



Title	STUDIES ON ELECTRICALLY CONDUCTIVE CRYSTALS INVOLVING METAL COMPLEXES
Author(s)	植山, 公助
Citation	大阪大学, 1985, 博士論文
Version Type	VoR
URL	https://hdl.handle.net/11094/719
rights	
Note	

The University of Osaka Institutional Knowledge Archive : OUKA

<https://ir.library.osaka-u.ac.jp/>

The University of Osaka

STUDIES ON ELECTRICALLY CONDUCTIVE CRYSTALS INVOLVING METAL COMPLEXES

(含金属錯体導電性結晶に関する研究)

KOSUKE UYAMA

OSAKA UNIVERSITY

1985

Preface

The works of this thesis were carried out under the guidance of Professor Toshio Tanaka at Department of Applied Chemistry, Faculty of Engineering, Osaka University.

Kosuke Ueyama

Department of Applied Chemistry,
Faculty of Engineering,
Osaka University,
Yamada-oka, Suita
Osaka 565,
Japan

January, 1985.

List of Publications

- 1 Syntheses and Electrical Resistivities of TTF and TSF Salts with Tris(oxalato)silicate, -germate, and -stannate
Kosuke Ueyama, Gen-etsu Matsubayashi, and Toshio Tanaka
Inorg. Chim. Acta, 87, 143, 1984.
- 2 Preparation and properties of TTF and TSF Salts with Planar Platinum(II) and Copper(II) Oxalate Anions
Kosuke Ueyama, Atsushi Tanaka, Gen-etsu Matsubayashi, and Toshio Tanaka
Inorg. Chim. Acta, in press.
- 3 Syntheses and Electrical Properties of TCNQ⁻ Radical Anion Salts of Some Tris(β -diketonato)siliconium(IV) Cations and X-Ray Crystal Structure of the 1:2 Salt of Tris(acetylacetonato)siliconium(IV) with TCNQ
Kosuke Ueyama, Gen-etsu Matsubayashi, Ichiro Shimohara, Tosio Tanaka, and Kazumi Nakatsu
J. Chem. Res., (S), (M), in press.
- 4 X-Ray Crystal Structures and Properties of Tris(tetrathiafulvalenium) Tetrachlorodimethylstannate(IV) and Tetra-thiafulvalenium Trichlorodimethylstannate(IV)
Gen-etsu Matsubayashi, Kosuke Ueyama, and Toshio Tanaka
J. Chem. Soc., Dalton Trans., in press.
- 5 Preparation and Electrical Resistivities of TTF and TSF Salts with the $[\text{SnR}_2\text{Cl}_n]^{2-n}$ Anions ($n = 3$ or 4 : $R = \text{Et}$ or Ph) and X-Ray Crystal Structure of $[\text{TTF}]_3[\text{SnEt}_2\text{Cl}_4]$
Kosuke Ueyama, Gen-etsu Matsubayashi, Ryuichi Shimizu, and Toshio Tanaka, in preparation.
- 6 X-Ray Crystal Structure and Properties of Tris(tetrathiafulvalenium) Hexachloroplatinate
Kosuke Ueyama, Gen-etsu Matsubayashi, and Toshio Tanaka, in preparation.
- 7 Electrical Properties and Configurations of TTF and TSF Salts with *cis*-Dialkylbis(oxalato)stannate(IV) Anions
Gen-etsu Matsubayashi, Koji Miyake, Kosuke Ueyama, and Toshio Tanaka, in preparation.

Contents

General Introduction	1
Chapter 1 Syntheses and Electrical Properties of TCNQ ⁻ Radical Anion Salts of Some Tris(β -diketonato)- siliconium(IV) Cations and X-Ray Crystal Structure of the 1:2 Salt of Tris(acetyl- acetionato)siliconium(IV) with TCNQ	3
Chapter 2 Syntheses and Electrical Properties of TTF and TSF Salts with Oxalato-metallate Anions	31
2-1 Tris(oxalato)silicate(IV), -germate(IV), and -stannate(IV) Anion Salts	31
2-2 Planar Platinum(II) and Copper(II) Oxalate Anion Salts	43
2-3 <i>cis</i> -Dialkylbis(oxalato)stannate(IV) Anion Salts	54
Chapter 3 Structures and Electrical Properties of TTF and TSF Salts with Chlorodiorganostannate(IV) Anions	66
3-1 X-Ray Crystal Structures and Properties of Tris- (tetrathiafulvalenium) Tetrachlorodimethyl- stannate(IV) and Tetrathiafulvalenium Trichloro- dimethylstannate(IV)	66
3-2 Preparation and Electrical Resistivities of TTF and TSF Salts with the $[\text{SnR}_2\text{Cl}_n]^{2-n}$ Anions ($n =$ 3 or 4: $\text{R} = \text{Et}$ or Ph) and X-Ray Crystal Structure of $[\text{TTF}]_3[\text{SnEt}_2\text{Cl}_4]$	83

Chapter 4	X-Ray Crystal Structure and Properties of Tris-	101
	(tetrathiafulvalenium) Hexachloroplatinate	
Conclusion		110
Acknowledgements		112

General Introduction

Organic solids are usually electrical insulators. Electrically conductive organic compounds known as "Organic metals" attract great attention, providing new insights into the solid state properties of organic compounds and prospects of many technological applications in future. Moreover, superconductors at high temperatures may be hoped to appear in this field.

Tetracyano-*p*-quinodimethane (TCNQ) is known as a good electron acceptor and is easily reduced to give a stable radical anion.¹ On the other hand, tetrathiafulvalene (TTF) and tetraselenafulvalene (TSF) are good electron donors, being oxidized to give stable radical cations.² To date, many TCNQ, TTF, and TSF salts with organic and inorganic counter ions (or molecules) have been prepared as electrically conductive compounds.³

The geometries and formal charges of counter ions (or molecules) may affect on the stacking modes of TCNQ and TTF (or TSF) molecules, and subsequently on the electrical properties of the salts. Although planar cations and anions have usually been used as the counterparts in the TCNQ⁻ radical anion and TTF⁺ radical cation salts, respectively, some TCNQ salts with non-planar cations exhibit metal-to-semiconductor transitions near room temperature.⁴ Furthermore, tetramethyltetraselenafulvalene salts with cubic hexafluorophosphate and perchlorate anions undergo to transfer to a superconductor below 1 K.⁵ Thus, bulky ions may be of interest as raw materials for obtaining TCNQ, TTF, and TSF salts with any new properties.

The objects of this thesis are to synthesize TCNQ, TTF, and TSF salts containing bulky metal complex ions for which few attentions have been paid, and to clarify their electrical properties

and the stacking modes of donor and acceptor molecules in the salts. In particular, it should be noted that the TTF or TSF salts with dichlorodiorganostannate(IV) and hexachloroplatinate(IV) anions in this thesis has been found to assume a new stacking mode containing the trimer units of donor molecules to form a two-dimensional layer.

Chapter 1 describes the preparation of TCNQ salts with some bulky tris(β -diketonato)siliconium(IV) cations and electrical resistivities, together with the crystal structure of the tris(acetylacetonato)siliconium-TCNQ (1:2) salt. In chapter 2, the electrical properties and the configurations of TTF and TSF salts with some metal oxalate anions are described. Chapter 3 deals with TTF and TSF salts with several chlorodiorganostannate(IV) anions, whose resistivities are interpreted based on the crystallographic analyses of three salts; $[\text{TTF}][\text{SnMe}_2\text{Cl}_3]$, $[\text{TTF}]_3[\text{SnMe}_2\text{Cl}_4]$, and $[\text{TTF}]_3^-[\text{SnEt}_2\text{Cl}_4]$. The crystal structure and the electrical properties of $[\text{TTF}]_3[\text{PtCl}_6]$ are elucidated in Chapter 4.

Referenes

- 1 A. F. Garito and A. J. Heeger, *Acc. Chem. Res.*, 1974, 7, 232.
- 2 J. B. Torrance, *Acc. Chem. Res.*, 1979, 12, 79.
- 3 A. R. Siedle, G. A. Candela, T. F. Finnegan, R. P. van Duyne, T. Cape, G. F. Kokoszka, P. M. Woyciesjes, J. A. Hashmall, M. Glick, and W. Ilsley, *Ann. N. Y. Acad. Sci.*, 1978, 313. T. J. Kistenmacher, M. Rossi, C. C. Chiang, R. P. van Duyne, and A. R. Siedle, *Inorg. Chem.*, 1980, 19, 3604. M. Bousseau, L. Valade, M. F. Bruniquel, P. Cassoux, M. Garbauskas, L. Interrante, and J. Kasper, *Nouv. J. Chim.*, 1984, 8, 3.
- 4 Bert van Bodegom, *Acta Crystallogr.*, 1981, B37, 857.
- 5 K. Bechgaard, *Mol. Cryst. Liq. Cryst.*, 1982, 79, 1.

CHAPTER 1

SYNTHESES AND ELECTRICAL PROPERTIES OF $\text{TCNQ}^{\cdot-}$ RADICAL ANION SALTS OF SOME $\text{TRIS}(\beta\text{-DIKETONATO})\text{SILICONIUM(IV)}$ CATIONS AND X-RAY CRYSTAL STRUCTURE OF THE 1:2 SALT OF $\text{TRIS}(\text{ACETYLACETONATO})\text{SILICONIUM(IV)}$ WITH TCNQ

1. Introduction

A number of 7,7,8,8-teracyano-*p*-quinodimethane (TCNQ) radical anion salts have been synthesized as electrically conductive low-dimensional materials since TCNQ appeared in 1960.^{1,2} Most of those are known to have compositions 1:1 (simple salts) and 1:2 (complex salts) with a univalent counter cation. There have sometimes been found unusual compositions such as 1:3,³ 2:3,⁴⁻⁹ and 4:7¹⁰ in the complex salts of univalent cations. Isolation of TCNQ salts with such unusual compositions may be possible by using bulky or nonplanar cations. Some of these exhibit considerably low electrical resistivities, as seen in the complex salts with dimethyldiphenyl- and diethyldiphenylphosphonium cations,¹¹ and with 1,1,4,4-tetraphenyl-1,4-diphosphoniacyclohexa-2,5-diene dication.¹² In addition, an unusual semiconductor-to-metal transition was observed near room temperature in the complex salt of TCNQ with the *N*-ethyl-*N*-methylmorpholinium cation.¹³

The work in the present chapter is to investigate such unusual compositions or properties in the $\text{TCNQ}^{\cdot-}$ radical anion salts, using siliconium(IV) cations as bulky counterparts. This chapter describes the synthesis and electrical resistivities of the $\text{TCNQ}^{\cdot-}$ radical anion salts with some $\text{tris}(\beta\text{-diketonato})$ -

siliconium(IV) cations (β -diketonato = MeC(O)CHC(O)Me , $\text{Bu}^t\text{C(O)CHC(O)Bu}^t$, PhC(O)CHC(O)Ph , and MeC(O)C(Et)C(O)Me), which are the first TCNQ salts containing silicon atoms. Moreover, X-ray crystal structures of two 1:2 salt of the $[\text{Si}^{\text{IV}}(\text{MeC(O)CHC(O)Me})_3]^+$ cation with TCNQ having different crystalline forms are described.

2. Experimental

Preparation of TCNQ Salts with Tris(β -diketonato)siliconium(IV) Cations. To a benzene/methanol (1:1 v/v, 2 cm³) solution of $[\text{Si}(\text{MeC(O)CHC(O)Me})_3]^+\text{Cl}^-\cdot\text{HCl}^{14}$ (0.38 g, 0.96 mmol) was added Li^+TCNQ^- (0.41 g, 1.0 mmol) in the same mixed solvent (20 cm³) with stirring. A yellow precipitate which appeared immediately was filtered off, and the filtrate was evaporated to one third volume under reduced pressure. The resulting solution was allowed to stand in a refrigerator for 5 h to give dark violet microcrystals of $[\text{Si}(\text{MeC(O)CHC(O)Me})_3]^+\text{TCNQ}^-\cdot\text{C}_6\text{H}_6$ (1a), which were collected by filtration, washed with benzene, and dried *in vacuo*, 77 % yield. The reaction of $[\text{Si}(\text{MeC(O)CHC(O)Me})_3]^+\text{Cl}^-\cdot\text{HCl}^{14}$ (0.95 g, 2.4 mmol) with Li^+TCNQ^- (0.75 g, 3.6 mmol) in ethanol/methanol (1:1 v/v, 50 cm³), however, afforded a black microcrystalline complex salt $[\text{Si}(\text{MeC(O)CHC(O)Me})_3]^+(\text{TCNQ})_2^-$ in 41 % yield based on the siliconium(IV) cation; black plates (2a-I) and black columns (2a-II) were obtained by recrystallization from acetonitrile at room temperature and below -10 °C, respectively.

The reaction of $[\text{Si}(\text{MeC(O)C(Et)C(O)Me})_3]^+\text{Cl}^-\cdot\text{HCl}^{14}$ with Li^+TCNQ^- in ethanol gave a black microcrystalline complex salt $[\text{Si}(\text{MeC(O)C(Et)C(O)Me})_3]^+(\text{TCNQ})_3^-$ (2b) in a 30 % yield, but the corresponding simple salt was not obtained even though the

reaction was attempted in various organic solvents. On the other hand, $[\text{Si}(\text{Bu}^t\text{C}(\text{O})\text{CHC}(\text{O})\text{Bu}^t)_3]^+\text{Cl}^-\cdot\text{HCl}^{14}$ and $[\text{Si}(\text{PhC}(\text{O})\text{CHC}(\text{O})\text{Ph})_3]^+\text{Cl}^-^{14}$ reacted with Li^+TCNQ^- in ethanol to yield violet micro-crystalline simple salts, $[\text{Si}(\text{Bu}^t\text{C}(\text{O})\text{CHC}(\text{O})\text{Bu}^t)_3]^+\text{TCNQ}^-$ (1c) and $[\text{Si}(\text{PhC}(\text{O})\text{CHC}(\text{O})\text{Ph})_3]^+\text{TCNQ}^-$ (1d) in 60 and 80 % yields, respectively, irrespective of the mole ratios of the reactants.

To a hot acetonitrile (10 cm^3) solution of 1d (0.74 g, 0.82 mmol) was added neutral TCNQ (0.33 g, 1.6 mmol) in hot acetonitrile (20 cm^3), and the mixture was refluxed for several min.. After cooling to room temperature, the solution was allowed to stand in a refrigerator overnight to give a complex salt $[\text{Si}(\text{PhC}(\text{O})\text{CHC}(\text{O})\text{Ph})_3]^+(\text{TCNQ})_2^-$ (2d) as blue plates, which were collected by filtration and dried *in vacuo*, 60 % yield. The analogous reaction of 1d with TCNQ at mole ratio 1:2 in hot acetonitrile afforded a complex salt $[\text{Si}(\text{PhC}(\text{O})\text{CHC}(\text{O})\text{Ph})_3]^+(\text{TCNQ})_{2.5}^-$ (3d) as violet needles, which were purified by recrystallization from acetonitrile, 87 % yield. On the other hand, several attempts to prepare $[\text{Si}(\text{Bu}^t\text{C}(\text{O})\text{CHC}(\text{O})\text{Bu}^t)_3]^+ - \text{TCNQ}$ complex salts were unsuccessful; TCNQ and 1c only were recovered.

Properties and analytical data of the simple and complex salts obtained are listed in Table 1.

Physical Measurements. Electrical resistivities as compacted samples, magnetic susceptibilities and electronic absorption spectra were measured as described previously.¹⁵ The measurement of resistivities in the crystalline states was performed by the conventional two-probe method.

X-Ray Crystal Structure Determinations. (a) *Black Plates of $[\text{Si}(\text{MeC}(\text{O})\text{CHC}(\text{O})\text{Me})_3]^+(\text{TCNQ})_2^-$ (2a-I).* The space group and

Table 1. Physical properties and analyses of the TCNQ⁻ salts

No.	Salt	Crystal form	m.p. / °C (decomp.)	Found (Calcd.) %		
				C	H	N
1a ~~	[Si (MeC (O) CHC (O) Me) ₃] ⁺ TCNQ ⁻ ·C ₆ H ₆	Purple microcrystals	> 99	64.5 (65.2)	5.1 (5.1)	9.4 (9.2)
1c ~~	[Si (Bu ^t C (O) CHC (O) Bu ^t) ₃] ⁺ TCNQ ⁻	Violet microcrystals	> 180	69.25 (69.1)	7.9 (7.9)	7.4 (7.2)
1d ~~	[Si (PhC (O) CHC (O) Ph) ₃] ⁺ TCNQ ⁻	Purple microcrystals	> 204	75.4 (75.9)	4.2 (4.1)	6.1 (6.2)
2a-I ~~	[Si (MeC (O) CHC (O) Me) ₃] ⁺ (TCNQ) ₂ ⁻	Black plates	> 148	64.1 (63.8)	4.2 (4.0)	15.4 (15.3)
2b ~~	[Si (MeC (O) C (Et) C (O) Me) ₃] ⁺ (TCNQ) ₃ ⁻	Violet microcrystals	> 146	66.4 (67.0)	4.5 (4.5)	16.5 (16.4)
2d ~~	[Si (PhC (O) CHC (O) Ph) ₃] ⁺ (TCNQ) ₂ ⁻	Purple plates	> 239	74.75 (74.9)	3.6 (3.7)	10.35 (10.1)
3d ~~	[Si (PhC (O) CHC (O) Ph) ₃] ⁺ (TCNQ) _{2.5} ⁻	Purple needles	> 246	74.2 (74.55)	3.7 (3.6)	11.6 (11.6)

initial unit-cell parameters were determined from oscillation and Weissenberg photographs. Accurate parameters were obtained by the least-squares treatment of angular coordinates of 50 reflections with 2θ values from 20° to 36° which were measured on a computer-controlled Rigaku four-circle diffractometer with Mo- $K\alpha$ ($\lambda = 0.71069 \text{ \AA}$) radiation.

Crystal data for $\tilde{2}a$ -I. $C_{39}H_{29}N_8O_6Si$, $M = 733.80$. Monoclinic, space group $P2_1/a$; $a = 34.981(5)$, $b = 13.543(2)$, $c = 7.837(1) \text{ \AA}$, $\beta = 95.15(1)^\circ$, $V = 3698(1) \text{ \AA}^3$; $Z = 4$, $D_c = 1.318(1) \text{ g cm}^{-3}$; $F(000) = 1524$, $(Mo-K\alpha) = 1.69 \text{ cm}^{-1}$.

A specimen, approximately $0.46 \times 0.25 \times 0.15 \text{ mm}$, was used for the data collection on the diffractometer. Intensity data were measured by using a graphite-monocromatized Mo- $K\alpha$ radiation and the ω - 2θ scan technique at the 2θ scan rate 4° min^{-1} . The scan width in ω was $(0.6 + 0.34\tan\theta)^\circ$ and 20 s background counts were taken on either side of every scan. Five check reflections were monitored before every 50 measurements. No significant intensity variation was observed throughout the data collection. The intensities were corrected for Lorentz and polarization effects. No correction was made for absorption. Of 6640 independent reflections measured in the range of $2^\circ < 2\theta < 50^\circ$, 4610 reflections with $|F_o| > 3\sigma(F)$ were used for the structure determination. The coordinates of all the non-hydrogen atoms were obtained by the direct (MULTAN) method¹⁶ and successive Fourier syntheses. Positions of hydrogen atoms except for those of a part of methyl groups of the acetylacetonato ligand were clarified from a difference-Fourier map based on the anisotropic refinement of all the non-hydrogen atoms. Block-diagonal least-squares refinement with anisotropic thermal parameters for all the non-hydrogen atoms and with isotropic thermal parameters for the clarified hydrogen atoms

led to final residual indices $R = \Sigma ||F_o| - |F_c|| / \Sigma |F_o| = 0.064$ and $R' = [\Sigma w(|F_o| - |F_c|)^2 / \Sigma w|F_o|^2]^{1/2} = 0.081$ with the weighting scheme, $1/w = \sigma^2(F_o) + 0.0005(F_o)^2$. The final difference-Fourier map had no positive maxima $> 1 \text{ e } \text{\AA}^{-3}$. The atomic scattering factors used throughout the refinement were taken from the table.¹⁷ The final atomic coordinates with standard deviations for salt 2a-I are given in Table 2.

Table 2. Final atomic coordinates ($\times 10^4$; H, $\times 10^3$) for $[\text{Si}(\text{MeC}(\text{O})\text{CHC}(\text{O})\text{Me})_3]^+(\text{TCNQ})_2^-$ (2a-I) with estimated standard deviations in parentheses

Atom	X	Y	Z
Si	2464.3(3)	6251.8(9)	3026(1)
O1	2061.5(7)	5626(2)	3702(3)
O2	2242.7(7)	7419(2)	3026(3)
O3	2866.4(7)	6853(2)	2304(3)
O4	2627.3(7)	6382(2)	5215(3)
O5	2704.2(7)	5102(2)	3060(3)
O6	2284.2(7)	6134(2)	861(3)
N1	-1551(1)	-101(3)	-946(5)
N2	-916(1)	112(3)	5984(5)
N3	377(1)	1861(3)	-3659(5)
N4	1000(1)	2065(3)	1363(5)
N5	-1366.9(9)	2590(3)	664(5)
N6	-666(1)	2741(3)	5414(4)
N7	522(1)	4544(3)	-4584(4)
N8	1214(1)	4691(3)	152(5)
C1	1428(1)	5206(4)	4258(6)
C2	1716(1)	5957(4)	3796(5)
C3	1625(1)	6943(4)	3511(6)
C4	1889(1)	7639(4)	3137(5)
C5	1791(2)	8711(4)	2850(7)
C6	3486(1)	7558(4)	2154(6)
C7	3184(1)	7087(3)	3173(5)

Table 2. Continued

Atom	X	Y	Z
C8	3249(1)	6944(4)	4904(5)
C9	2966(1)	6626(3)	5884(5)
C10	3025(1)	6568(4)	7798(5)
C11	2852(1)	3443(3)	2484(6)
C12	2647(1)	4378(3)	1988(5)
C13	2418(1)	4466(3)	487(5)
C14	2251(1)	5337(3)	-53(5)
C15	2017(1)	5454(4)	-1734(5)
C16	-600(1)	662(3)	1945(5)
C17	-615(1)	794(3)	125(5)
C18	-305(1)	1120(3)	-623(4)
C19	51(1)	1328(3)	365(5)
C20	66(1)	1190(3)	2181(5)
C21	-246(1)	874(3)	2939(5)
C22	-1269(1)	94(3)	1741(5)
C23	-921(1)	329(3)	2725(5)
C24	-916(1)	209(3)	4534(5)
C25	370(1)	1770(3)	-2216(5)
C26	371(1)	1656(3)	-399(5)
C27	720(1)	1876(3)	581(5)
C28	-395(1)	3345(3)	1293(4)
C29	-428(1)	3460(3)	-526(4)
C30	-125(1)	3771(3)	-1367(4)
C31	238(1)	3982(3)	-463(4)
C32	270(1)	3877(3)	1361(4)
C33	-29(1)	3565(3)	2206(4)
C34	-1070(1)	2789(3)	1305(5)
C35	-703(1)	3013(3)	2158(4)
C36	-673(1)	2869(3)	3969(5)
C37	526(1)	4429(3)	-3134(5)
C38	549(1)	4299(3)	-1328(4)
C39	916(1)	4511(3)	-473(5)
H3	138(1)	714(3)	361(5)
H8	346(1)	712(3)	547(5)
H111	311(1)	362(4)	297(6)
H112	270(1)	313(3)	330(6)

Table 2. Continued

Atom	X	Y	Z
H113	288(1)	306(4)	145(6)
H13	242(1)	397(3)	-15(5)
H151	212(2)	503(4)	-238(7)
H152	170(2)	572(4)	-149(7)
H153	210(2)	602(4)	-236(7)
H17	-87(1)	74(3)	-58(4)
H18	-31(1)	126(3)	-186(4)
H20	31(1)	136(3)	290(4)
H21	-25(1)	77(3)	412(4)
H29	-66(1)	333(2)	-117(4)
H30	-16(1)	390(2)	-258(4)
H32	50(1)	403(2)	200(4)
H33	0(1)	346(3)	345(4)

(b) Black columns of $[\text{Si}(\text{MeC}(\text{O})\text{CHC}(\text{O})\text{Me})_3]^+(\text{TCNQ})_2^-$ ($\underline{2a-II}$).

Accurate parameters were determined by the least-squares treatment of angular coordinates of 40 reflections in the range $20^\circ < 2\theta < 30^\circ$.

Crystal data for $\underline{2a-II}$. $\text{C}_{39}\text{H}_{29}\text{N}_8\text{O}_6\text{Si}$, $M = 733.80$. Triclinic, space group $P\bar{1}$; $a = 7.941(2)$, $b = 33.04(1)$, $c = 7.775(1)$ Å, $\alpha = 95.92(2)$, $\beta = 98.55(3)$, $\gamma = 76.86(2)^\circ$, $V = 1959.3(8)$ Å³; $Z = 2$, $D_c = 1.244(1)$ g cm⁻³; $F(000) = 762$, $(\text{Mo-K}\alpha) = 1.69$ cm⁻¹.

Data collection using a specimen, approximately $0.44 \times 0.18 \times 0.44$ mm and the structure solution were carried out by a similar procedure to that for $\underline{2a-I}$. Of 6877 independent reflections ($2^\circ < 2\theta < 50^\circ$), only 2724 had structure amplitudes larger than three times their standard deviations. The coordinates of non-hydrogen atoms of the $[\text{Si}(\text{MeC}(\text{O})\text{CHC}(\text{O})\text{Me})_3]^+$ cation and of one TCNQ moiety were found by the MULTAN procedure and Fourier syntheses.

The atomic positions of the other TCNQ molecule, however, have not been determined probably because of a large disorder of the molecule. Block-diagonal least-squares refinement with anisotropic thermal parameters for non-hydrogen atoms of the $[\text{Si}(\text{MeC}(\text{O})\text{CHC}(\text{O})-\text{Me})_3]^+$ cation and of one TCNQ molecule gave the residual index $R = \Sigma ||F_o| - |F_c|| / \Sigma |F_o| = 0.24$.

Crystallographic calculations were performed on an ACOS 900S computer at the Crystallographic Research Center, Institute for Protein Research, Osaka University. Figures 1, 2, and 5 - 7 were drawn with a local version of ORTEP-II.¹⁸

3. Results and Discussion

Crystal Structure of 2a-I. A projection of the crystal structure of 2a-I along the c^* axis is given in Figure 1, which demonstrates that the TCNQ molecules stack in plane-to-plane, forming columns parallel to the b axis. In the columns, TCNQ-A is crystallographically nonequivalent with TCNQ-B, while their molecular planes are parallel to those of TCNQ-A' and TCNQ-B', respectively, owing to the center of symmetry. Overlaps of the adjacent TCNQ molecules in a column are shown in Figure 2. TCNQ-A and TCNQ-B are almost parallel to each other with the dihedral angle of 1.8° between their least-squares planes, and they overlap in a manner of the ring-external-bond type. The average distance from the non-hydrogen atoms of the TCNQ-B molecule to the TCNQ-A molecular plane is 3.14 \AA , which is compatible with the TCNQ - TCNQ spacing (3.17 \AA) in TCNQ-tetrathiafulvalene.^{19,20} Thus, there is a strong interaction between TCNQ-A and TCNQ-B. TCNQ-A and TCNQ-A' as well as TCNQ-B and TCNQ-B' are both parallel to each other and they also assume the ring-external-bond type

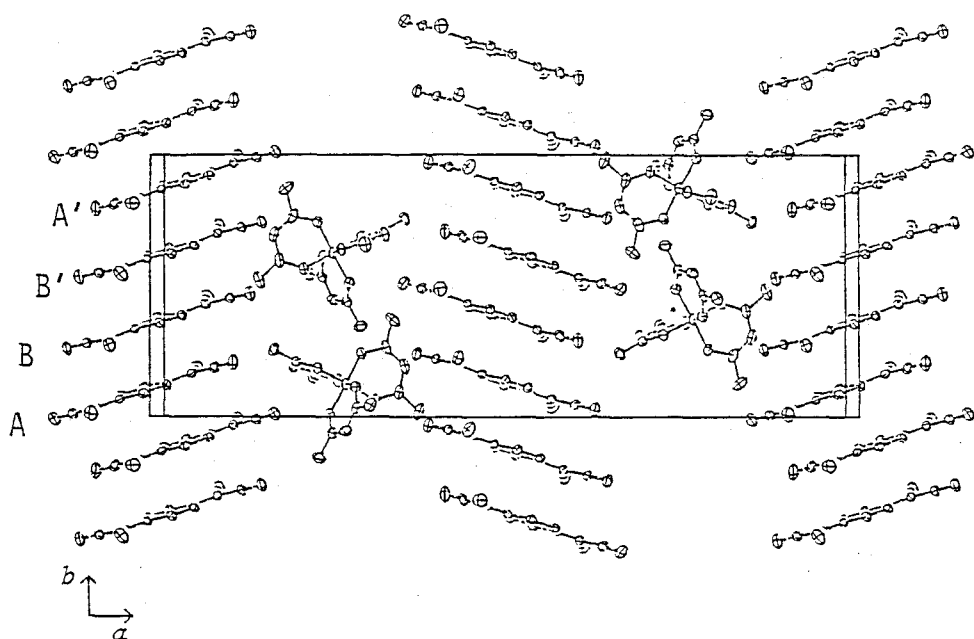


Figure 1. Projection of the crystal structure of 2a-I along the c^* axis.

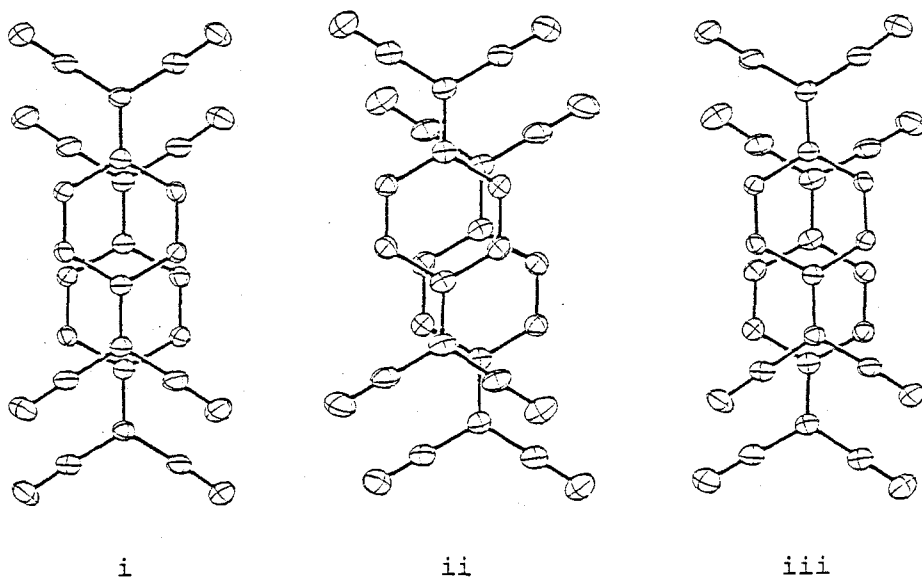


Figure 2. Overlap of the adjacent TCNQ molecules of 2a-I; TCNQ-A and TCNQ-B (i), TCNQ-A and TCNQ-A' (ii), and TCNQ-B and TCNQ-B' (iii).

overlap, respectively, although there can be seen a slightly sideways sliding in the TCNQ-A/TCNQ-A' overlap. The spacing of TCNQ-A/TCNQ-A' and TCNQ-B/TCNQ-B' molecular planes are 3.34 and 3.21 Å, respectively. Thus, the three different overlap modes and distances between the TCNQ molecules indicate that the columns are constructed by tetramer units consisting of a pair of dimers (TCNQ-A/TCNQ-B and TCNQ-B'/TCNQ-A'). Similar packings have been reported for other 1:2 complex salts of methyltriphenylarsenium²¹ and 4-ethylmorpholinium cations²² with TCNQ, and for 1:4 complex salts of diquaterized 4,4'-bipyridinium and related dications with TCNQ.^{23,24} The columns are located closely to one another along the *c* axis with intermolecular nitrogen-hydrogen contacts of 2.71 - 3.07 Å (see Figure 3), which are slightly larger than those in the 1:1 salt of TCNQ with dibenzothiophene (2.70 - 2.77 Å).²⁵ Adjacent TCNQ columns from sheets approximately parallel to the *bc* plane, and the successive sheets are interleaved along the *a* axis by the [Si(MeC(O)-CHC(O)Me)₃]⁺ cation.

Figure 4 shows the molecular geometries of TCNQ-A and TCNQ-B. Deviations of non-hydrogen atoms from the least-squares plane are given in Table 3. In the TCNQ-A molecule two C(CN)₂ groups are slightly twisted to the same side by 1.7° and 1.9° against the least-squares cyclohexadiene plane. On the contrary, the TCNQ-B molecule assumes approximately a shallow boat form. The bond lengths of these molecules are intermediate between those of neutral TCNQ²⁶ and those of the TCNQ⁻ radical anion in M⁺TCNQ⁻, where M = Na,²⁷ K,²⁸ and Rb.²⁹ This is consistent with the charge on each TCNQ; 0.6 e⁻ for TCNQ-A and 0.5 e⁻ for TCNQ-B, which was estimated on the basis of the mean bond lengths of TCNQ molecules according to the method of Flandrois and Chasseau.³⁰

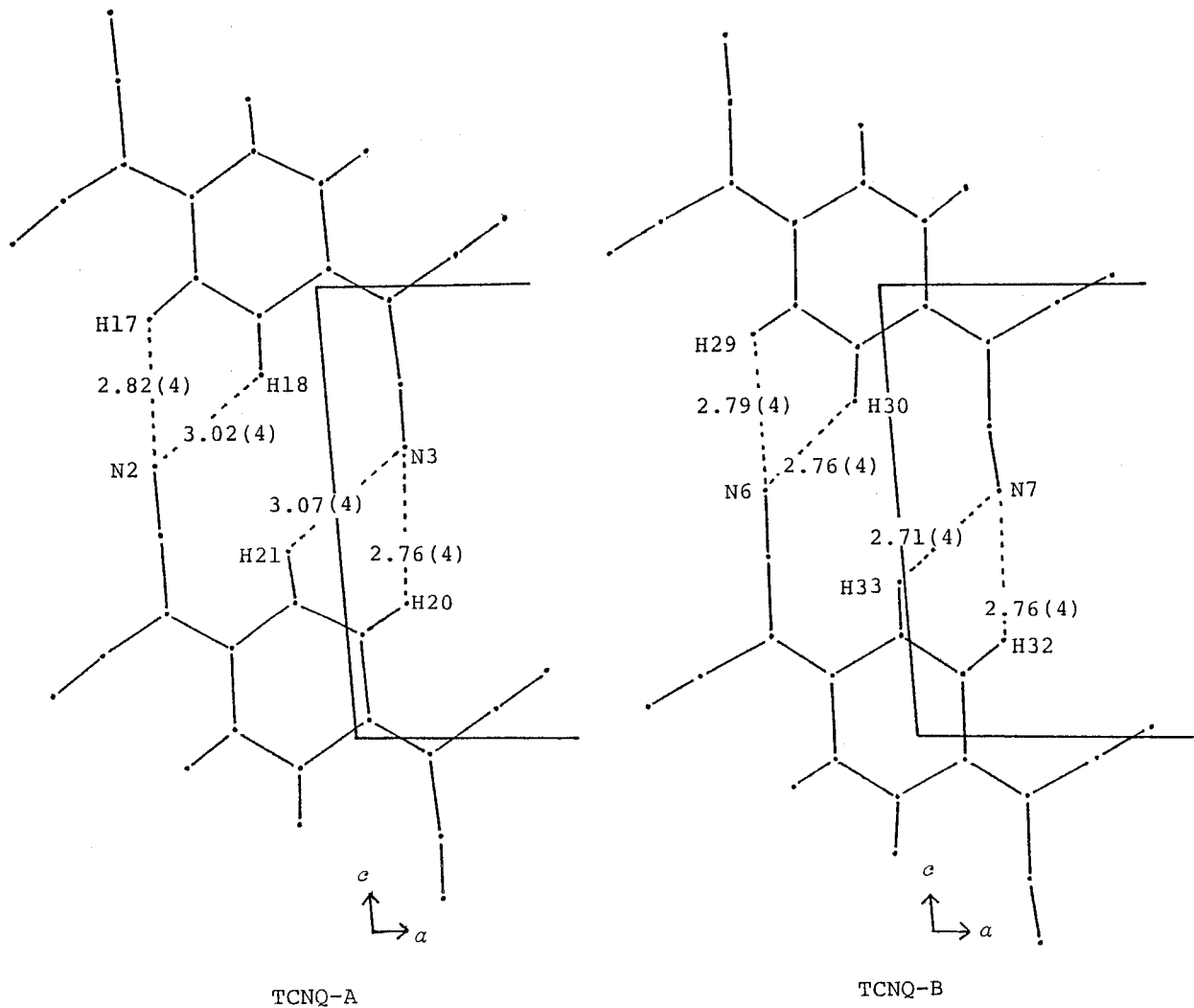


Figure 3. Distances (\AA) between the TCNQ molecules belonging to the adjacent columns of $2a\text{-I}$ along the b axis.

Table 3. The least-squares planes of TCNQ-A and TCNQ-B of 2a-I and the deviations of atoms from the plane

TCNQ-A			
Cyclohexadiene ring			
$-0.3030X + 0.9468Y + 0.1080Z = 1.6887$			
Atom	deviation (\AA)	Atom	deviation (\AA)
C16*	0.001	C24	0.029
C17*	- 0.005	C25	- 0.045
C18*	0.006	C26	- 0.001
C19*	- 0.002	C27	0.015
C20*	- 0.002	N1	- 0.074
C21*	0.003	N2	0.058
C22	- 0.039	N3	- 0.088
C23	- 0.002	N4	0.044

TCNQ-B			
Cyclohexadiene ring			
$-0.2948X + 0.9502Y + 0.1014Z = 4.8409$			
Atom	deviation (\AA)	Atom	deviation (\AA)
C28*	- 0.000	C36	- 0.059
C29*	- 0.000	C37	0.003
C30*	0.004	C38	- 0.008
C31*	- 0.007	C39	- 0.028
C32*	0.007	N5	- 0.032
C33*	- 0.003	N6	- 0.086
C34	- 0.018	N7	0.011
C35	- 0.023	N8	- 0.041

* These atoms make the cyclohexadiene.

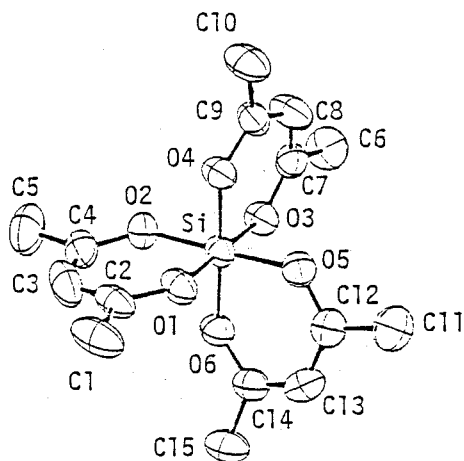


Figure 5. The structure of $[\text{Si}(\text{MeC}(\text{O})\text{CHC}(\text{O})\text{Me})_3]^+$ of 2a-I. Hydrogen atoms are omitted for simplification.

Figure 5 shows an ORTEP drawing of the cation moiety of 2a-I, and the bond distances and angles are listed in Table 4. The silicon atom is coordinated by six oxygen atoms of the acetylacetonato ligands with Si-O distances of 1.761(3) - 1.768(3) Å to assume an octahedral geometry. Since this is the first X-ray structure determination of the tris(β -diketonato)siliconium(IV) cation salt, no comparative distance for an Si-O bond placed in the same geometry is available. The structure, however, is quite similar to that of $(-)_589[\text{Ge}(\text{MeC}(\text{O})\text{CHC}(\text{O})\text{Me})_3]\text{ClO}_4$ with Ge-O distances of 1.860(5) - 1.875(5) Å.³¹ The difference between the Si-O and Ge-O distances can essentially be ascribed to the bulkiness of the Si^{4+} and Ge^{4+} ions, whose radii are 0.54 and 0.67 Å, respectively.³²

Each acetylacetonato ligand in the present salt assumes a planar skeleton with a deviation of ± 0.091 Å from the least-squares

Table 4. Bond distances (\AA) and angles ($^\circ$) in the cation moiety of 2a-I with the estimated standard deviations in parentheses

Si - O1	1.766(3)	C1 - C2	1.500(7)
Si - O2	1.761(3)	C2 - C3	1.385(7)
Si - O3	1.762(3)	C3 - C4	1.370(7)
Si - O4	1.767(3)	C4 - C5	1.503(7)
Si - O5	1.768(3)	C6 - C7	1.519(6)
Si - O6	1.763(3)	C7 - C8	1.368(5)
O1 - C2	1.298(5)	C8 - C9	1.376(6)
O2 - C4	1.283(5)	C9 - C10	1.497(6)
O3 - C7	1.290(4)	C11 - C12	1.489(6)
O4 - C9	1.295(4)	C12 - C13	1.369(5)
O5 - C12	1.294(5)	C13 - C14	1.367(6)
O6 - C14	1.294(5)	C14 - C15	1.495(5)
O1 - Si - O2	93.9(1)	O1 - C2 - C1	115.4(4)
O3 - Si - O4	93.9(1)	O2 - C4 - C5	115.0(4)
O5 - Si - O6	93.6(1)	O3 - C7 - C6	115.5(3)
		O4 - C9 - C10	115.5(3)
Si - O1 - C2	128.6(3)	O5 - C12 - C11	115.7(3)
Si - O2 - C4	129.5(3)	O6 - C14 - C15	114.5(4)
Si - O3 - C7	128.2(2)		
Si - O4 - C9	128.5(2)	C1 - C2 - C3	122.9(4)
Si - O5 - C12	127.8(2)	C3 - C4 - C5	123.2(4)
Si - O6 - C14	128.0(2)	C6 - C7 - C8	121.3(3)
		C8 - C9 - C10	122.3(3)
O1 - C2 - C3	121.6(4)	C11 - C12 - C13	121.9(4)
O2 - C4 - C3	121.8(4)	C13 - C14 - C15	123.2(4)
O3 - C7 - C8	123.1(4)		
O4 - C9 - C8	122.1(3)	C2 - C3 - C4	123.3(4)
O5 - C12 - C13	122.4(4)	C7 - C8 - C9	122.3(4)
O6 - C14 - C13	122.2(3)	C12 - C13 - C14	122.8(4)

plane consisting of the non-hydrogen atoms. The silicon atom, however, deviates from these planes by $0.179 - 0.208 \text{ \AA}$, which is similar to the deviation ($0.105 - 0.337 \text{ \AA}$) of the germanium atom in $(-)_589[\text{Ge}(\text{MeC}(\text{O})\text{CHC}(\text{O})\text{Me})_3]\text{ClO}_4$.³¹ The dihedral angles between the plane consisting of silicon and two chelating oxygen atoms and the plane of an acetylacetonato ligands are 13.6 , 8.7 , and 8.7° which are compared with those (17.4 , 13.4 , and 5.1°) of $(-)_589[\text{Ge}(\text{MeC}(\text{O})\text{CHC}(\text{O})\text{Me})_3]^+$.³¹

Crystal Structure of 2a-II. The positions of the cation moiety and one TCNQ molecule of 2a-II were determined as illustrated in Figure 6. Another TCNQ molecule is expected to exist approximately along the c axis, however the position has not been revealed presumably owing to a great disorder. The clarified TCNQ molecules construct columns stacked in the c direction, the molecular planes being parallel to each other with overlap of the ring-external-bond type. TCNQ-A overlaps with TCNQ-A' effectively with an interplanar

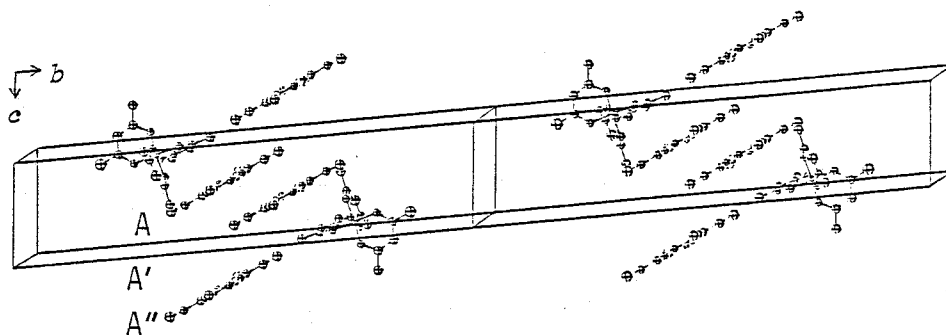


Figure 6. Projection of the structure of 2a-II on the bc plane, showing two unit cells.

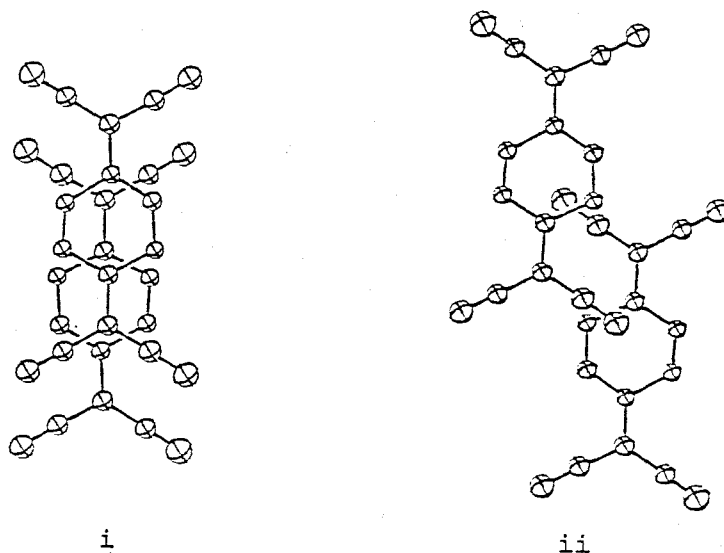


Figure 7. Overlap of the adjacent TCNQ molecules of 2a-II; TCNQ-A and TCNQ-A' (i), and TCNQ-A' and TCNQ-A" (ii).

distance of 3.23 \AA , while the overlap of TCNQ-A'/TCNQ-A" is small, with an interplanar distance of 3.45 \AA , as illustrated in Figure 7.

In spite of the insufficient overlap of TCNQ molecules in the columns, the resistivity in the crystals was measured to be fairly small along the c axis, as described below. This finding suggests that the undetermined TCNQ molecules may be arranged to form columns along the c axis with a sufficient TCNQ/TCNQ overlap, although they are disordered.

Electrical Resistivities. The temperature dependences of specific resistivities measured as compacted samples indicated

that all the salts are typical semiconductors in the temperature range measured (20 - 90 °C), except for 2a-I which exhibited a significant deviation of the $\log \rho - 1/T$ plot from a straight line around room temperature. Table 5 summarizes the specific resistivities (ρ) and activation energies (E_a) calculated from $\rho = \rho_0 \exp(E_a/kT)$, together with the magnetic susceptibilities of the salts. The resistivities of simple salts 1a, 1c, and 1d fall in the range $10^6 - 10^8 \Omega \text{ cm}$ which is about 10^3 times larger than those of the TCNQ^- radical anion simple salts with alkali metal cations.³³ This may be due to the bulky cations of the present salts. In addition, there seems to be a trend that the siliconium cation with more bulky β -diketonato ligands requires more TCNQ molecules to

Table 5. Specific resistivities (ρ)^a, activation energies (E_a), and magnetic susceptibilities (χ_m)^b of the TCNQ^- salts

Salt	$\rho_{298}/\Omega \text{ cm}$	E_a/eV	$\chi_m/10^{-4} \text{ emu mol}^{-1}$
<u>1a</u>	4.0×10^6	0.19	- 0.58
<u>1c</u>	2.0×10^8	0.93	7.2
<u>1d</u>	1.6×10^8	0.32	- 1.6
<u>2a-I</u>	2.9×10^2	c	4.5
<u>2a-II</u>	4.3×10	0.11	2.1
<u>2d</u>	1.8×10^2	0.21	7.5
<u>2d</u>	2.9×10^4	0.24	6.6
<u>3d</u>	8.3×10	0.23	5.1

^a Measured in the compacted samples. ^b Measured at room temperature. ^c Not determined owing to no linear relation between $\log \rho$ and $1/T$ around 298 K.

stabilize the complex salts (compare $\underline{2b}$ and $\underline{3d}$). In view of these results, the bulkiness of the cation may control the interplanar distance of TCNQ in the columnar structure.

The resistivities of salts $\underline{2a-I}$ and $\underline{2a-II}$ measured in the single crystalline states are summarized in Table 6. Salt $\underline{2a-I}$ shows the smallest resistivity along the b axis, which is approximately parallel to the TCNQ columns. Along the a axis, the TCNQ columns are separated by the cation moiety and the resistivity has the largest value. The intermediate resistivity along the c axis may be explainable by the TCNQ/TCNQ interaction between the nitrogen and hydrogen atoms parallel to the c axis (Figure 3), although this is weak. Salt $\underline{2a-II}$ exhibits the smallest resistivity along the c axis, which is parallel to the direction of the TCNQ stack with an effective overlap, though a part of TCNQ molecules is disordered and the position has not been determined as described in the previous section.

Figure 8 shows the temperature dependence of the resistivities of crystals $\underline{2a-I}$ and $\underline{2a-II}$ which were measured along the axes with

Table 6. Anisotropy of the resistivities (ρ)^{*} in the crystalline states of $\underline{2a-I}$ and $\underline{2a-II}$

axis	$\underline{2a-I}$ $\rho / \Omega \text{ cm}$	$\underline{2a-II}$ $\rho / \Omega \text{ cm}$
a	9.2×10^3	2.6×10^2
b	7.7×10	5.3×10^4
c	1.2×10^3	4.0×10

* Measured at 298 K.

the smallest resistivity, b and c respectively. Although the linear $\log \rho - 1/T$ relationship is observed for $2a-II$ in the temperature range measured ($-30 - 45^\circ C$), $2a-I$ exhibits two distinct transition points below room temperature. This may be associated with the fact that $2a-I$ is crystallized into a stable form only near room temperature, however details have not elucidated in this study.

Electronic Spectra and Magnetic Susceptibilities. Figure 9 shows the electronic absorption spectra of three simple salts $1a$,

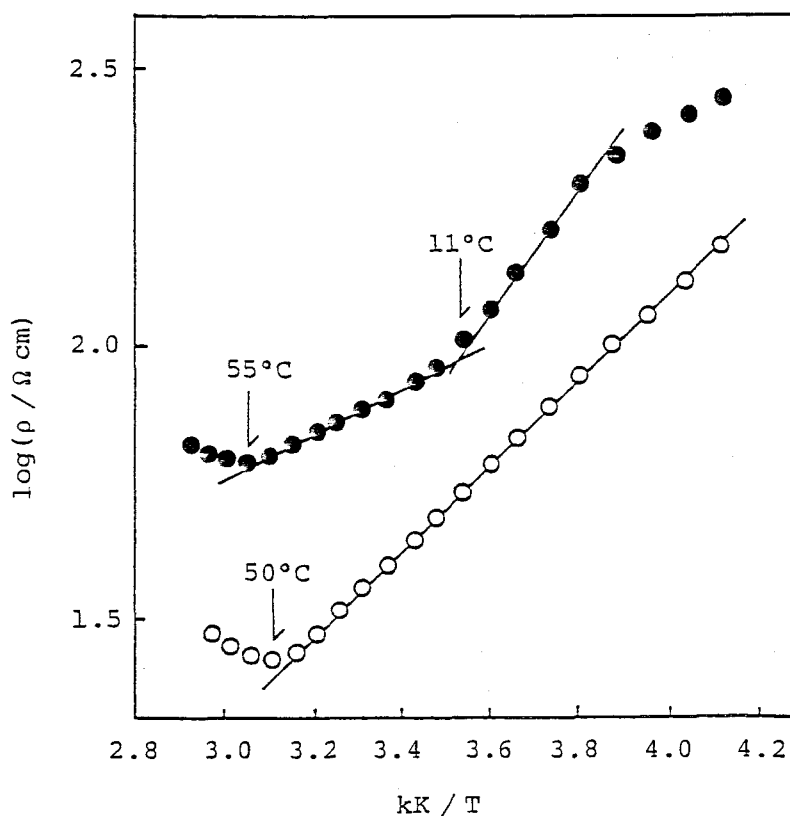


Figure 8. Temperature dependence of electrical resistivities of the crystal of $2a-I$ along the b axis (●) and $2a-II$ along the c axis (○).

$\underline{\underline{lc}}$, and $\underline{\underline{ld}}$ in the solid state as well as the spectrum of $\underline{\underline{lc}}$ in acetonitrile. The solid state spectrum of $\underline{\underline{lc}}$ is very similar in appearance to the solution spectrum of this salt, indicating that the $\text{TCNQ}^{\cdot-}$ radical anion in solid $\underline{\underline{lc}}$ may exist as a monomer. This is compatible not only with a large paramagnetism but also with a high resistivity of $\underline{\underline{lc}}$ in the solid state (Table 5). Thus, $\underline{\underline{lc}}$ is suggested to exist as alternate stacks of the $[\text{Si}(\text{Bu}^t\text{C}(\text{O})\text{CHC}(\text{O})-\text{Bu}^t)_3]^+$ cation and $\text{TCNQ}^{\cdot-}$ radical anion. Both $\underline{\underline{la}}$ and $\underline{\underline{ld}}$ display a moderate intense band around 14500 cm^{-1} assignable to the $(\text{TCNQ})_2^{2-}$ dimer^{34,35} in accordance with the diamagnetism of these salts at room temperature, though the diamagnetic susceptibilities are small (Table 5). In addition, the spectrum of $\underline{\underline{la}}$ shows a distinct band due to charge transfer (CT) transition between the $\text{TCNQ}^{\cdot-}$ radical

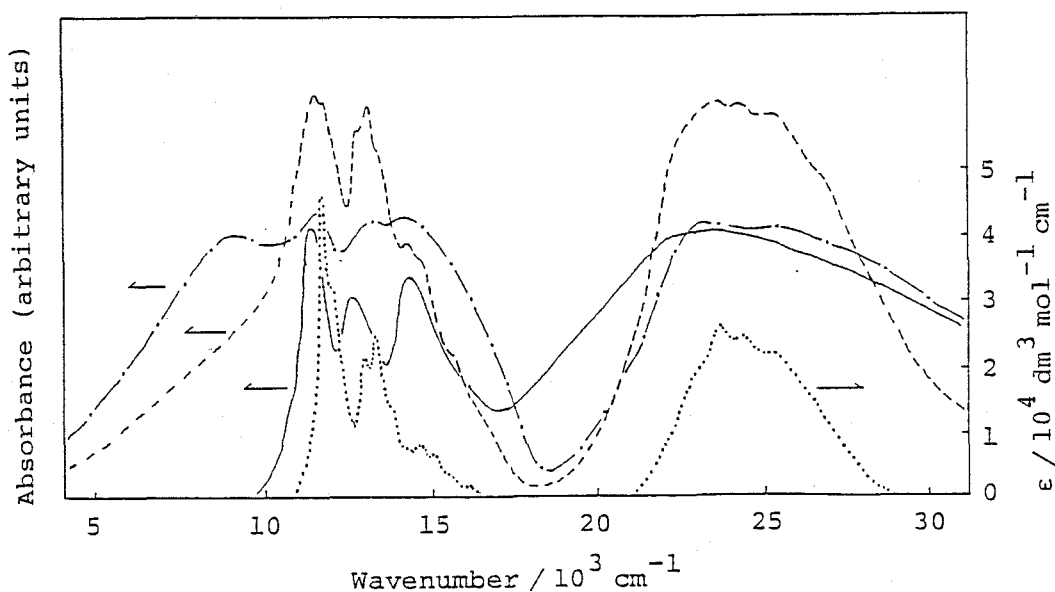


Figure 9. Absorption spectra of $\underline{\underline{la}}$ (---), $\underline{\underline{lc}}$ (---), and $\underline{\underline{ld}}$ (—) in the solid states (nujol mulls), and $\underline{\underline{lc}}$ (-----) in acetonitrile.

anions³³ around 9000 cm^{-1} , while no corresponding band is observed in the spectrum of 1d. On the other hand, these two salts exhibit two absorption bands without fine structure around 11500 and 13000 cm^{-1} which may be assigned to transitions to the first locally excited (LE_1) state of monomeric $TCNQ^{\cdot-}$ radical anions.³⁵ These spectral features are unusual in $TCNQ^{\cdot-}$ radical anion salts and suggest that the $TCNQ^{\cdot-}$ radical anion essentially exists as dimers, though the CT interaction may be extremely weak, particularly in 1d. This assumption explains the small diamagnetic susceptibilities of 1a and 1d (Table 5).

Figure 10 shows the electronic absorption spectra of complex salts 2a-I and 2d in the solid state. The spectral appearance of 2a-I resembles well those of most 1:2 complex salts of TCNQ such as $(Et_3NH)^+(TCNQ)_2^{\cdot-}$,³⁵ $(MePh_3P)^+(TCNQ)_2^{\cdot-}$,³⁴ and $(SCH_2CH_2SCNMe_2)^+ (TCNQ)_2^{\cdot-}$,¹⁵ which were reported to involve the monomeric $TCNQ^{\cdot-}$

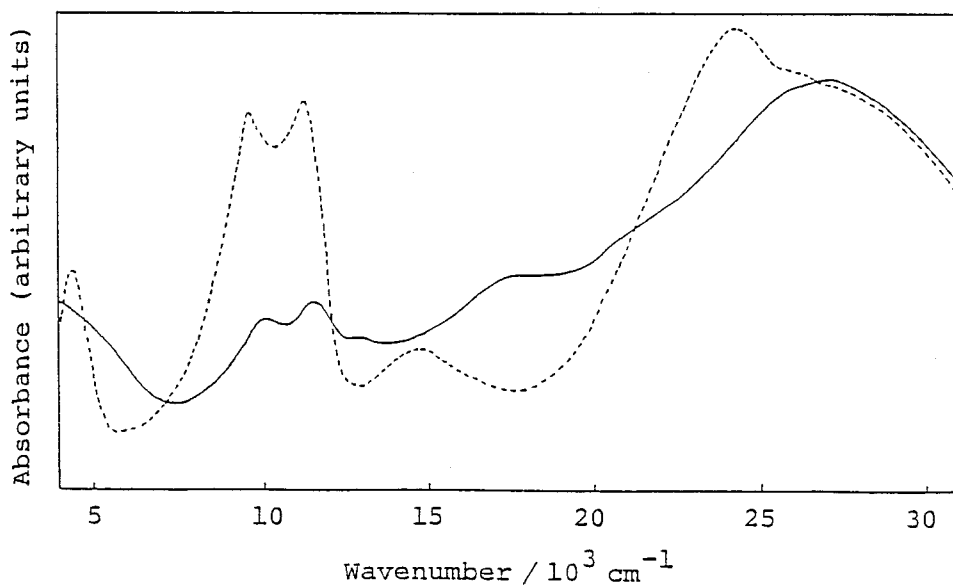


Figure 10. Absorption spectra of 2a-I (—) and 2d (-----) in the solid states (nujol mulls).

radical anion as well as neutral TCNQ in a columnar structure. Such a spectral feature is consistent with the paramagnetic property of 2a-I at room temperature. In addition, 2a-I exhibited a very broad absorption band in the infrared region assignable to the CT transition between the partially negatively charged TCNQ species,³⁵ which is compatible with a relatively low resistivity of this salt. It is noteworthy that the bands due to the monomeric $\text{TCNQ}^{\cdot-}$ radical anion are much stronger in 2d (9500 and 10500 cm^{-1}) than in 2a-I (10000 and 11500 cm^{-1}), and the CT band between the $\text{TCNQ}^{\cdot-}$ moieties³⁴ of 2d (4500 cm^{-1}) occurs at a higher energy than that of 2a-I (below 4000 cm^{-1}). These observations indicate that the CT interaction between the TCNQ moieties in 2d is weaker than in 2a-I . This is consistent with the fairly high resistivity of 2d (see Table 5).

Complex salts 2a-II , 2b , and 3d with compositions 1:2, 1:3, and 1:2.5, respectively, exhibited spectra very similar to 2a-I .

5. Summary

Several 7,7,8,8-tetracyano-*p*-quinodimethane (TCNQ) radical anion salts with tris(β -diketonato)siliconium(IV) cations were prepared; $[\text{Si}(\text{MeC}(\text{O})\text{CHC}(\text{O})\text{Me})_3]^+ \text{TCNQ}^{\cdot-} \cdot \text{C}_6\text{H}_6$, $[\text{Si}(\text{Bu}^t\text{C}(\text{O})\text{CHC}(\text{O})\text{Bu}^t)_3]^+ \text{TCNQ}^{\cdot-}$, $[\text{Si}(\text{PhC}(\text{O})\text{CHC}(\text{O})\text{Ph})_3]^+ \text{TCNQ}^{\cdot-}$, $[\text{Si}(\text{MeC}(\text{O})\text{CHC}(\text{O})\text{ME})_3]^+ (\text{TCNQ})_2^{\cdot-}$, $[\text{Si}(\text{MeC}(\text{O})\text{C}(\text{Et})\text{C}(\text{O})\text{Me})_3]^+ (\text{TCNQ})_3^{\cdot-}$, and $[\text{Si}(\text{PhC}(\text{O})\text{CHC}(\text{O})\text{Ph})_3]^+ (\text{TCNQ})_n^{\cdot-}$ ($n = 2$ and 2.5). For $[\text{Si}(\text{MeC}(\text{O})\text{CHC}(\text{O})\text{Me})_3]^+ (\text{TCNQ})_2^{\cdot-}$, monoclinic and triclinic crystals were obtained by recrystallization from acetonitrile. The monoclinic crystals belong to the space group $P2_1/a$ with $a = 34.981(5)$, $b = 13.543(2)$, $c = 7.837(1)$ Å, $\beta = 95.15(1)^\circ$, $U = 3698(1)$ Å³, $Z = 4$, and $D_c = 1.318(1)$ g cm⁻³.

The X-ray structure was solved by the direct method and refined to final R value of 0.064 for 4610 independent reflections with $|F_o| > 3\sigma(F)$. TCNQ molecules stack in columns along the b axis, consisting of tetramer units with the mean interplanar spacing of 3.14 (A/A'), 3.21 (B/B'), and 3.34 Å (A/B). Adjacent columns form sheets parallel to the bc plane and successive sheets are separated along the a axis by the cation moieties. The triclinic crystals belong to the space group $P\bar{1}$ with $a = 7.941(2)$, $b = 33.04(1)$, $c = 7.775(1)$ Å, $\alpha = 95.92(2)$, $\beta = 98.55(3)$, $\gamma = 76.86(2)^\circ$, $V = 1959.3$ 1959.3(8) Å³, $Z = 2$, and $D_c = 1.244(1)$ g cm⁻³. In the X-ray structure analysis for this salt by the direct method, the refinement was limited with an R value of 0.24 for 2724 independent reflections with $|F_o| > 3\sigma(F)$, where the positions of the cation moiety and one of two independent TCNQ molecules were determined, the other TCNQ molecule being not clarified owing to a large disorder. The stacks of TCNQ molecules in all the salts obtained are discussed on the basis of electronic absorption spectra and magnetic susceptibilities. Electrical resistivities of the simple and complex TCNQ⁻ salts fall in the ranges $10^6 - 10^8$ and $10^1 - 10^4$ Ω cm, respectively, for the compacted samples at 298 K. Anisotropy of the resistivities was determined for two kinds of crystals of $[\text{Si}(\text{MeC}(\text{O})\text{CHC}(\text{O})\text{Me})_3]^+(\text{TCNQ})_2^-$.

5. References

- 1 D. S. Acker, R. J. Harder, W. R. Hertler, W. Mahler, L. R. Melby, R. E. Benson, and W. E. Mochel, *J. Am. Chem. Soc.*, 1960, 82, 6408.
- 2 J. B. Torrance, *Acc. Chem. Res.*, 1979, 12, 79
- 3 T. Iinuma and T. Tanaka, *Inorg. Chim. Acta*, 1981, 49, 79.

- 4 L. R. Melby, R. J. Harder, W. R. Hertler, W. Mahler, R. E. Benson, and W. E. Mochel, *J. Am. Chem. Soc.*, 1962, 84, 3374.
- 5 W. J. Siemons, P. E. Bierstedt, and R. G. Kepler, *J. Chem. Phys.*, 1963, 39, 3523.
- 6 S. Araki and T. Tanaka, *Bull. Chem. Soc. Jpn.*, 1978, 51, 1311.
- 7 R. Harms, H. J. Keller, D. Nöthe, and D. Wehe, *Acta Crystallogr.*, 1982, B38, 2838.
- 8 C. J. Fritchie, Jr. and P. Arthur, Jr., *Acta Crystallogr.*, 1966, 21, 139.
- 9 T. Sundaresan and S. C. Wallwork, *Acta Crystallogr.*, 1972, B28, 491.
- 10 Y. Yumoto and T. Tanaka, *Chem. Lett.*, 1980, 123.
- 11 G. J. Ashwell, D. W. Allen, G. H. Cross, D. A. Kennedy, and I. W. Nowell, *Solid State Commun.*, 1982, 43, 731.
- 12 M. Lequan, R. M. Lequan, P. Betall, J. F. Halet, and L. Ouahab, *Tetrahedron Lett.*, 1983, 24, 3107.
- 13 Bert van Bodegom, *Acta Crystallogr.*, 1981, B37, 857, and references therein.
- 14 W. Dilthey, *Berichte*, 1903, 36, 923.
- 15 S. Araki, H. Ishida, and T. Tanaka, *Bull. Chem. Soc. Jpn.*, 1978, 51, 407.
- 16 P. Main, S. E. Hull, L. Lessinger, G. Germain, J-P. Declercq and M. M. Woolfson, A System of Computer Programs for the Automatic Solution of Crystal Structures from X-ray Diffraction Data, MULTAN 78, University of York, 1978.
- 17 'International Table for X-Ray Crystallography,' vol. IV, Kynoch Press, Birmingham (1974).
- 18 C. K. Johnson. ORTEP-II: A FORTRAN Thermal-Ellipsoid Plot Program for Crystal Structure Illustrations, ORNL-5138, March 1976. Oak Ridge National Laboratory.

- 19 T. E. Phillips, T. J. Kistenmacher, J. P. Ferraris, and D. O. Cowan, *J. Chem. Soc., Chem. Commun.* 1973, 471.
- 20 T. J. Kistenmacher, T. E. Phillips, and D. O. Cowan, *Acta Crystallogr.*, 1974, B30, 763.
- 21 A. T. McPhail, G. M. Semeniuk, and D. B. Chesut, *J. Chem. Soc. A*, 1971, 2174.
- 22 Beat van Bodegom and Jan L. De Boer, *Acta Crystallogr.*, 1981, B37, 119.
- 23 G. J. Ashwell, *Phys. Status Solidi B*, 1978, 86, 705.
- 24 G. J. Ashwell, G. H. Cross, D. A. Kennedy, I. W. Nowell, and J. G. Allen, *J. Chem. Soc., Perkin Trans. 2*, 1983, 1787.
- 25 J. D. Wright and Z. A. Ahmad, *Acta Crystallogr.*, 1981, B37, 1848.
- 26 R. E. Long, R. A. Sparks, and K. N. Trueblood, *Acta Crystallogr.*, 1965, 18, 932.
- 27 M. Konno and Y. Saito, *Acta Crystallogr.*, 1974, B30, 1294.
- 28 M. Konno, T. Ishii, and Y. Saito, *Acta Crystallogr.*, 1977, B33 763.
- 29 A. Hoekstra, T. Spoelder, and A. Vos, *Acta Crystallogr.*, 1972, B28, 14.
- 30 P. S. Flandrois and D. Chasseau, *Acta Crystallogr.*, 1977, B33, 2744.
- 31 T. Ito, K. Toriumi, F. B. Ueno, and K. Saito, *Acta Crystallogr.*, 1980, B36, 2998.
- 32 J. E. Huheey, 'Inorganic Chemistry, Principles of Structure and Reactivity,' 2nd ed., Haper & Row Publishers. New York, 1979, p. 71.
- 33 2×10^5 , 3×10^4 , 5×10^3 , and $3 \times 10^4 \Omega \text{ cm}$ for $M^+ \text{TCNQ}^-$, where $M = \text{Li, Na, K, and Cs}$ respectively, ref. 4.
- 34 Y. Iida, *Bull. Chem. Soc. Jpn.*, 1969, 42, 71; 637.

35 J. Tanaka, M. Tanaka, T. Kawai, T. Takabe, and O. Maki,
Bull. Chem. Soc. Jpn., 1976, 49, 2358.

CHAPTER 2

SYNTHESES AND ELECTRICAL PROPERTIES OF TTF AND TSF SALTS WITH OXALATO-METALLATE ANIONS

2-1

TRIS(OXALATO)SILICATE(IV), -GERMATE(IV), AND -STANNATE(IV) ANION SALTS

1. Introduction

Low-dimensional organic crystals containing the radical cations of tetrathiafulvalene (TTF), tetraselenafulvalene (TSF), and their derivatives have been investigated extensively.¹ Among these, tetramethyltetraselenafulvalene (TMTSF) salts with cubic inorganic anions, $(\text{TMTSF})_2\text{X}$ ($\text{X}^- = \text{ClO}_4^-, \text{ReO}_4^-, \text{PF}_6^-, \text{SbF}_6^-, \text{and TaF}_6^-$), have been shown to exhibit metallic conductivities and to transfer to a superconducting state around 1 K under atmospheric or high pressures.² On the other hand, there have been reported some TTF salts with planar metal chelate anions,³⁻⁷ such as bis(dithiolene)metal anions, whose electrical resistivities fall in the range of semiconductors more than $1 \times 10^3 \Omega \text{ cm}$.³⁻⁶ Thus the author undertook to study on TTF and TSF salts with cubic metal chelate anions; no such TTF and TSF salts has been reported so far.

This section deals with the preparations and electrical resistivities of TTF and TSF salts with tris(oxalato)metallate anions, $\text{M}(\text{OX})_3^{2-}$ ($\text{M} = \text{Si, Ge, and Sn; OX}^{2-} = \text{C}_2\text{O}_4^{2-}$). The stack of these salts in the crystalline state are discussed on the basis of electronic and ESR spectra, and on magnetic susceptibilities.

2. Experimental

Materials. Tetrathiafulvalene (TTF),⁸ tetraselenafulvalene (TSF),⁹ tetrathiafulvalenium tetrafluoroborate, $[\text{TTF}]_3[\text{BF}_4]_2$,¹⁰ and tetraselenafulvalenium tetrafluoroborate, $[\text{TSF}]_3[\text{BF}_4]_2$,¹¹ were prepared according to the literature. Bis(tetrabutylammonium) tris(oxalato)silicate, $[\text{Bu}^n_4\text{N}]_2[\text{Si}(\text{OX})_3]$, and bis(tetraethylammonium) tris(oxalato)germate and -stannate, $[\text{Et}_4\text{N}]_2[\text{Ge}(\text{OX})_3]$ and $[\text{Et}_4\text{N}]_2[\text{Sn}(\text{OX})_3]$, were obtained by the modified literature methods.¹²

Preparation of Tetrathia- and Tetraselenafulvalenium Tris(oxalato)metallates. An acetonitrile (10 cm³) solution of $[\text{Bu}^n_4\text{N}]_2[\text{Si}(\text{OX})_3]$ (150 mg, 0.19 mmol) was added to an acetonitrile (50 cm³) solution of $[\text{TTF}]_3[\text{BF}_4]_2$ (140 mg, 0.18 mmol) under nitrogen atmosphere and the mixture was allowed to stand in a refrigerator overnight. The resulting black microcrystals of $[\text{TTF}]_2[\text{Si}(\text{OX})_3] \cdot 0.5\text{MeCN}$ (1) were collected by filtration and dried *in vacuo*, 75 % yield. The involvement of acetonitrile was confirmed by the ¹H NMR spectrum. The reaction of $[\text{Et}_4\text{N}]_2[\text{Ge}(\text{OX})_3]$ with $[\text{TTF}]_3[\text{BF}_4]_2$ in acetonitrile similarly afforded dark brown microcrystals of $[\text{TTF}]_2[\text{Ge}(\text{OX})_3] \cdot 0.5\text{MeCN}$ (2) in an 83 % yield, whereas black microcrystals of $[\text{TTF}]_{2.8}[\text{Sn}(\text{OX})_3]$ (3a) were obtained in a 64 % yield by the reaction of $[\text{Et}_4\text{N}]_2[\text{Sn}(\text{OX})_3]$ with $[\text{TTF}]_3[\text{BF}_4]_2$ in the same solvent. On the other hand, $[\text{TSF}]_3[\text{BF}_4]_2$ reacted with $[\text{Bu}^n_4\text{N}][\text{Si}(\text{OX})_3]$, $[\text{Et}_4\text{N}]_2[\text{Ge}(\text{OX})_3]$, and $[\text{Et}_4\text{N}]_2[\text{Sn}(\text{OX})_3]$ in acetonitrile to give $[\text{TSF}]_2[\text{Si}(\text{OX})_3]$ (4) $[\text{TSF}]_2[\text{Ge}(\text{OX})_3] \cdot 0.5\text{MeCN}$ (5b), and $[\text{TSF}]_2[\text{Sn}(\text{OX})_3]$ (6) as black microcrystals, in 68, 47, and 59 % yields, respectively.

Electrocrystallization. An acetonitrile (10 cm^3) solution both containing TTF (24 mg, 0.12 mmol) and $[\text{Et}_4\text{N}]_2[\text{Sn}(\text{OX})_3]$ (300 mg, 0.47 mmol) was subjected to controlled current ($I = 5\text{ }\mu\text{A}$) electrolysis in a cell with two platinum ($0.3\text{ mm } \phi$) electrodes under nitrogen atmosphere for 10 days. Black microcrystals of $[\text{TTF}]_{2.8}^+[\text{Sn}(\text{OX})_3] \cdot 0.5\text{MeCN}$ (3b) thus produced on the anode were collected and dried *in vacuo* (6 mg). The electrolysis of an acetonitrile solution containing TSF and $[\text{Et}_4\text{N}]_2[\text{Ge}(\text{OX})_3]$ under the same conditions afforded black microcrystals of $[\text{TSF}]_2[\text{Ge}(\text{OX})_3]$ (5a). Electrocrystallization from an acetonitrile solution containing TSF and $[\text{Bu}_4^{\text{n}}\text{N}]_2[\text{Si}(\text{OX})_3]$ or $[\text{Et}_4\text{N}]_2[\text{Sn}(\text{OX})_3]$, however, gave 4 or 6, which is the same product as that obtained in the reaction of $[\text{TSF}]_3[\text{BF}_4]_2$ with $[\text{Bu}_4^{\text{n}}\text{N}]_2[\text{Si}(\text{OX})_3]$ or $[\text{Et}_4\text{N}]_2[\text{Sn}(\text{OX})_3]$ in acetonitrile.

Analyses and melting points of the salts obtained are summarized in Table 1.

Physical Measurements. Electrical resistivities (ρ) were measured for compacted samples (about 10 mg) in the -25 to $+30\text{ }^\circ\text{C}$ range by the conventional two-probe method, as described previously.¹³ Electronic absorption spectra were recorded on a Union SM-401 spectrophotometer. Electronic powder reflectance spectra were measured with a Hitachi 340 spectrophotometer equipped with a Hitachi NIR (near IR) or R-10A (UV and visible) integrating sphere unit. X-ray photoelectron spectra were measured as described elsewhere.¹⁴ Magnetic susceptibilities were measured by the Gouy method at room temperature. ESR measurements were carried out using a JEOL-3X spectrometer.

Table 1. Analyses and melting points of TTF and TSF salts*

No.	Salt	Found (Calcd.) %			m.p. (dec.) °C
		C	H	N	
1 ~	[TTF] ₂ [Si(OX) ₃]·0.5MeCN	31.91 (31.64)	1.53 1.33	0.96 0.97)	> 195
2 ~	[TTF] ₂ [Ge(OX) ₃]·0.5MeCN	29.89 (29.89)	1.47 1.25	0.79 0.91)	> 200
3a ~	[TTF] _{2.8} [Sn(OX) ₃]	28.55 (28.68)	1.32 1.18)		> 185
3b ~	[TTF] _{2.8} [Sn(OX) ₃]·0.5MeCN	29.06 (29.31)	1.72 1.31	0.43 0.72)	> 180
4 ~	[TSF] ₂ [Si(OX) ₃]	19.80 (20.09)	1.08 0.75)		> 300
5a ~	[TSF] ₂ [Ge(OX) ₃]	19.01 (19.29)	1.04 0.72)		> 300
5b ~	[TSF] ₂ [Sn(OX) ₃]·0.5MeCN	19.94 (20.00)	1.03 0.85	0.56 0.61)	> 300
6 ~	[TSF] ₂ [Sn(OX) ₃]	18.55 (18.53)	1.06 0.69)		> 300

* 3b and 5a were prepared by electrocrystallization, and others by the reaction of [TTF]₃[BF₄]₂ and [TSF]₃[BF₄]₂ with [M(OX)₃] salts in acetonitrile.

3. Results and Discussion

Electrical Resistivities and Electronic Spectra. Temperature dependence of the specific resistivities of the TTF and TSF salts indicated that all the salts behave as a typical semiconductor in the temperature range measured (-25 to +30 °C). Table 2 lists the specific resistivities of the TTF and TSF salts at 25 °C ($\rho_{25\text{ °C}}$) and the activation energies (E_a) determined from the equation $\rho = \rho_0 \exp(E_a/kT)$, where ρ_0 , k , and T stand for a constant value, Boltzmann's constant, and the temperature, respectively, as well as their electronic reflectance spectra. The resistivities of the TTF salts obtained in this work ($10^4 - 10^5 \text{ } \Omega \text{ cm}$ at 25 °C) fall in the same range as those of TTF salts with bis(dithiolene)-metal complexes,³⁻⁶ which have been suggested to adopt the columnar structure of the TTF^+ radical cation in the crystals. The TSF salts obtained exhibit resistivities and activation energies smaller than the corresponding TTF salts. This is consistent with the lower charge transfer (CT) energy between the TSF^+ radical cations than between the TTF^+ radical cations, as described below. The involvement of acetonitrile molecules in the crystals causes an appreciable increase in the resistivity (Table 2). Differential thermal analyses of the salts containing acetonitrile molecules showed no desolvation of acetonitrile, even at around 150 °C. Thus, acetonitrile molecules may be located stably in the crystal lattice.

Figure 1 shows the powder reflectance spectra of 1 and 3a, together with the electronic absorption spectrum of 1 in acetonitrile. The solution spectrum exhibits bands at 29500, 22900 and 17200 cm^{-1} , due to the TTF^+ radical cation.¹⁵ Thus, the bands appeared in the $17000 - 35000 \text{ cm}^{-1}$ region of the reflectance

Table 2. Electrical resistivity (ρ), activation energy (E_a), and reflectance spectra of the TTF and TSF salts

Salt	$\rho_{25} \text{ } ^\circ\text{C} / \Omega \text{ cm}$	E_a / eV	LE band / 10^3 cm^{-1}			CT band / 10^3 cm^{-1}	
						D^\dagger/D^\ddagger^a	D^\dagger/D^0^a
1 ~	2.9×10^5	0.35	28.4	b	19.1	13.3	
2 ~	2.1×10^5	0.47	28.7	23.3	19.3	13.6	
3a ~ ~	3.9×10^4	0.43	27.3	b	19.4	13.6	8.9
3b ~ ~	1.2×10^5	0.41	27.7	b	19.2	12.8	8.9
4 ~	1.3×10^3	0.27	27.9	b	16.5	11.4	
5a ~ ~	2.9×10^4	0.28	27.8	b	16.1	12.3	
5b ~ ~	8.2×10^4	0.32	27.0	22.6	16.4	11.8	
6 ~	1.0×10^3	0.25	27.6	b	16.7	12.5	

^a D = TTF or TSF. ^b The position has not been determined, it being obscured by the high frequency bands.

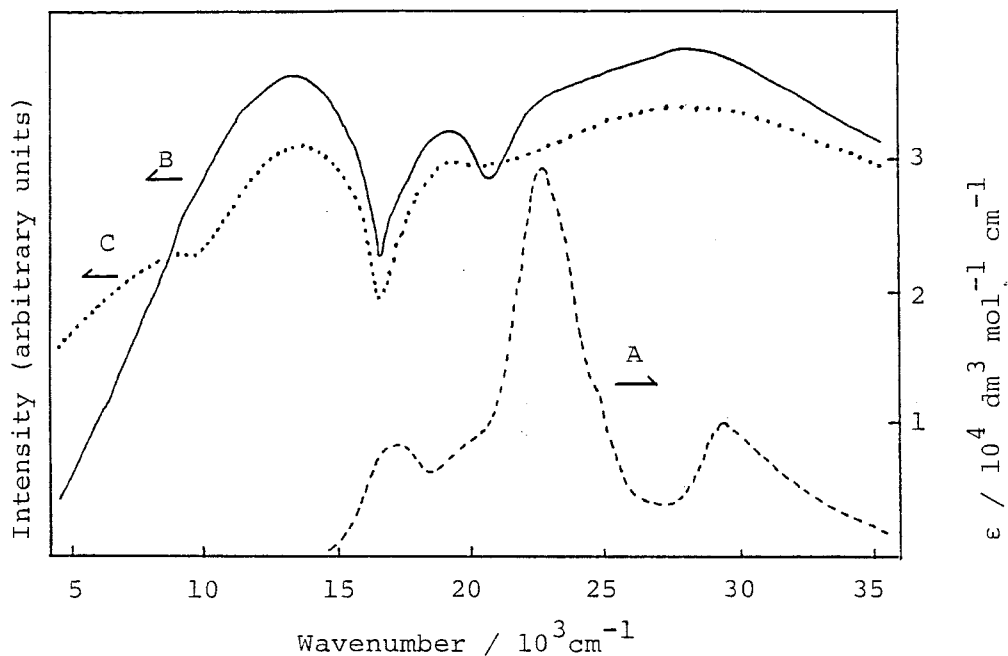


Figure 1. The absorption spectrum of 1 in acetonitrile (A), and the powder reflectance spectra of 1 (B) and 3a (C).

spectrum of 1 may be ascribed to the local excitation (LE) of TTF^+ , some of which are shifted to high frequencies on the salt formation. Such high frequency shifts have also been reported for the powder absorption spectrum of $(\text{TTF})\text{Cl}$ ¹⁶ and the polarized absorption spectrum of $(\text{TTF})\text{ClO}_4$.¹⁷ The band at 13300 cm^{-1} observed in the reflectance spectrum of 1 can reasonably be assigned to an inter-molecular CT transition in a TTF^+ dimer.^{16,17} Salt 2 exhibited a spectrum very similar to 1 (Table 2).

The spectrum of 3a in acetonitrile showed an absorption maximum at 31300 cm^{-1} , characteristic of neutral TTF in addition to three bands of TTF^+ whose frequencies are almost the same as those of 1 shown in Figure 1. The powder reflectance spectrum of 3a shows a band at 8900 cm^{-1} , assignable to a CT transition between the TTF^+ radical cation and neutral TTF,¹⁸ as well as that due to a CT

transition between the $\text{TTF}^{\cdot+}$ radical cations at 13600 cm^{-1} . Salt 3b also exhibits the bands due to the CT transitions, not only between two $\text{TTF}^{\cdot+}$ radical cations, but also between the $\text{TTF}^{\cdot+}$ radical cation and neutral TTF (Table 2). Thus, 3a and 3b are suggested to involve the stack of $\text{TTF}^{\cdot+}/\text{TTF}^{\cdot+}/\text{TTF}^0$ in the crystalline state. This is contrast to $[\text{TTF}]_3[\text{SnCl}_6]$, which contains the $\text{TTF}^{\cdot+}/\text{TTF}^0/\text{TTF}^{\cdot+}$ stack, as confirmed by the electronic reflectance spectrum and X-ray crystallographic analysis.¹⁹

All the TSF salts obtained here have the composition as simple salts, $[\text{TSF}]_2[\text{M}(\text{OX})_3]$ ($\text{M} = \text{Si}, \text{Ge}, \text{and Sn}$), with or without inclusion of acetonitrile. The powder reflectance spectra of those salts are very similar to the corresponding TTF simple salts, although all the LE and CT bands of the TSF salts appeared in lower frequencies than those of the TTF salts (Table 2). Thus, the present TSF salts may involve a $\text{TSF}^{\cdot+}$ radical cation dimer in the crystalline state. The binding energies of Sn $3d_{3/2}$ and $3d_{5/2}$ electrons for 3a (494.1 ± 0.2 and 485.6 ± 0.2 eV, respectively) and for 6 (494.2 ± 0.2 and 485.9 ± 0.2 eV, respectively) determined from the X-ray photoelectron spectra were very close to those of $[\text{Et}_4\text{N}]_2[\text{Sn}(\text{OX})_3]$ (494.5 ± 0.2 and 485.8 ± 0.2 eV, respectively). In view of this result, no appreciable charge transfer may occur between the $[\text{Sn}(\text{OX})_3]^{2-}$ anion and the $\text{TTF}^{\cdot+}$ or $\text{TSF}^{\cdot+}$ radical cation.

Magnetic Susceptibilities and Spectra. Except for 3b and 5a, whose amounts required for the measurement of magnetic susceptibilities have not been obtained by electrocrystallization, all the TTF and TSF salts exhibit diamagnetic properties at room temperature, as shown in Table 3. The magnetic susceptibilities obtained for the TTF and TSF salts are close to those of the corresponding tetraalkylammonium salts; $[\text{Bu}_4^{\text{n}}\text{N}]_2[\text{Si}(\text{OX})_3]$

Table 3. Molar magnetic susceptibilities (χ_M)^a and ESR g values^b of the TTF and TSF salts

Salt	$\chi_M / \text{emu mol}^{-1}$	g_{max}	g_{int}	g_{min}
1	-1.4×10^{-4}	2.012	2.007	2.002
2	-4.1×10^{-4}	2.016	2.007	2.002
3a	-4.1×10^{-4}	2.016	2.007	2.002
4	-1.7×10^{-4}	2.067	2.022	1.995
5b	-3.8×10^{-4}	2.036	2.019	1.999
6	-4.0×10^{-4}	2.059	2.022	1.997

^a Measured at room temperature. ^b Measured at 77 K.

($-1.0 \times 10^{-4} \text{ emu mol}^{-1}$), $[\text{Et}_4\text{N}]_2[\text{Ge}(\text{OX})_3]$ ($-3.7 \times 10^{-4} \text{ emu mol}^{-1}$), and $[\text{Et}_4\text{N}]_2[\text{Sn}(\text{OX})_3]$ ($-4.0 \times 10^{-4} \text{ emu mol}^{-1}$), respectively. This is consistent with the fact that the TTF^+ and TSF^+ radical cations exist as dimers in the crystalline state as described above, except for 3a and 3b, which may involve the stack of $\text{TTF}^+/\text{TTF}^+/\text{TTF}^0$ in the crystalline state.

ESR spectra of the TTF and TSF salts (polycrystalline samples) at 77 K gave three kinds of weak signals with anisotropic g values (Table 3). Those values indicate that all the spins observed are associated with the TTF^+ and TSF^+ radical cations, which assume dimers through rather weak spin-pairing. The TTF salts, 1, 2, and 3a, have almost the same g values, which are also close to those of $[\text{TTF}]_3[\text{BF}_4]_2$ ($g_{\text{max}} = 2.0145$, $g_{\text{int}} = 2.0074$, $g_{\text{min}} = 2.0020$),¹¹ $[\text{TTF}]\text{Cl}_{0.9}$ ($g_{\text{max}} = 2.0127$, $g_{\text{int}} = 2.009$, $g_{\text{min}} = 2.0026$),¹¹ $[\text{TTF}]-[\text{CuS}_4\text{C}_4(\text{CF}_3)_4]$ ($g_{\text{max}} = 2.015$, $g_{\text{int}} = 2.007$, $g_{\text{min}} = 2.002$).²⁰ On the other hand, the TSF salts, 4, 5b, and 6, as well as $[\text{TSF}]_3[\text{BF}_4]_2$

($g_{\max} = 2.0551$, $g_{\text{int}} = 2.0196$, $g_{\min} = 1.9954$)¹¹ exhibit not only a somewhat wide variation in the anisotropic g values (in particular g_{\max}) with changing the counter anion, but also about five times broader signals than the TTF analogs. Such broad signals of the TSF salts may arise from an increasingly rapid spin-lattice relaxation associated with an effective spin-orbit coupling in the heavier Se atoms.^{21,22}

4. Summary

Several tetrathiafulvalene (TTF) and tetraselenafulvalene (TSF) salts of tris(oxalato)silicate, -germate, and -stannate, $[\text{TTF}]_x^- [\text{M}(\text{C}_2\text{O}_4)_3] \cdot n\text{MeCN}$ ($x = 2$ and $n = 0.5$ for $\text{M} = \text{Si}$ and Ge , and $x = 2.8$ and $n = 0$ for $\text{M} = \text{Sn}$) and $[\text{TSF}]_2 [\text{M}(\text{C}_2\text{O}_4)_3] \cdot n\text{MeCN}$ ($n = 0$ for $\text{M} = \text{Si}$, Sn and $n = 0.5$ for $\text{M} = \text{Ge}$), have been prepared by the reaction of $[\text{TTF}]_3 [\text{BF}_4]_2$ or $[\text{TSF}]_3 [\text{BF}_4]_2$ with $[\text{R}_4\text{N}]_2 [\text{M}(\text{C}_2\text{O}_4)_3]$ ($\text{R} = \text{Et}$ or Bu^n) in acetonitrile.

Electrocrystallization for the $\text{TTF}-[\text{Et}_4\text{N}]_2 [\text{Sn}(\text{C}_2\text{O}_4)_3]$ and $\text{TSF}-[\text{Et}_4\text{N}]_2 [\text{Ge}(\text{C}_2\text{O}_4)_3]$ systems in acetonitrile afforded $[\text{TTF}]_{2.8}^- [\text{Sn}(\text{C}_2\text{O}_4)_3] \cdot 0.5\text{MeCN}$ and $[\text{TSF}]_2 [\text{Ge}(\text{C}_2\text{O}_4)_3]$, respectively. Electrical resistivities of the TTF salts as compacted samples at 25 °C fall in the range $10^4 - 10^5 \Omega \text{ cm}$ and those of the TSF salts in the range $10^3 - 10^4 \Omega \text{ cm}$.

Electronic reflectance spectra of the TTF and TSF salts show bands at $13300 - 13600 \text{ cm}^{-1}$ and $11400 - 12500 \text{ cm}^{-1}$ due respectively to the $(\text{TTF}^+)_2$ and $(\text{TSF}^+)_2$ dimers. In addition, $[\text{TTF}]_{2.8}^- [\text{Sn}(\text{C}_2\text{O}_4)_3]$ exhibited a band at 8900 cm^{-1} , ascribed to a charge transfer transition between neutral TTF and the TTF^+ radical cation. All the salts display weakly diamagnetic properties, consistent with

the appearance of anisotropic weak ESR signals attributable to the TTF^+ and TSF^+ radical cations.

5. References

- 1 A. R. Siedle, G. A. Candela, T. F. Finnegan, R. P. Van Duyne, T. Cape, G. F. Koksza, P. M. Woyciejes, J. A. Hashmall, M. Glick, and W. Ilsley, *Ann. N. Y. Acad. Sci.*, 1978, 313.
- 2 K. Bechgaard, *Mol. Cryst. Liq. Cryst.*, 1982, 79, 1.
- 3 F. Wudl, C. H. Ho, and A. Nagel, *J. Chem. Soc., Chem. Commun.*, 1973, 923.
- 4 M. G. Miles and J. D. Wilson, *Inorg. Chem.*, 1975, 14, 2357.
- 5 P. Calas, J. M. Fabre, M. Khalife-El-Saleh, A. Mas, E. Torreilles, and L. Giral, *Tetrahedron Lett.*, 1975, 4475
- 6 L. V. Interrante, K. W. Browall, H. R. Hart, Jr., I. S. Jacobs, G. D. Warkins, and S. H. Wee, *J. Am. Chem. Soc.*, 1975, 97, 889.
- 7 G. C. Pavassiliou, *Mol. Cryst. Liq. Cryst.*, 1982, 86, 159.
- 8 L. R. Melby, H. D. Hartzler, and W. A. Sheppard, *J. Org. Chem.*, 1974, 39, 2456.
- 9 M. V. Lakshmikantham and M. P. Cava, *J. Org. Chem.*, 1976, 41, 882.
- 10 F. Wudl, *J. Am. Chem. Soc.*, 1975, 97, 1962.
- 11 W. M. Walsh, Jr., L. W. Rupp, Jr., F. Wudl, M. L. Kaplan, D. E. Schafer, G. A. Thomas, and R. Gemmer, *Solid State Commun.*, 1980, 33, 413.
- 12 V. G. Schott and D. Lange, *Z. Anorg. allgem. Chem.*, 1972, 391, 27.
- 13 S. Araki, H. Ishida, and T. Tanaka, *Bull. Chem. Soc. Jpn.*, 1978, 51, 407.
- 14 G. Matsubayashi, K. Kondo, and T. Tanaka, *Inorg. Chim. Acta.*, 1983, 69, 167.

- 15 S. Hünig, G. Kiesslich, H. Quast, and D. Scheutzow, *Justus Liebigs Ann. Chem.*, 1973, 310.
- 16 J. B. Torrance, B. A. Scott, B. Welber, F. B. Kaufman, and P. E. Sieden, *Phys. Rev. B*, 1979, 19, 730.
- 17 T. Sugano, K. Yakushi, and H. Kuroda, *Bull. Chem. Soc. Jpn.*, 1978, 51, 1041.
- 18 Similar assignments have been given for the $\sim 5000\text{ cm}^{-1}$ and $< 9000\text{ cm}^{-1}$ bands of $\text{TTF-Cl}_{0.80}$ and $\text{TTF-Br}_{0.71}$; ref. 16 and 17, respectively.
- 19 K. Kondo, G. Matsubayashi, T. Tanaka, H. Yoshioka, and K. Nakatsu, *J. Chem. Soc., Dalton Trans.*, 1984, 379.
- 20 J. W. Bray, H. R. Hart, Jr., L. V. Interrante, I. S. Jacobs, J. S. Kasper, G. D. Watkins, S. H. Wee, and J. C. Bonner, *Phys. Rev. Lett.*, 1975, 35, 744.
- 21 Y. Tomkiewicz, E. M. Engler, and T. D. Schltz, *Phys. Rev. Lett.*, 1975, 35, 456.
- 22 F. Wudl, D. E. Schafer, W. M. Walsh, Jr., L. W. Rupp, F. J. DiSalvo, J. V. Waszczak, M. L. Kaplan, and G. A. Thomas, *J. Chem. Phys.*, 1977, 66, 377.

PLANAR PLATINUM(II) AND COPPER(II) OXALATE ANION SALTS

1. Introduction

Tetrathiafulvalene (TTF) and tetraselenafulvalene (TSF) are known to form electrically conductive salts with several metal complex anions containing organic ligands.^{1,2} The previous section described the preparation of TTF and TSF salts with tris(oxalato)-metallate anions (metal = Si(IV), Ge(IV), and Sn(IV)) having a bulky configuration, which behave as semiconductors with specific resistivities of $1 \times (10^3 - 10^5) \Omega \text{ cm}$ as compacted samples at 25 °C.² On the other hand, the square-planar bis(oxalato)platinate anion as rubidium and potassium salts was reported to assume a columnar structure with a platinum-platinum interaction when partially oxidized and to exhibit a high electrical conductivity.³⁻⁵ Sodium, potassium, and ammonium bis(oxalato)cuprates also are known as polymers with metal-to-ligand intermolecular contacts in the anionic moieties.^{6,7} Thus, it may be of interest to study the electrical conduction of TTF and TSF salts with these planar bis(oxalato)-metallate anions in relation to the stack of TTF or TSF and the anionic moieties.

This section describes the preparation of TTF and TSF salts with planar bis(oxalato)platinate, dichloro(oxalato)platinate, and bis(oxalato)cuprate anions, and their electrical resistivities. The stack of the TTF or TSF molecule as well as the electronic interaction between TTF or TSF and the anionic moieties in the crystals is discussed based on electronic reflectance, X-ray photoelectron, and ESR spectra.

2. Experimental

Materials. TTF,⁸ TSF,⁹ [TTF]₃[BF₄]₂,¹⁰ [TSF]₃[BF₄]₂,¹¹ [NH₄]₂[Cu(OX)₂],⁶ and [Buⁿ₄N]₂[Pt(OX)₂]¹² (OX²⁻ = C₂O₄²⁻) were prepared according to the literature methods. [Buⁿ₄N]₂[Pt(OX)Cl₂] was obtained by the reaction of K₂PtCl₆ with K₂C₂O₄ at mole ratio 1:3 in water; the precipitate of K₂[Pt(OX)₂] produced¹² was filtered, and the filtrate was evaporated to a half-volume to give a red precipitate (1.4 g), which was collected by filtration and dissolved in water (10 cm³), followed by the addition of an aqueous solution (10 cm³) of [Buⁿ₄N]Br (1.9 g). A precipitate formed was dissolved in dichloromethane. Removal of the solvent afforded a pale red powder, which was washed with diethyl ether to give the product (0.73 g), m.p. 114 - 119 °C. Anal. Calcd for C₃₄H₇₂N₂O₄Cl₂Pt; C, 48.68; H, 8.65; N, 3.34; Cl, 8.45 %. Found: C, 48.31; H, 8.72; N, 3.41; Cl, 8.58 %.

Preparation of TTF and TSF salts. An acetonitrile (35 cm³) solution containing [TTF]₃[BF₄]₂ (47 mg, 60 μmol) and [Buⁿ₄N]₂⁻[Pt(OX)₂] (63 mg, 74 μmol) was allowed to stand in a refrigerator for several hours under nitrogen atmosphere. The resulting dark brown precipitate of [TTF]_{2.7}[Pt(OX)₂]·0.5MeCN (1) was filtered and dried *in vacuo*, 71 % yield based on [TTF]₃[BF₄]₂. Similarly, [TTF]_{2.7}[Pt(OX)Cl₂]·MeCN (2) was obtained in a 48 % yield by the reaction of [TTF]₃[BF₄]₂ with [Buⁿ₄N]₂[Pt(OX)Cl₂] in acetonitrile. [TSF]_{4.5}[Pt(OX)₂] (4) and [TSF]_{3.5}[Pt(OX)Cl₂] (5) also were prepared in 29 and 20 % yields, respectively, by the reaction of [TSF]₃⁻[BF₄]₂ with [Buⁿ₄N]₂[Pt(OX)₂] or [Buⁿ₄N]₂[Pt(OX)Cl₂] in acetonitrile. Analogous reactions of [NH₄]₂[Cu(OX)₂] in dimethyl sulfoxide with [TTF]₃[BF₄]₂ and [TSF]₃[BF₄]₂ in acetonitrile afforded

$[\text{TTF}]_3[\text{Cu}(\text{OX})_2] \cdot 1.5\text{Me}_2\text{SO}$ (3) and $[\text{TSF}]_3[\text{Cu}(\text{OX})_2] \cdot 2\text{Me}_2\text{SO}$ (6) in 50 and 64 % yields, respectively. Mole ratios of the TTF^+ radical cation to neutral TTF^0 in the salts obtained were determined not only by electronic absorption spectra in MeCN or in Me_2SO but also by elemental analyses. The involvement of solvent molecules in the salts was confirmed by ^1H NMR spectra in conc. HNO_3 .

Properties and analytical data for the TTF and TSF salts are listed in Table 1.

Physical Measurements. Powder electronic reflectance,² ESR,² and X-ray photoelectron spectra¹³ were recorded as described elsewhere. Electrical resistivities were measured as compacted samples by the conventional two-probe method.¹⁴

3. Results and Discussion

Electrical Resistivity. All the salts obtained behave as semiconductors in the temperature range measured; -40 to +50 °C. The resistivities (ρ) at 25 °C measured for compacted samples and activation energies (E_a) for the electrical conduction calculated from the equation $\rho = \rho_0 \exp(E_a/kT)$ are summarized in Table 2, which lists also electronic reflectance and ESR spectral data of the salts. The $\rho_{25\text{ }^\circ\text{C}}$ values of the TTF and TSF salts are in the order of $10^2 - 10^4 \text{ } \Omega \text{ cm}$, suggesting a columnar structure of the TTF^+ or TSF^+ radical cation and its neutral molecule in the crystals. These values are somewhat smaller than $\rho_{25\text{ }^\circ\text{C}}$ for tris(oxalato)metallate anion simple salts of TTF and TSF ($1 \times (10^3 - 10^5) \text{ } \Omega \text{ cm}$),² which may be due to the fact that all the present salts contain both neutral TTF or TSF as well as the TTF^+ or TSF^+ radical cation.

Table 1. Properties and analyses of the TTF and TSF salts

No.	Salt	Color	m.p. (dec.) / °C	Found (Calcd) *	
				% C	% H
1 ~	[TTF] _{2.7} [Pt(OX) ₂]·0.5MeCN	Dark brown	> 300	26.74 (26.99)	1.55 (1.31)
2 ~	[TTF] _{2.7} [Pt(OX)Cl ₂]·MeCN	Brown	> 145	25.21 (25.63)	1.78 (1.47)
3 ~	[TTF] ₃ [Cu(OX) ₂]·1.5Me ₂ SO	Brown	195 - 197	30.45 (30.96)	2.19 (2.18)
4 ~	[TSF] _{4.5} [Pt(OX) ₂]	Dark green	> 300	17.46 (17.44)	1.11 (0.85)
5 ~	[TSF] _{3.5} [Pt(OX)Cl ₂]	Dark green	> 300	15.95 (16.00)	1.09 (1.82)
6 ~	[TSF] ₃ [Cu(OX) ₂]·2Me ₂ SO	Dark green	> 300	19.16 (19.87)	1.52 (1.51)

* % N: 0.64 (0.74) for 1 and 1.55 (1.48) for 2.

Table 2. Electrical resistivities ($\rho_{25} \text{ }^{\circ}\text{C}$), activation energies (E_a), and powder reflectance and ESR spectra of the TTF and TSF salts

Salt	$\rho_{25} \text{ }^{\circ}\text{C}/\Omega \text{ cm}$	E_a/eV	LE band of D^a			CT band/ 10^3 cm^{-1}		ESR parameter of $D^{a,b}$		
			10^3 cm^{-1}			$D^{\dagger}/D^{\ddagger a}$	$D^{\dagger}/D^0 a$	g_{max}	g_{int}	g_{min}
1	1.2×10^3	0.25	29.0	c	18.5	13.1	8.8	2.015	2.008	2.000
2	2.6×10^4	0.40	29.5	c	18.4	13.2	8.6		2.010	
3	9.3×10^3	0.18	29.4	24.8	20.0	14.0	8.9		2.006 ^d	
4	7.2×10^2	0.18	27.9	24.9	16.6	12.3	8.8	2.061	2.018	1.998
5	5.8×10^2	0.10	27.5	22.5	16.5	11.8	8.8	2.065	2.024	1.998
6	2.1×10^3	0.12	27.9	22.7	16.7	10.5	8.7		2.009 ^d	

^a D = TTF or TSF. ^b Measured at 77 K. ^c Observed by the higher frequency bands.

^d See the text for signals due to the $[\text{Cu}(\text{OX})_2]^{2-}$ moiety.

In addition, the planar metallate anions may be more favorable than the tris(oxalato)metallate anions with octahedral configurations for the stack of the donor molecules. The TSF salts exhibit resistivities and activation energies smaller than the corresponding TTF salts. This is consistent with the observation that the charge transfer (CT) energy between the TSF⁺ radical cations is smaller than that between the TTF⁺ radical cations, as described below.

Configurations of the Salts. Figure 1 shows the electronic reflectance spectra of salts 1 and 4. The two bands around 18500 and 30000 cm⁻¹ observed in 1 may be ascribed to local electronic excitations of both the TTF⁺ radical cation and neutral TTF⁰. The bands around 13100 and 8800 cm⁻¹ are reasonably assigned to CT

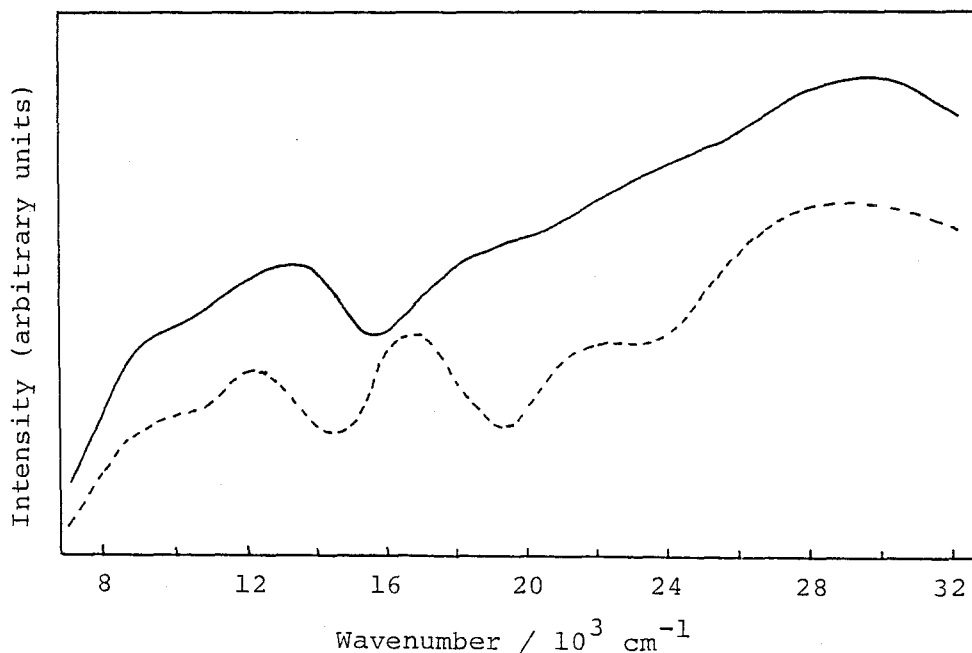


Figure 1. Powder reflectance spectra of 1 (—) and 4 (---).

transitions between the $\text{TTF}^{\cdot+}$ radical cations¹⁵ and between $\text{TTF}^{\cdot+}$ and TTF^0 ,¹⁶ respectively. Similar spectra were observed in salts 2 and 3. Salt 4 exhibits the corresponding two bands; CT transitions between $\text{TSF}^{\cdot+}$ and TSF^+ , and between $\text{TSF}^{\cdot+}$ and TSF^0 around 12300 and 8800 cm^{-1} , respectively. Similar spectra were observed also in salts 5 and 6 (Table 2). These findings suggest the columnar structure of donor molecules which involves both the $\text{D}^{\cdot+}/\text{D}^+$ and $\text{D}^{\cdot+}/\text{D}^0$ ($\text{D} = \text{TTF}$ and TSF) arrangements. Such a structure is compatible with considerably low resistivities of those salts, as mentioned above.

Table 3 lists the binding energies of Pt $4f_{5/2}$ and $4f_{7/2}$ electrons of two TTF salts, 1 and 2, and related platinum(II and IV) complexes obtained from X-ray photoelectron spectra (XPS); the TSF salts, 4 and 5, have been unsuccessful to obtain well-resolved XPS spectra. The binding energies of Pt $4f_{5/2}$ and $4f_{7/2}$ electrons in the TTF salts are fairly smaller (1.1 - 1.4 eV) than those in the tetrabutylammonium salts of $[\text{Pt}^{\text{II}}(\text{OX})_2]^{2-}$ and $[\text{Pt}^{\text{II}}(\text{OX})\text{Cl}_2]^{2-}$ anions, and much smaller than those of $\text{K}_2\text{Pt}^{\text{IV}}\text{Cl}_6$. This result

Table 3. Binding energies (eV) of the Pt $4f_{5/2}$ and $4f_{7/2}$ electrons of some platinum(II and IV) salts

Salt	Pt $4f_{5/2}$	Pt $4f_{7/2}$
$[\text{TTF}]_{2.7}[\text{Pt}(\text{OX})_2] \cdot 0.5\text{MeCN}$	74.3	70.9
$[\text{Bu}^n_4\text{N}]_2[\text{Pt}(\text{OX})_2]$	75.5	72.3
$[\text{TTF}]_{2.7}[\text{Pt}(\text{OX})\text{Cl}_2] \cdot \text{MeCN}$	73.9	70.4
$[\text{Bu}^n_4\text{N}]_2[\text{Pt}(\text{OX})\text{Cl}_2]$	75.2	71.5
K_2PtCl_6	79.0	75.6

indicates that the platinum(II) moieties in the TTF salts are somewhat reduced through a transfer of some negative charges from the TTF moieties. Such a reduced species is in contrast to partially oxidized $[\text{Pt}(\text{OX})_2]^{2-}$ which form anion stacks exhibiting high electrical conductivities.³⁻⁵ A similar negative charge transfer from TTF^+ and/or TTF^0 moieties to metal-containing anions has been reported to occur also for $[\text{TTF}]_3[\text{SnCl}_6]$, $[\text{TTF}]_3[\text{SnMe}_2\text{Cl}_4]$, and $[\text{TTF}][\text{SnMe}_2\text{Cl}_3]$.¹⁷

The TTF and TSF salts with uni- and bis(oxalato)platinate exhibited anisotropic weak ESR signals at 77 K, though the signal of salt 2 has been isotropic, indicating that all the spins observed are ascribed to TTF^+ and TSF^+ radical cations forming dimers through a weak spin-pairing. The g values obtained (Table 2) are close to those of the TTF and TSF salts with tris(oxalato)silicate, -germate, and -stannate anions reported previously.²

The NH_4^+ and Na^+ salts of $[\text{Cu}(\text{OX})_2]^{2-}$ are known to assume an infinite columnar structure which involves a face-to-face weak interaction among the anion moieties, and to give ESR signals at $g = 2.31$ and $g = 2.08$ together with a weak signal around 1600 G.^{6,7} On the other hand, the powder spectrum of salt 3 exhibits signals due to the $[\text{Cu}(\text{OX})_2]^{2-}$ anion with an extremely anisotropic mode at $g_1 = 2.321$, $g_2 = 2.112$, and $g_3 = 1.855$ (Figure 2) in addition to a weak signal due to the TTF^+ radical cation exhibiting as a weakly interacting dimer at $g = 2.006$. The occurrence of the signal with such a low g_3 value suggests the presence of a dimeric species of $[\text{Cu}(\text{OX})_2]^{2-}$ with a weak interaction between two anions rather than any polymeric ones, as was reported for $[\text{Cu}(\text{pip})_2]_2(\text{im})(\text{NO}_3)_3$ (pip = 2-[(2-(2pyridyl)ethylimino)methyl]pyridine and im = imidazolate anion).¹⁸ The appearance of the half band due to $\Delta M = \pm 2$ at 1600 G is compatible with the interaction

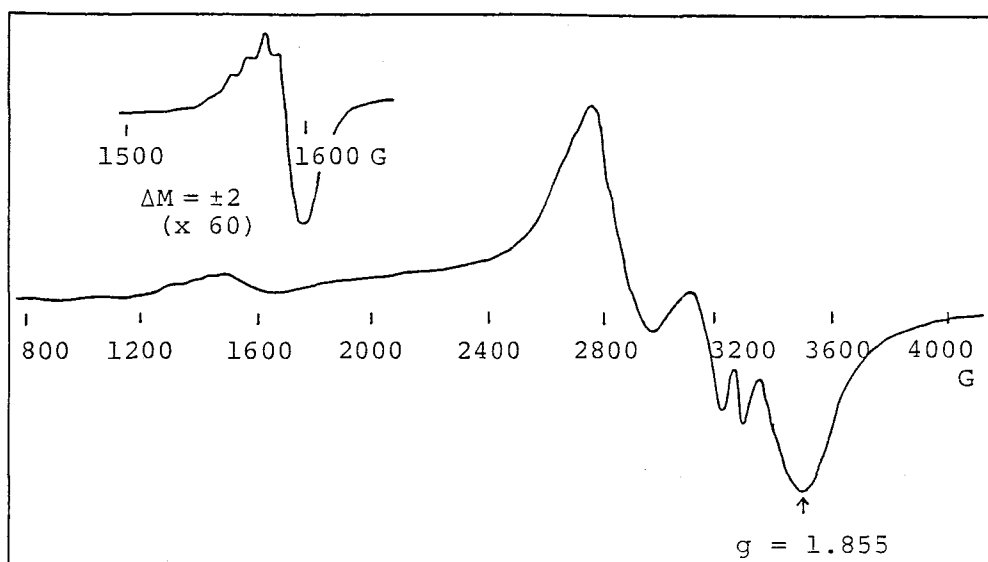


Figure 2. The powder ESR spectrum of 3 at 77 K.

between two copper(II) ions in the dimeric species. The TSF salt 6 also gave anisotropic signals due to the $[\text{Cu}(\text{OX})_2]^{2-}$ anion ($g_1 = 2.268$, $g_2 = 2.112$, and $g_3 = 1.877$) and a weak signal due to the TSF^+ radical cation at $g = 2.009$, together with the $\Delta M = \pm 2$ resonance at 1600 G; the spectral feature is very similar to that of salt 3.

4. Summary

Tetrathiafulvalene (TTF) and tetraselenafulvalene (TSF) salts with bis(oxalato)platinate, dichloro(oxalato)platinate, and bis(oxalato)cuprate anions have been prepared by the reaction of $[\text{TTF}]_3[\text{BF}_4]_2$ or $[\text{TSF}]_3[\text{BF}_4]_2$ with the oxalato-metallates either in acetonitrile or in dimethyl sulfoxide. These salts contain neutral TTF^0 or TSF^0 as well as the TTF^+ or TSF^+ radical cation. Electronic reflectance spectra of the salts show a band due to dimeric

$(\text{TTF}^{\dagger})_2$ or $(\text{TSF}^{\dagger})_2$ in the 13100 - 14000 or 10500 - 12300 cm^{-1} region, as well as a band due to a $\text{TTF}^{\dagger}/\text{TTF}^0$ or $\text{TSF}^{\dagger}/\text{TSF}^0$ charge transfer transition in the 8600 - 8900 cm^{-1} range. X-Ray photoelectron spectra of the TTF salts with oxalato-platinates indicate the occurrence of some negative charge transfer from the TTF moiety to the platinate anion. It is suggested also that the planar bis-(oxalato)cuprate anions in the TTF and TSF salts exist as a dimer based on the ESR spectra. All the salts behave as semiconductors with the electrical resistivities in the order $10^2 - 10^4 \Omega \text{ cm}$ as compacted samples at 25 °C.

5. References

- 1 F. Wudl, C. H. Ho, and A. Nagel, *J. Chem. Soc., Chem. Commun.*, 1973, 923. L. V. Interrante, K. W. Browall, H. R. Hart, Jr., I. S. Jacobs, G. D. Watkins, and S. H. Wee, *J. Am. Chem. Soc.*, 1975, 97, 889. J. S. Kasper, L.V. Interrante, and C. A. Secaur, *J. Am. Chem. Soc.*, 1975, 97, 891. J. W. Bray, H. R. Hart, Jr., L. V. Interrante, I. S. Jacobs, J. S. Kasper, G. D. Watkins, S. H. Wee, and J. S. Bonner, *Phys. Rev. Lett.*, 1975, 35, 744. M. G. Miles and J. D. Wilson, *Inorg. Chem.*, 1975, 10, 2357. P. Calas, J. M. Fabre, M. Khalife-El-Saleh, A. Mas, E. Torreilles, and L. Giral, *Tetrahedron Lett.*, 1975, 4475. G. C. Paoavassiliou, Papavassiliou, *Mol. Cryst. Liq. Cryst.*, 1982, 86, 159.
- 2 K. Ueyama, G. Matsubayashi, and T. Tanaka, *Inorg. Chim. Acta*, 1984, 87, 143.
- 3 J. S. Miller and A. J. Epstein, *Prog. Inorg. Chem.*, 1976, 20, 1.
- 4 H. Kobayashi, I. Shirotani, A. Kobayashi, and Y. Sasaki, *Solid State Commun.*, 1977, 23, 409. A. Kobayashi, Y. Sasaki,

- I. Shirotani, and H. Kobayashi, *Solid State Commun.*, 1978, 26, 653.
- 5 A. Kobayashi, Y. Sasaki, and H. Kobayashi, *Bull. Chem. Soc. Jpn.*, 1979, 52, 3682.
- 6 D. Y. Jeter and W. E. Hatfield, *Inorg. Chim. Acta*, 1972, 6, 523.
- 7 A. Gleizes, F. Maury, and J. Galy, *Inorg. Chem.*, 1980, 19, 2074.
- 8 L. R. Melby, H. D. Hartzler, and W. A. Sheppard, *J. Org. Chem.*, 1974, 39, 2456.
- 9 M. V. Lakshmikanthan and M. P. Cava, *J. Org. Chem.*, 1976, 41, 882.
- 10 F. Wudl, *J. Am. Chem. Soc.*, 1975, 97, 1962.
- 11 W. M. Walsh, Jr., L. W. Rupp, Jr., F. Wudl, M. L. Kaplan, D. E. Schafer, and G. A. Thomas, *Solid State Commun.*, 1980, 33, 413.
- 12 J. S. Miller, A. L. Balch, and C. Hartman, *Inorg. Syn.*, 1979, 19, 13.
- 13 G. Matsubayashi, K. Kondo, and T. Tanaka, *Inorg. Chim. Acta*, 1983, 69, 167.
- 14 S. Araki, H. Ishida, and T. Tanaka, *Bull. Chem. Soc. Jpn.*, 1978, 51, 407.
- 15 T. Sugano, K. Yakushi, and H. Kuroda, *Bull. Chem. Soc. Jpn.*, 1978, 51, 1041.
- 16 J. B. Torrance, B. A. Scott, B. Welber, F. B. Kaufman, and P. E. Sieden, *Phys. Rev.*, 1979, B19, 730.
- 17 G. Matsubayashi, K. Ueyama, and T. Tanaka, *J. Chem. Soc., Dalton Trans.*, in press.
- 18 G. Kolks, C. R. Frihart, P. K. Coughlin, and S. J. Lippard, *Inorg. Chem.*, 1981, 20, 2933.

cis-DIALKYL BIS (OXALATO) STANNATE (IV) ANION SALTS

1. Introduction

Several tetrathiafulvalene (TTF) and tetraselenafulvalene (TSF) salts with metal-complex anions have been prepared, and their low-dimensional structures and electrical properties have been investigated.¹ The previous sections described the preparation and electrical conductivities of TTF and TSF salts with tris(oxalato)-metallate anions (metal = Si(IV), Ge(IV), and S (IV))² and bis-(oxalato)metallate anions (metal = Pt(II) and Cu(II)).³ In the former anions with bulky *hexa*-coordinate structures, TTF⁺ or TSF⁺ simple salts containing only the radical cation have mainly been obtained, whereas complex salts containing both the TTF⁺ (or TSF⁺) radical cation and neutral TTF⁰ (or TSF⁰) have been obtained in the latter anions with planar structures. On the other hand, polarizable bulky *hexa*-coordinated anions may be of interest as a counterpart to prepare TTF and TSF salts in the viewpoints of stacking modes of the donor molecules and their interactions with the anions.

This section describes the preparation of TTF and TSF salts with *cis*-dialkylbis(oxalato)stannate(IV) anions (alkyl = Me and Et) and their electrical resistivities. Configurations of the anions and TTF or TSF stacks and their electrical interactions are discussed on the basis of electronic reflectance, infrared, and X-ray photoelectron spectra.

2. Experimental

Preparation of $[\text{Bu}^n_4\text{N}]_2[\text{R}_2\text{Sn}(\text{OX})_2]$ ($\text{R} = \text{Me}$ and Et , $\text{OX}^{2-} = \text{C}_2\text{O}_4^{2-}$).
To an acetone (30 cm^3) solution containing tetrabutylammonium bromide (1.93 g, 6.0 mmol) and oxalatosilver(I) (2.0 g, 6.6 mmol) was added an acetone (10 cm^3) solution of dichlorodimethyltin(IV) (0.66 g, 3.0 mmol) with stirring at 0°C . The mixture was stirred at room temperature for 4 h, followed by the filtration to remove silver chloride and -bromide. The filtrate was dried under reduced pressures to give crude $[\text{Bu}^n_4\text{N}]_2[\text{MeSn}(\text{OX})_2]$, which was recrystallized from a mixture of acetone and diethyl ether, affording white crystals (1.4 g), 53 % yield, m.p. 114°C . Anal. Found: C, 55.44; H, 9.59; N, 3.33 %. Calcd for $\text{C}_{38}\text{H}_{78}\text{N}_2\text{O}_8\text{Sn}$: C, 56.37; H, 9.71; N, 3.46 %.

$[\text{Bu}^n_4\text{N}]_2[\text{Et}_2\text{Sn}(\text{OX})_2]$ was similarly prepared by the reaction of a mixture of tetrabutylammonium bromide and oxalatosilver(I) with dichlorodiethyltin(IV) in acetone, 50 % yield, m.p. $92\text{--}94^\circ\text{C}$. Anal. Found: C, 56.86; H, 10.06; N, 3.23 %. Calcd for $\text{C}_{40}\text{H}_{82}\text{N}_2\text{O}_8\text{Sn}$: C, 57.35; H, 9.87; N, 3.34 %.

Preparation of the TTF and TSF Salts. An acetonitrile (35 cm^3) solution containing $[\text{TTF}]_3[\text{BF}_4]_2^4$ (50 mg, 86 μmol) and $[\text{Bu}^n_4\text{N}]_2[\text{MeSn}(\text{OX})_2]$ (35 mg, 43 μmol) was allowed to stand in a refrigerator for 2 h under nitrogen atmosphere. The resulting dark brown precipitate of $[\text{TTF}]_2[\text{MeSn}(\text{OX})_2] \cdot 0.67\text{MeCN}$ (1a) was filtered and dried *in vacuo*, 98 % yield based on $[\text{Bu}^n_4\text{N}]_2[\text{Me}_2\text{Sn}(\text{OX})_2]$. Similarly, the reaction of $[\text{TTF}]_3[\text{BF}_4]_2$ with $[\text{Bu}^n_4\text{N}]_2[\text{Et}_2\text{Sn}(\text{OX})_2]$ in acetonitrile afforded $[\text{TTF}]_{2.5}[\text{Et}_2\text{Sn}(\text{OX})_2] \cdot 0.2\text{MeCN}$ (2a) in a 90 % yield.

$[\text{TSF}]_2[\text{MeSn}(\text{OX})_2]$ (3a) and $[\text{TSF}]_2[\text{Et}_2\text{Sn}(\text{OX})_2]$ (4a) were analogously obtained in 90 and 95 % yields, respectively, by the

reaction of $[\text{TSF}]_3[\text{BF}_4]_2^5$ with the corresponding oxalato-stannate anion salts. The TTF and TSF salts were obtained by electrocrystallization; an acetonitrile (10 cm^3) solution containing TTF (50 mg, 0.24 mmol) and $[\text{Bu}_4^{\text{n}}\text{N}]_2[\text{Me}_2\text{Sn}(\text{OX})_2]$ (810 mg, 1.0 mmol) was electrolyzed in a cell consisting of a platinum wire (anode) and a graphite rod (cathode) under a constant current ($5 \mu\text{A}$) for 3 weeks to afford $[\text{TTF}]_{2.5}[\text{Me}_2\text{Sn}(\text{OX})_2] \cdot 0.67\text{MeCN}$ (1b) (20 mg). $[\text{TTF}]_{3.3}[\text{Et}_2\text{Sn}(\text{OX})_2]$ (2b), $[\text{TSF}]_{4.0}[\text{Me}_2\text{Sn}(\text{OX})_2]$ (3b), and $[\text{TSF}]_{2.2}[\text{Et}_2\text{Sn}(\text{OX})_2]$ (4b) were similarly obtained by electrocrystallization from an acetonitrile solution containing TTF or TSF and the oxalato-stannates.

Mole ratios of the TTF^+ radical cation to neutral TTF^0 in the salts obtained were determined by both electronic absorption spectra in acetonitrile and elemental analyses. The involvement of solvent molecules in the salts was confirmed by ^1H NMR spectra in conc. HNO_3 .

Properties and analytical data for the salts are summarized in Table 1.

Physical Measurements. Powder electronic reflectance,² infrared,⁶ ^1H NMR,⁶ and X-ray photoelectron spectra⁷ were recorded as described elsewhere. Electrical resistivities were measured as compacted pellets by the conventional two-probe method.⁸

3. Results and Discussion

Electrical Resistivity. All the salts obtained behave as typical semiconductors; plots of $\log \rho$ (ρ = specific resistivities) vs. $1/T$ gave linear relationships in the 243 - 308 K range, while some deviations from the linearity were observed for all the salts above ca. 308 K. The electrical resistivities at 298 K and

Table 1. Properties and analyses of the TTF and TSF salts

No	Salt	Color	m.p.(dec.)	Found (Calcd) %		
			°C	C	H	N
1a ~~	$[\text{TTF}]_2 [\text{Me}_2\text{Sn}(\text{OX})_2] \cdot 0.6\text{MeCN}$	Dark brown	> 144	30.77 (30.42)	2.42 2.10	0.95 1.11)
1b ~~	$[\text{TTF}]_{2.5} [\text{Me}_2\text{Sn}(\text{OX})_2] \cdot 0.7\text{MeCN}$	Black	> 141	31.13 (31.13)	2.23 2.11	1.18 1.13)
2a ~~	$[\text{TTF}]_{2.5} [\text{Et}_2\text{Sn}(\text{OX})_2] \cdot 0.2\text{MeCN}$	Dark brown	> 141	32.21 (32.23)	2.69 2.38	0.32 0.32)
2b ~~	$[\text{TTF}]_{3.3} [\text{Et}_2\text{Sn}(\text{OX})_2]$	Black	> 121	32.16 (32.51)	2.65 2.28)	
3a ~~	$[\text{TSF}]_2 [\text{Me}_2\text{Sn}(\text{OX})_2]$	Dark green	> 113	19.34 (19.50)	1.52 1.27)	
3b ~~	$[\text{TSF}]_{4.0} [\text{Me}_2\text{Sn}(\text{OX})_2]$	Black	> 111	18.20 (19.04)	1.45 1.17)	
4a ~~	$[\text{TSF}]_2 [\text{Et}_2\text{Sn}(\text{OX})_2]$	Dark green	> 111	20.96 (21.13)	1.86 1.60)	
4b ~~	$[\text{TSF}]_{2.2} [\text{Et}_2\text{Sn}(\text{OX})_2]$	Black	> 137	20.92 (20.96)	1.83 1.56)	

activation energies (E_a) calculated for the temperature dependence of electrical conduction are summarized in Table 2, which lists also relevant wavenumbers in the electronic reflectance and infrared spectra.

The $\rho_{298\text{ K}}$ values of salts 1a, 3a, and 4a containing the TTF^+ or TSF^+ radical cation without neutral TTF^0 or TSF^0 fall in $1 \times (10^3 - 10^5) \Omega \text{ cm}$, which are similar to those of the TTF^- and TSF^- tris(oxalato)metallate anions (metal = Si(IV), Ge(IV), and Sn(IV)).² Complex salts which contain both TTF^+ or TSF^+ radical cation and neutral TTF^0 or TSF^0 exhibit small resistivities in the order of $1 \times (10^1 - 10^3) \Omega \text{ cm}$ except for 4a involving solvent molecules. In particular, salt 3b containing more amounts of neutral TSF^0 molecules display a smaller resistivity. The $\rho_{298\text{ K}}$ values of the complex salts are compared with the TTF or TSF complex salts with bis(oxalato)platinate(II) and -cuplate(II) anions.³

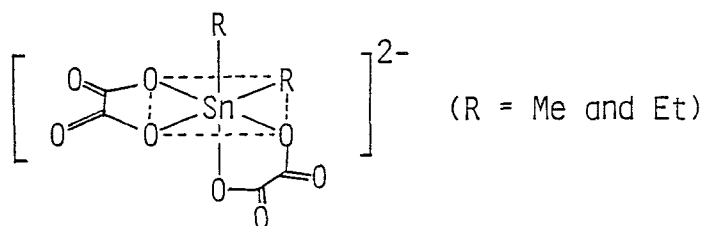
Configuration of the Dialkylbis(oxalato)stannate(IV) Anions (alkyl = Me and Et). The ^1H NMR spectrum of $[\text{Bu}_4^{\text{n}}\text{N}]_2[\text{Me}_2\text{Sn}(\text{OX})_2]$ in chloroform-d showed a Sn-methyl proton signal at δ 0.29, which was accompanied with the satellites due to the spin-spin coupling with $^{117/119}\text{Sn}$ nuclei [$^2J(^{119}\text{Sn}-\text{CH}_3) = 78.6 \text{ Hz}$ and $^2J(^{117}\text{Sn}-\text{CH}_3) = 75.6 \text{ Hz}$]. The $^2J(^{117/119}\text{Sn}-\text{CH}_3)$ value of dimethylstannate(IV) compounds are known to reflect the s-character of the Sn-C bond⁹ which may be related with C-Sn-C angles.¹⁰ The 2J value obtained here is rather close to those of Me_2SnCl_2 with a tetrahedral geometry (68.9 Hz in carbon tetrachloride,¹⁰ and bis(8-hydroxyquinolinato)dimethylstannate(IV) (71.2 Hz)¹¹ with the C-Sn-C angle of 110.7° ,¹² whereas, in contrast to the $^2J(^{119}\text{Sn}-\text{CH}_3)$ values of *trans*- $\text{Me}_2\text{SnCl}_2\text{L}_2$ [L = pyridine (112.0 Hz),¹³ dimethyl sulfoxide (114.8 Hz),¹⁴ and hexamethylphosphoric triamide (121.1 Hz)¹⁴],

Table 2. Electrical resistivities ($\rho_{298\text{ K}}$), activation energies (E_a), and powder reflectance and infrared spectra of the TTF and TSF salts

Salt	$\rho_{298\text{ K}}$ $\Omega\text{ cm}$	E_a eV	LE band of D ^a			CT band / 10^3 cm^{-1}		$\nu(\text{C=O})^b$ cm^{-1}
			10^3 cm^{-1}			$\text{D}^+/\text{D}^+{}^a$	$\text{D}^+/\text{D}^0{}^a$	
1a	3.2×10^5	0.30	29.4	18.9		12.8		1640
1b	1.4×10^3	0.20	27.8	19.1		12.8	8.5	1640
2a	2.0×10^6	0.31	29.4	19.9		13.5	8.8	1630
2b	3.4×10^2	0.26	29.4	19.2		12.5	9.1	1630
3a	1.8×10^4	0.28	25.0	22.7	16.4	11.8		1624
3b	8.9×10^1	0.15	27.8	23.7	16.5	12.2	9.0	1630
4a	6.8×10^3	0.20	27.8	22.2	16.7	11.8		1620
4b	7.2×10^2	0.13	28.6	20.3	16.1	11.8	8.8	1622

^a D = TTF or TSF. ^b Frequencies of the most intense carbonyl stretching bands of the oxalato ligands, measured in Nujol mulls. Cf. 1650 cm^{-1} for $[\text{Bu}_4^{\text{n}}\text{N}]_2[\text{Me}_2\text{Sn}(\text{OX})_2]$ and 1640 cm^{-1} for $[\text{Bu}_4^{\text{n}}\text{N}]_2[\text{Et}_2\text{Sn}(\text{OX})_2]$.

trans-Me₂SnCl₂(N-substituted picolinaldimines) (111.5 - 114.6 Hz),¹⁵
trans-Me₂SnCl₂(phen) (phen = substituted *o*-phenanthrolines (110.8 -
 115.6 Hz),¹⁶ and *trans*-dimethylbis(acetylacetonato)stannate(IV)
 (99.5 Hz).^{11,17} In view of these results, the present anion
 reasonably assumes the *cis*-configuration (I). The [Et₂Sn(OX)₂]²⁻



anion exhibited the ³J(¹¹⁹Sn-CH₃) value of 126 Hz (at δ 0.99) in
 dimethyl sulfoxide-d₆.¹⁸

Configuration of the TTF and TSF Salts. In the electronic
 reflectance spectra, bands at higher frequencies than 16000 cm⁻¹
 observed for all the salts are ascribed to local excitations of the
 TTF⁺ or TSF⁺ radical cation (D⁺) as well as the neutral TTF⁰ or TSF⁰
 molecule (D⁰) (D = TTF and TSF).¹⁹ In addition, 1a, 3a, and 4a
 exhibit a band at 12800, 11800, and 11800 cm⁻¹, respectively, which
 are due to the (TTF⁺)₂ or (TSF⁺)₂ radical cation dimers.²⁰ Since
 these salts have fairly large resistivities, the electronic inter-
 action between the neighboring dimers may be small. The remaining
 salts display a band around 9000 cm⁻¹ as well as a band around 12000
 or 13000 cm⁻¹ ascribed to the (D⁺)₂ dimers. The former band is
 assigned to the charge transfer transition between D⁺ and D⁰.¹⁹
 Thus, these salts are suggested to assume a columnar structure
 containing both D⁺/D⁺ and D⁺/D⁰ arrangements, which is consistent
 with rather small resistivities of these salts except for 4a

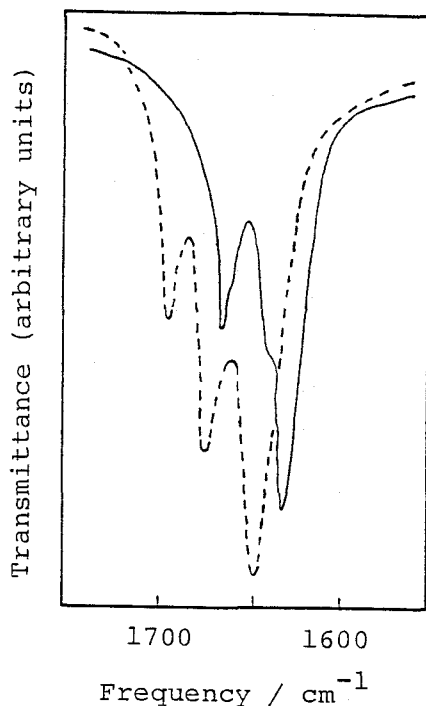


Figure 1. Infrared spectra of $[\text{Bu}_4\text{N}]_2[\text{Me}_2\text{Sn}(\text{OX})_2]$ (----) and 1a (—) in Nujol mulls.

involving solvent molecules, as mentioned above.

The oxalato-metal complexes exhibit the characteristic three $\nu(\text{C}=\text{O})$ bands near 1650 cm^{-1} .²¹ As is shown in figure 1, all the $\nu(\text{C}=\text{O})$ bands of $[\text{Bu}_4\text{N}]_2[\text{Me}_2\text{Sn}(\text{OX})_2]$ are shifted to low frequencies in 1a. This is also the cases with other TTF salts as well as the salts (Table 2), while no low frequency shift of $\nu(\text{C}=\text{O})$ bands has been observed in the oxalato ligand of TTF- and TSF- $[\text{M}(\text{OX})_3]$ salts ($\text{M} = \text{Si}(\text{IV}), \text{Ge}(\text{IV}),$ and $\text{Sn}(\text{IV})$).² The low frequency shift of $\nu(\text{C}=\text{O})$ in the present salts suggestive of an interaction between negatively polarized carbonyl-oxygen and positively polarized sulfur of the TTF^+ radical cation.²² The carbonyl-oxygen of $[\text{cis-R}_2\text{Sn}(\text{OX})_2]^{2-}$ ($\text{R} = \text{Me}$ and Et) may be negatively polarized by

Table 3. Binding energies (eV) of the Sn 3d_{3/2} and 3d_{5/2} electrons of some dialkylbis(oxalato)stannate(IV)

Salt	Sn 3d _{3/2}	Sn 3d _{5/2}
[Bu ⁿ ₄ N] ₂ [Me ₂ Sn(OX) ₂]	494.2	485.7
1a	494.2	485.7
1b	494.2	485.7
3a	494.2	485.7
[Bu ⁿ ₄ N] ₂ [Et ₂ Sn(OX) ₂]	493.6	485.3
2a	493.2	484.8
4a	493.7	485.6

the electron-donation of the alkyl group in the *trans* position of the oxalato ligand.

Table 3 summarized the binding energies of Sn 3d_{3/2} and 3d_{5/2} electrons of the TTF salts and tetrabutylammonium salt of [*cis*-R₂Sn(OX)₂]²⁻ which were determined by the X-ray photoelectron spectroscopy. The binding energies are essentially constant in all the salts, indicating that the interaction between TTF moieties and the [R₂Sn(OX)₂]²⁻ anions is too weak to change the electronic state of the tin atom.

4. Summary

TTF and TSF salts with [*cis*-R₂Sn(OX)₂]²⁻, [TTF or TSF]_{2.0-4.0}⁺ [*cis*-R₂Sn(OX)₂] (R = Me and Et; OX²⁻ = C₂O₄²⁻) were prepared, by the reaction of [TTF or TSF]₃[BF₄]₂ with [*cis*-R₂Sn(OX)₂]²⁻ in acetonitrile and by electrolysis of TTF or TSF in acetonitrile solution containing [Buⁿ₄N]₂[*cis*-R₂Sn(OX)₂] as electrolytes. All

the salts behave as typical semiconductors with electrical resistivities of $1 \times (10^1 - 10^7) \Omega \text{ cm}$ at 25 °C as compacted pellets. TTF or TSF molecules (D) in the complex salts are stacked in a column with D^+/D^+ and D^+/D^0 interactions in the solids, as discussed on the basis of electronic reflectance spectra. Electronic interactions between TTF or TSF moieties and the polarized $[\text{cis-R}_2\text{Sn}(\text{OX})_2]^{2-}$ anions are noticed from the infrared spectra.

5. References

- 1 F. Wudl, C. H. Ho, and A. Nagel, *J. Chem. Soc., Chem. Commun.*, 1973, 923. L. V. Interrante, K. W. Browall H. R. Hart, Jr., I. S. Jacobs, G. D. Watkins, and S. H. Wee, *J. Am. Chem. Soc.*, 1975, 97, 889. J. S. Kasper, L.V. Interrante, and C. A. Secaur, *J. Am. Chem. Soc.*, 1975, 97, 891. J. W. Bray, H. R. Hart, Jr., L. V. Interrante, I. S. Jacobs, J. S. Kasper, G. D. Watkins, S. H. Wee, and J. S. Bonner, *Phys. Rev. Lett.*, 1975, 35, 744. M. G. Miles and J. D. Wilson, *Inorg. Chem.*, 1975, 10, 2357. P. Calas, J. M. Fabre, M. Khalife-El-Saleh, A. Mas, E. Torreilles, and L. Giral, *Tetrahedron Lett.*, 1975, 4475. G. C. Papavassiliou, *Mol. Cryst. Liq. Cryst.*, 1982, 86, 159.. M. Bousseau, L. Valade, M. F. Bruniquel, P. Cassoux, M. Garbauskas, L.Interrante, and J. Kasper, *Nouv. J. Chim.*, 1984, 8, 3.
- 2 K. Ueyama, G. Matsubayashi, and T. Tanaka, *Inorg. Chim. Acta*, 1984, 87, 143.
- 3 K. Ueyama, A. Tanaka, G. Matsubayashi, and T. Tanaka, *Inorg. Chim. Acta*, in press.
- 4 F. Wudl, *J. Am. Chem. Soc.*, 1975, 97, 1962.
- 5 W. M. Walsh, Jr., L.W. Rupp, Jr., F. F. Wudl, M. L. Kaplan,

- D. E. Schafer, G. A. Thomas, and R. Gemmer, *Solid State Commun.*, 1980, 33, 413.
- 6 H. Koezuka, G. Matsubayashi, and T. Tanaka, *Inorg. Chem.*, 1974, 13, 443.
- 7 G. Matsubayashi, K. Kondo, and T. Tanaka, *Inorg. Chim. Acta*, 1983, 69, 167.
- 8 S. Araki, H. Ishida, and T. Tanaka, *Bull. Chem. Soc. Jpn.*, 1978, 51, 407.
- 9 J. R. Holmes and H. D. Kaesz, *J. Am. Chem. Soc.*, 1961, 83, 3903.
- 10 G. Matsubayashi, Y. Kawasaki, T. Tanaka, and R. Okawara, *Bull. Chem. Soc. Jpn.*, 1967, 40, 1566.
- 11 M. M. McGrady and R. S. Tobias, *J. Am. Chem. Soc.*, 1965, 87, 1909.
- 12 E. O. Schlemper, *Inorg. Chem.*, 1967, 6, 2012.
- 13 H. Fujiwara, F. Sasaki, and Y. Sasaki, *J. Phys. Chem.*, 1979, 83, 2400.
- 14 V. S. Peterosyan, V. I. Bakhmutov, and O. A. Reutov, *J. Organomet. Chem.*, 1974, 72, 79.
- 15 G. Matsubayashi, M. Okunaka, and T. Tanaka, *J. Organomet. Chem.*, 1973, 56, 215.
- 16 W. D. Honnick, M. C. Hughes, C. D. Schaeffer, Jr., and J. J. Zuckerman, *Inorg. Chem.*, 1976, 15, 1391.
- 17 Y. Kawasaki, T. Tanaka, and R. Okawara, *Bull. Chem. Soc. Jpn.*, 1964, 37, 903.
- 18 The $^3J(^{119}\text{Sn}-\text{CH}_3)$ value was measured for $[\text{PPh}_3\text{CH}_2\text{Ph}][\text{Et}_2\text{Sn}(\text{OX})_2]$.
- 19 J. B. Torrance, B. A. Scott, B. Welber, F. B. Karfman, and P. E. Sieden, *Phys. Rev.*, 1979, B19, 730.
- 20 T. Sugano, K. Yakushi, and H. Kuroda, *Bull. Chem. Soc. Jpn.*, 1978, 51, 1041.
- 21 K. Nakamoto, 'Infrared and Raman Spectra of Inorganic and

Coordination Compounds,' 3rd ed., John Wiley & Sons, New York
(1978) p. 234.

22 W. D. Grobman and B. D. Silverman, *Solid State Commun.*, 1976,
19, 319.

STRUCTURES AND ELECTRICAL PROPERTIES OF TTF AND TSF SALTS WITH
CHLORODIORGANOSTANNATE(IV) ANIONS

3-1

X-RAY CRYSTAL STRUCTURES AND PROPERTIES OF TRIS(TETRATHIA-
FULVALENium) TETRACHLORODIMETHYLSTANNATE(IV) AND TETRATHIA-
FULVALENium TRICHLORODIMETHYLSTANNATE(IV)

1. Introduction

Recently, the preparations and electrical properties of some tetrathiafulvalene (TTF)-halogenostannate(IV) anion salts and the X-ray crystal structure of $[\text{TTF}]_3[\text{SnCl}_6]^{1-}$ have been reported. This salt contains a two-dimensional layer structure of TTF molecules with intermolecular sulfur-sulfur van der Waals contacts, and exhibits a rather small resistivity ($410 \, \Omega \, \text{cm}$ at $25 \, ^\circ\text{C}$ as a compacted sample). Thus, an electrical current path through the layer has been suggested. The $[\text{TTF}]_3[\text{SnMe}_2\text{Cl}_4]^{1-}$ salt has been reported also to display a smaller resistivity ($16 \, \Omega \, \text{cm}$ at $25 \, ^\circ\text{C}$ as a compacted sample) than $[\text{TTF}]_3[\text{SnCl}_6]^{1-}$. Here, the author has undertaken to clarify the mechanism of electrical conduction in the TTF-chlorostannate(IV) anion salts based on a structural viewpoint.

This section describes the X-ray crystal structures of $[\text{TTF}]_3[\text{SnMe}_2\text{Cl}_4]^{1-}$ and $[\text{TTF}][\text{SnMe}_2\text{Cl}_3]$. Electrical resistivities of these salts, as well as electronic reflectance and X-ray photoelectron spectra, are discussed based on these crystal structures.

2. Experimental

Preparation of [TTF]₃[SnMe₂Cl₄] (1) and [TTF][SnMe₂Cl₃] (2). Salts (1) and (2) were prepared by the reaction of [TTF]₃[BF₄]₂² (0.14 g, 0.18 mmol) in acetonitrile (60 cm³) with SnMe₂Cl₂ (1.23 g, 3.6 mmol) and [Et₄N]Cl (0.075 g, 0.45 mmol) in the same solvent (15 cm³) under nitrogen atmosphere; the mixed solution was allowed to stand at room temperature for 3 d, giving a mixture (0.057 g) of black square-plates of (1) (density, 1.79 g cm⁻³) and black cubes of (2) (density, 2.02 g cm⁻³), from which (1) and (2) were readily separated from each other in 1,3-dibromopropane (density, 1.98 g cm⁻³). The two resulting crystals of (1) (0.048 g) and of (2) (0.009 g) were collected and washed with diethyl ether and dried *in vacuo*. Salt (1) obtained here was identical with black square-plates afforded by the electrocrystallization of TTF³ in the presence of SnMe₂Cl₂ and [Et₄N]Cl as an electrolyte in acetonitrile.¹

Physical Measurements. Electronic powder reflectance¹ and X-ray photoelectron spectra⁴ were recorded as described elsewhere. The electrical resistivities of the salts were measured as compacted samples by the conventional two-probe technique.¹

X-Ray Crystal Structure of Salts (1) and (2). Cell constants (Table 1) were obtained from the least-squares fit of angular coordinates of 25 reflections with 2θ values from 21 to 36° for (1) and from 30 to 41° for (2), which were measured on computer-controlled Rigaku four-circle diffractometers at Kwansei Gakuin University and at the crystallographic Research Center, Osaka University, respectively. Intensity data were collected on the same

Table 1. Summary of crystal data and experimental details of the structural study of salts (1) and (2)

	Salt (1)	Salt (2)
Formula	$C_{20}H_{18}Cl_4S_{12}Sn$	$C_8H_{10}Cl_3S_4Sn$
Crystal system	Tetragonal	Triclinic
Space group	$P4/mbm$	$P\bar{1}$
$a / \text{\AA}$	11.725(1)	9.348(1)
$b / \text{\AA}$	11.725(1)	10.475(1)
$c / \text{\AA}$	12.194(3)	8.4517(9)
$\alpha / ^\circ$		92.47(1)
$\beta / ^\circ$		102.53(1)
$\gamma / ^\circ$		109.27(1)
$V / \text{\AA}^3$	1676.4(5)	756.7(2)
M	903.6	459.4
Z	2	2
$D_c / \text{g cm}^{-3}$	1.790(1)	2.016(1)
$D_m(\text{flotation}) / \text{g cm}^{-3}$	1.79	2.02
Crystal dimensions / mm	0.25 x 0.25 x 0.06	0.40 x 0.24 x 0.20
Radiation	Mo-K α ($\lambda = 0.71069 \text{\AA}$)	
Monochromator	Graphite	
μ / cm^{-1}	15.2	21.3
$F(000)$	869	446
Scan range / $^\circ$	$0.9 + 0.34 \tan \theta$	$1.0 + 0.35 \tan \theta$
2θ limits / $^\circ$	3 - 55	4 - 55
Reflections, total	1178	3556
Reflections, $ F_o > 3\sigma(F)$	847	3196

diffractometers. No intensity decay was observed during the data collections. Data were corrected for background, attenuators, and Lorentz and polarization effects in the usual fashion. No absorption correction was made. Experimental conditions for the data collections also are listed in Table 1.

Although for salt (1) three possible tetragonal space groups, $P\bar{4}b2$, $P4bm$, and $P4/mbm$, were indicated by oscillation and

Weissenberg photographs, the space group $P4/mbm$ was probed to be suitable in a successful analysis, which is the same as $[TTF]_3-[SnCl_6]$.¹ For (1) a Fourier map phased on the tin atom at the origin gave positions of chlorine and sulfur atoms. The carbon atoms of the Sn-Me groups, however, have not been found in Fourier maps after following refinements. The block-diagonal least-squares refinement, based on the position of the methyl-carbon atom calculated from the assumed Sn-C distance of 2.1 \AA ,^{5,6} with the occupancy of 0.5, under the assumption of the disorder with respect to methyl groups and chlorine atoms on the c plane, was converged. The refinement with anisotropic thermal parameters for all the nonhydrogen atoms led to residual indices $R = \Sigma ||F_o| - |F_c|| / \Sigma |F_o| = 0.052$ and $R' = [\Sigma w(|F_o| - |F_c|)^2 / \Sigma w|F_o|^2]^{1/2} = 0.070$. The weighting scheme, $1/w = \sigma^2(F_o) + 0.0007(F_o)^2$, was used. The structure of (2) was solved by the conventional Patterson and Fourier techniques. By assuming the space group $P\bar{1}$, the refinement with anisotropic thermal parameters for all the nonhydrogen atoms led to $R = 0.048$ and $R' = 0.062$, using the weighting scheme, $1/w = \sigma^2(F_o) + 0.001(F_o)^2$. No attempt has been made to refine hydrogen atoms at any stage of both the analyses. Atomic scattering factors used in these refinements were taken from the tabulation.⁷

The final atomic coordinates with standard deviations for (1) and (2) are given in Tables 2 and 3, respectively.

Crystallographic calculations were performed on an ACOS 900S computer at the Crystallographic Research Center, Institute for Protein Research, Osaka University. Figures were drawn by the local version of ORTEP-II program.⁸

Table 2. Atomic coordinates ($\times 10^4$) for $[\text{TTF}]_3[\text{SnMe}_2\text{Cl}_4]$
(1) with estimated standard deviations in parentheses

Atom	X	Y	Z
Sn	0	0	0
Cl(1)	0	0	2132(2)
Cl(2)	2190(4)	342(5)	0
S(1)	1226(1)	2007(1)	3684(1)
S(5)	4125(2)	875(2)	3667(7)
C(Me2)	1761(15)	316(18)	0
C(1)	1775(7)	2432(7)	2421(5)
C(3)	2076(5)	2925(5)	4445(6)
C(7)	4576(12)	423(12)	2309(35)
C(9)	5000	0	4445(39)

Table 3. Atomic coordinates ($\times 10^4$) for $[\text{TTF}][\text{SnMe}_2\text{Cl}_3]$
(2) with estimated standard deviations in parentheses

Atom	X	Y	Z
Sn	3613.1(3)	877.8(3)	1372.9(3)
Cl(1)	1756(1)	-222(1)	3155(2)
Cl(2)	5535(2)	1925(2)	-558(2)
Cl(3)	3254(2)	3060(1)	1717(2)
S(1)	-1189(1)	3846(1)	2016(1)
S(2)	1300(1)	6501(1)	3036(2)
S(3)	3253(1)	5121(1)	5637(2)
S(4)	745(2)	2508(1)	4602(2)
C(1)	5541(6)	1092(5)	3330(6)
C(2)	1880(6)	-149(5)	-755(6)
C(3)	-1443(6)	5185(5)	1013(6)
C(4)	-304(6)	6411(5)	1483(6)
C(5)	3519(7)	3757(6)	6564(7)
C(6)	2363(8)	2552(6)	6088(8)
C(7)	604(5)	4802(4)	3272(5)
C(8)	1448(5)	4202(4)	4386(5)

3. Results and Discussion

The Crystal Structure and Properties of Salt (1). Figures 1 and 2 illustrate the crystal structure of (1) together with the atom-labelling scheme. The bond distances and angles as well as relevant intermolecular atom-atom distances are listed in Table 4. The tin atom of the distorted octahedral $[\text{SnMe}_2\text{Cl}_4]^{2-}$ anion occupies (0, 0, 0) and (1/2, 1/2, 0), which is the same arrangement as that found in $[\text{TTF}]_3[\text{SnCl}_6]$.¹ An interesting feature of the present salt is the presence of disorder with respect to the methyl groups and chlorine atoms which are located on the *c* plane, as is apparent from Figure 1. The $[\text{SnMe}_2\text{Cl}_4]^{2-}$ anion as the tetramethyl- and tetraethylammonium salts was suggested to assume a *trans* geometry on the basis of vibrational and Mossbauer spectroscopies,^{9,10}

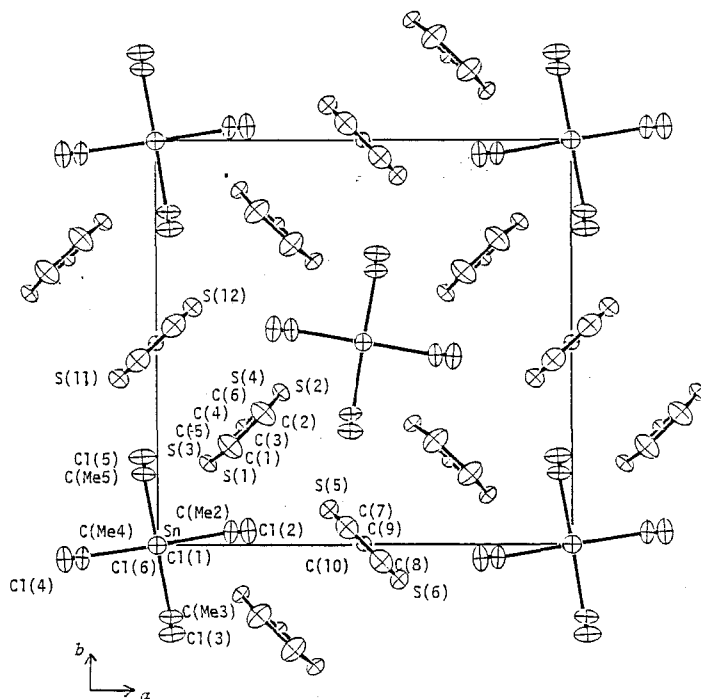


Figure 1. Projection of the crystal structure of $[\text{TTF}]_3[\text{SnMe}_2\text{Cl}_4]$ (1) along *c*.

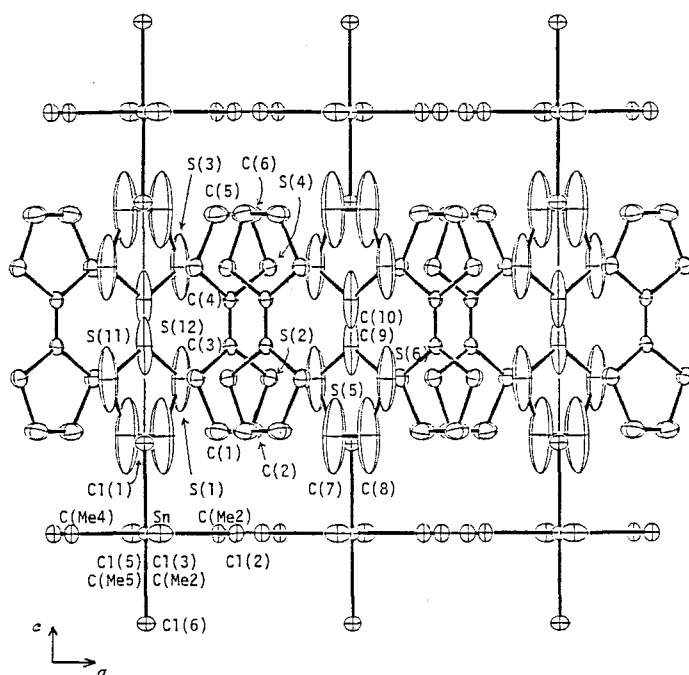


Figure 2. Projection of the crystal structure of $[\text{TTF}]_3[\text{SnMe}_2\text{Cl}_4]$ (1) along b .

This geometry is also the case with $[\text{pyridinium}]_2[\text{SnMe}_2\text{Cl}_4]$ as confirmed by the X-ray crystallographic analysis.¹¹ Thus, in the present salt the linear Me-Sn-Me and Cl-Sn-Cl skeletons seem to be disordered. The Sn-C(Me) (2.098(18) Å) and Sn-Cl distances (2.599(5), 2.600(3) Å) are close to those of the pyridinium salt; Sn-C(Me), 2.109(9); Sn-Cl, 2.603(2) and 2.625(2) Å.¹¹ The rather long Sn-Cl distances in the pyridinium salt come from the Cl---H-N hydrogen bonding,¹¹ while the long Sn-Cl bond for (1) may be due to the electronic interaction between Cl(1) and S(1) (3.244(2) Å). This interaction may force the methyl groups to be located on the c plane, which results in the disorder with respect to the methyl groups and chlorine atoms because of the presence of the 4-fold axis along the c axis.

Table 4. Selected distances (\AA) and angles ($^\circ$) for $[\text{TTF}]_3[\text{SnMe}_2\text{Cl}_4]$ (1) with estimated standard deviations in parentheses

Sn-Cl(1)	2.600(3)	S(5)-C(9)	1.734(26)
Sn-Cl(2)	2.599(5)	C(1)-C(2)	1.346(12)
Sn-C(Me2)	2.098(18)	C(3)-C(4)	1.354(10)
S(1)-C(1)	1.733(7)	C(7)-C(8)	1.404(20)
S(1)-C(3)	1.736(6)	C(9)-C(10)	1.354(67)
S(5)-C(7)	1.818(40)		
S(1)---Cl(1)	3.344(2)	S(1)---S(11)	3.498(3)
S(1)---S(5)	3.649(3)		
Cl(1)-Sn-Cl(2)	90	S(1)-C(3)-C(4)	112.3(5)
Cl(1)-Sn-C(Me2)	90	C(7)-S(5)-C(9)	98.8(15)
Cl(2)-Sn-C(Me2)	1.3(6)	S(5)-C(7)-C(8)	114.3(29)
C(1)-S(1)-C(3)	95.2(4)	S(5)-C(9)-S(6)	113.6(27)
S(1)-C(1)-C(2)	117.2(5)	S(5)-C(9)-C(10)	123.2(13)
S(1)-C(3)-S(2)	115.2(4)		

The arrangement of TTF molecules in the crystal is essentially the same as that found in $[\text{TTF}]_3[\text{SnCl}_6]$. The TTF molecules constitute a trimer unit, in which their cofacial planes parallel to the c axis are almost overlapped in an eclipsed manner, spaced by the same distance. The adjacent trimer units are perpendicular to each other to satisfy the tetragonal symmetry, and the centers of the TTF molecules occupy the (002) plane to form a layer of TTF (Figure 2).

The side-located TTF molecules within the trimer unit are almost planar, with C(3), C(4), and the sulfur atoms 0.03-0.08 \AA below (toward the central molecule) and the other carbon atoms 0.07 \AA above the least-squares best plane. All the atoms of the

central TTF molecule, although the molecule is strictly planar, have extremely large thermal factors. This is due to the fact that this molecule is rather loosely located compared with the other two TTF molecules in the trimer unit which are more strictly arranged through the sulfur-chlorine electrostatic interaction mentioned above. Although the bond distances in the central TTF molecule are not precisely determined because of the large thermal factors of the atoms, the bond distances in two other TTF molecules are very close to the corresponding distances in $[\text{TTF}]_3[\text{SnCl}_6]$. The C(3)-C(4) distance ($1.354(10) \text{ \AA}$) is lengthened and the C(3)-S(1) one ($1.736(6) \text{ \AA}$) is shortened compared with those ($1.349(3)$ and $1.757(2) \text{ \AA}$, respectively) of neutral TTF.¹² These parameters suggest the occurrence of a partial oxidation of the TTF molecule in (1).¹ The interplanar spacing within the trimer is $3.499(2) \text{ \AA}$, which is also very close to that of $[\text{TTF}]_3[\text{SnCl}_6]$ ($3.493(2) \text{ \AA}$). These values are longer than interplanar spacing of the TTF^+ radical cation dimer ($3.34 - 3.43 \text{ \AA}$) in $[\text{TTF}]\text{Br}$,¹³ $[\text{TTF}]\text{I}_3$,¹⁴ $[\text{TTF}][\text{ClO}_4]$,¹⁵ and $[\text{TTF}][\text{HgCl}_3]$ ¹⁶ and shorter than those ($3.554 - 3.607 \text{ \AA}$) of mixed-valence TTF salts with an eclipsed columnar structure, such as $[\text{TTF}]\text{Br}_{0.76}$,¹⁷ $[\text{TTF}]\text{I}_{0.71}$,¹⁸ and $[\text{TTF}][\text{SCN}]_{0.57}$.¹⁹

The closest sulfur-sulfur distance between the adjacent TTF trimer units is $3.649(3) \text{ \AA}$, which is not only significantly shorter than the sum of the van der Waals radii of sulfur atoms (3.70 \AA)²⁰ but also shorter than that found in $[\text{TTF}]_3[\text{SnCl}_6]$ (3.705 \AA).¹ The difference between the sulfur-sulfur contacts in these two salts may reflect on the electrical conduction; the specific resistivity ($16 \text{ } \Omega \text{ cm}$ at $25 \text{ } ^\circ\text{C}$ as a compacted sample) and the activation energy for conduction (0.028 eV) obtained for salt (1) are appreciably smaller than those ($410 \text{ } \Omega \text{ cm}$, 0.23 eV) for $[\text{TTF}]_3[\text{SnCl}_6]$.¹ Such a correlation between the sulfur-sulfur

Table 5. Binding energies (eV) of the Sn 3d_{3/2} and 3d_{5/2} electrons of some chlorostannate(IV) salts observed in X-ray photoelectron spectra

Salt	Sn 3d _{3/2}	Sn 3d _{5/2}
[TTF] ₃ [SnMe ₂ Cl ₄] (1)	494.0	485.5
[(CH ₂) ₂ - $\overset{\text{S}}{\text{<}}\text{C=NMe}_2$] ₂ [SnMe ₂ Cl ₄] ^a	494.3	486.0
[TTF] ₃ [SnCl ₆] ^b	493.8	485.5
[Bu ⁿ ₄ N] ₂ [SnCl ₆] ^b	495.0	486.5
[TTF][SnMe ₂ Cl ₃] (2)	493.9	485.3
[(CH ₂) ₃ - $\overset{\text{S}}{\text{<}}\text{C=NMe}_2$][SnMe ₂ Cl ₃] ^c	494.5	486.0

^a Ref. 28. ^b Ref. 1. ^c Ref. 29.

contact and the conduction supports the electrical conduction through the two-dimensional layer consisting of TTF-trimers with the network due to the sulfur-sulfur contacts.

The S(1)-Cl(1) distance (3.344(2) Å) also is shorter than the sum of the van der Waals radii of sulfur and chlorine atoms (3.65 Å), indicating the electrostatic interaction between these atoms, being similar to [TTF]₃[SnCl₆].¹ Table 5 lists the binding energies of Sn 3d_{3/2} and 3d_{5/2} electrons for the chlorostannate(IV) anion salts which have been determined from X-ray photoelectron spectra. The binding energies for (1) and [TTF]₃[SnCl₆] are smaller than those for [(CH₂)₂- $\overset{\text{S}}{\text{<}}\text{C=NMe}_2$]₂[SnMe₂Cl₄] and [Buⁿ₄N]₂[SnCl₆], respectively. This means that the tin atoms in the TTF salts are more reduced than in the latter salts, suggesting a partial, although slight, transfer of some negative charges from TTF⁺/TTF⁰ to the chlorostannate(IV) anions. This is consistent

with the above-mentioned sulfur-chlorine contacts.

The Crystal Structure and Properties of Salt (2). The projection of the unit cell contents of salt (2) is shown in Figure 3. The crystal structure consists of both dimeric units of TTF and of $[\text{SnMe}_2\text{Cl}_3]^-$. The bond distances, angles, and selected intermolecular atom-atom distances are summarized in Table 6. The TTF molecule is almost planar, with all the sulfur atoms and C(7) and C(8) 0.008 - 0.026 Å below (toward the other molecule of the dimer) and the other carbon atoms 0.019 - 0.028 Å above the least-squares plane. The C(7)-C(8) (1.400(7) Å), and C(7)-S(1,2) and C(8)-S(3,4) distances

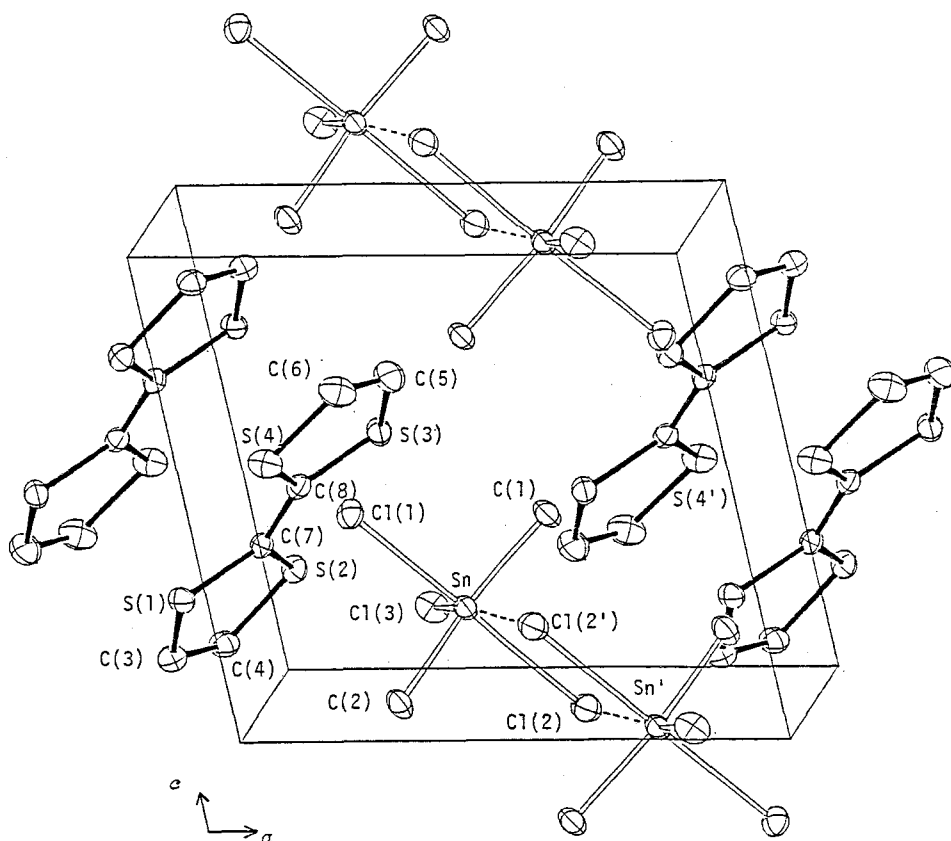


Figure 3. Projection of the crystal structure of $[\text{TTF}][\text{SnMe}_2\text{Cl}_3]$ (2) along the b^* axis.

Table 6. Selected distances (\AA) and angles ($^\circ$) for [TTF][SnMe₂Cl₃] (2) with estimated standard deviations in parentheses

Sn-Cl(1)	2.564(1)	S(2)-C(7)	1.718(4)
Sn-Cl(2)	2.687(2)	S(3)-C(5)	1.720(7)
Sn-Cl(3)	2.432(2)	S(3)-C(8)	1.720(4)
Sn-C(1)	2.108(5)	S(4)-C(6)	1.730(7)
Sn-C(2)	2.106(4)	S(4)-C(8)	1.710(4)
S(1)-C(3)	1.726(6)	C(3)-C(4)	1.346(6)
S(1)-C(7)	1.722(4)	C(5)-C(6)	1.338(8)
S(2)-C(4)	1.738(5)	C(7)-C(8)	1.400(7)
Cl(2)---S(a)	3.292(8)	S(2)---Cl(b)	3.311(7)
Sn---Cl(2')	3.367(6)		
Cl(1)-Sn-Cl(2)	117.57(5)	S(3)-C(8)-C(7)	122.2(3)
Cl(1)-Sn-Cl(3)	93.2(1)	S(4)-C(8)-C(7)	122.2(3)
Cl(2)-Sn-Cl(3)	89.0(1)	C(3)-S(1)-C(7)	94.9(2)
Cl(1)-Sn-C(1)	89.9(2)	C(4)-S(2)-C(7)	94.6(2)
Cl(1)-Sn-C(2)	90.6(2)	C(5)-S(3)-C(8)	95.4(2)
Cl(2)-Sn-C(1)	90.7(2)	C(6)-S(4)-C(8)	95.1(2)
Cl(2)-Sn-C(2)	87.9(2)	S(1)-C(7)-S(2)	116.3(3)
Cl(3)-Sn-C(1)	102.4(2)	S(1)-C(3)-C(4)	117.1(4)
Cl(3)-Sn-C(2)	103.2(2)	S(2)-C(4)-C(3)	117.1(4)
C(1)-Sn-C(2)	154.2(2)	S(3)-C(8)-S(4)	115.6(3)
S(1)-C(7)-C(8)	121.0(3)	S(3)-C(5)-C(6)	116.8(5)
S(2)-C(7)-C(8)	122.7(3)	S(4)-C(6)-C(5)	117.1(5)

(1.718(4) \AA , averaged), which are sensitive to the oxidation state of the TTF molecule, are close to the corresponding bond distances of [TTF][HgCl₃] (1.41(1) and 1.71(1) \AA)¹⁶ and of [TTF]I₃ (1.382(7) and 1.719(8) \AA , respectively).¹⁴ Thus, the TTF molecule in salt (2) may exist as the radical cation.

The molecular overlap of the TTF⁺ radical cation in a dimer

is nearly eclipsed with a significant lateral shift (0.621 \AA) along the in-plane molecular axis, as illustrated in Figure 4. It has theoretically been pointed out that dimeric $(\text{TTF})_2^{2+}$ cations prefer an eclipsed overlap configuration.²¹⁻²³ The nearly eclipsed overlap mode of the TTF^+ radical cation was reported on some salts containing $(\text{TTF})_2^{2+}$ dimers, such as $[\text{TTF}][\text{ClO}_4]$,¹⁵ $[\text{TTF}]\text{Br}$,¹⁷ and $[\text{TTF}][2,5\text{-difluoroTCNQ}]$.²⁴ The overlap of the TTF^+ radical cations with the appreciable lateral shift in the present salt is presumably due to the static interaction between the sulfur atom of TTF and closely located chlorine atom of the $[\text{SnMe}_2\text{Cl}_3]^-$ anion: $\text{S}(1)\text{-Cl(a)}$, $3.292(8) \text{ \AA}$ and $\text{S}(2)\text{-Cl(b)}$, $3.311(7) \text{ \AA}$ (Figure 4). Each dimer is appreciably separated with nearest interatomic sulfur-sulfur

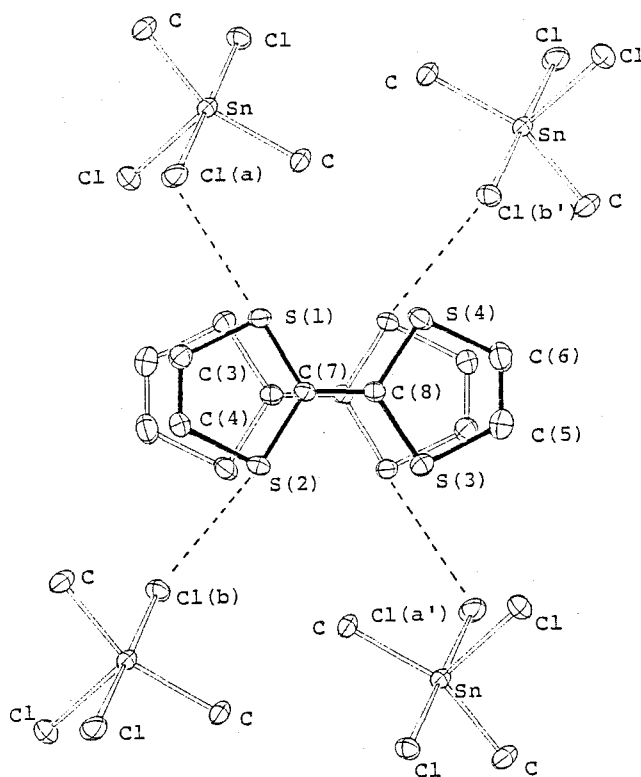


Figure 4. Molecular overlap of the $(\text{TTF})_2^{2+}$ dimer and sulfur-chlorine interactions in $[\text{TTF}][\text{SnMe}_2\text{Cl}_3]$ (2).

contact: S(2)---S(4'), 6.553(3) Å. Such a separation of (TTF)₂²⁺ dimers in the crystal is consistent not only with the appearance of the band at 12100 cm⁻¹ assignable to the (TTF)₂²⁺ dimer transition²⁵ in the powder reflectance spectrum but with a large electrical resistivity (1.3 x 10⁷ Ω cm at 25 °C as a compacted sample).

The [SnMe₂Cl₃]⁻ anion assumes as distorted trigonal bipyramidal geometry, which is essentially the same as the anion of [quinolinium][SnMe₂Cl₃].⁶ Bond distances between the tin and two axial chlorine atoms (2.564(1) and 2.687(2) Å) are significantly larger than the equatorial Sn-Cl bond (2.432(2) Å). This may be due to the static interaction between the axial chlorine and sulfur atoms, as described above. A transfer of some negative charges from the TTF⁺ radical cation to the [SnMe₂Cl₃]⁻ anion also is suggested from the binding energies of Sn 3d electrons (see Table 5). It is noteworthy that two [SnMe₂Cl₃]⁻ anions are arranged to form a dimeric unit; at a distance of 3.367(6) Å from the tin atom is located a chlorine atom of an adjacent anion. This configuration around the tin atoms is similar to that found for the quinolinium salt (Sn---Cl, 3.486(7) Å).⁶ Such a dimerized geometry was found also in InMe₂Cl (In---Cl, 3.450(9) Å)²⁶ and SnMe₂Cl₂ (Sn---Cl, 3.54 Å).²⁷ The C(1)-Sn-C(2) angle (154.2(2)°) for (2) is considerably larger than not only the value (120°) expected from the equatorial positions of carbon atoms in the trigonal bipyramidal geometry around the tin atom but also that of the anion of [SnMe₂-Cl(terpyridyl)]⁺[SnMe₂Cl₃]⁻ (140(2)°).⁵ This may be resulted from a repulsion of the methyl group of [SnMe₂Cl₃]⁻ with that of the adjacent anion through the dimeric formation.

4. Summary

A single-crystal X-ray structure analysis has been performed for $[\text{TTF}]_3[\text{SnMe}_2\text{Cl}_4]$ obtained by electrocrystallization of tetra-thiafulvalene (TTF) in the presence of SnMe_2Cl_2 and $[\text{Et}_4\text{N}]\text{Cl}$ in acetonitrile. The crystals are tetragonal, space group $P4/\text{mbm}$, with $Z = 2$. The cell constants are $a = 11.725(1)$, $c = 12.194(3) \text{ \AA}$, and $V = 1676.4(5) \text{ \AA}^3$. The block-diagonal least-squares refinement, based on 847 independent reflections with $|F_o| > 3\sigma(F)$, yields an R factor of 0.052. TTF molecules exist as trimers, which are located perpendicularly to each other, forming a two-dimensional network with somewhat close sulfur-sulfur contact among the trimers. The $[\text{SnMe}_2\text{Cl}_4]^{2-}$ anions are disordered with respect to the Sn-Me and Sn-Cl bonds. On the other hand, an X-ray structure analysis of $[\text{TTF}][\text{SnMe}_2\text{Cl}_3]$ obtained by the reaction of $[\text{TTF}]_3[\text{BF}_4]_2$ with SnMe_2Cl_2 and $[\text{Et}_4\text{N}]\text{Cl}$ in acetonitrile has shown that both TTF^+ radical cations and $[\text{SnMe}_2\text{Cl}_3]^-$ anions exist as dimers. The crystals are triclinic, space group $P\bar{1}$, with cell dimensions $a = 9.384(1)$, $b = 10.475(1)$, $c = 8.4517(9) \text{ \AA}$, $\alpha = 92.47(1)$, $\beta = 102.53(1)$, $\gamma = 109.27(1)^\circ$, $V = 756.7(2) \text{ \AA}^3$, and $Z = 2$. The least-squares refinement, based on 3196 independent reflections with $|F_o| > 3\sigma(F)$ yields an R factor of 0.048.

5. References

- 1 K. Kondo, G. Matsubayashi, T. Tanaka, H. Yoshioka, and K. Nakatsu, *J. Chem. Soc. Dalton Trans.*, 1984, 379.
- 2 F. Wudl, *J. Am. Chem. Soc.*, 1975, 97, 1962.
- 3 L. R. Melby, H. D. Hartzler, and W. A. Sheppard, *J. Org. Chem.*,

- 1974, 39, 2456.
- 4 G. Matsubayashi, K. Kondo, and T. Tanaka, *Inorg. Chim. Acta*, 1983, 69, 167.
- 5 F. W. B. Einstein and B. R. Penfold, *J. Chem. Soc. (A)*, 1968, 3019.
- 6 A. J. Buttenshaw, M. Duchene, and M. Webster, *J. Chem. Soc. Dalton Trans.*, 1975, 2230.
- 7 'International Tables for X-Ray Crystallography,' Kynoch Press, Birmingham, 1974, vol. 4.
- 8 C. K. Johnson, ORTEP-II, Report ORNL 5138, Oak Ridge National Laboratory, Tennessee, 1976.
- 9 J. P. Clark and C. J. Wilkins, *J. Chem. Soc. (A)*, 1966, 871.
- 10 I. R. Beattie, F. C. Stokes, and L. E. Alexander, *J. Chem. Soc. Dalton Trans.*, 1973, 465.
- 11 L. E. Smart and M. Webster, *J. Chem. Soc. Dalton Trans.*, 1976, 1924.
- 12 T. E. Phillips, T. J. Kistenmacher, J. P. Ferraris, and D. O. Cowan, *J. Chem. Soc. Chem. Comm.*, 1973, 471.
- 13 B. A. Scott, S. J. La Placa, J. B. Torrance, B. D. Silverman, and B. Webster, *J. Am. Chem. Soc.*, 1977, 99, 6631.
- 14 R. C. Teitelbaum, T. J. Marks, and C. K. Johnson, *J. Am. Chem. Soc.*, 1980, 102, 2986.
- 15 K. Yakushi, S. Nishimura, T. Sugano, H. Kuroda, and I. Ikemoto. *Acta, Crystallogr.*, 1980, B36, 358.
- 16 T. J. Kistenmacher, M. Rossi, C. C. Chiang, R. P. van Duyne, and A. R. Siedle, *Inorg. Chem.*, 1980, 19, 3604.
- 17 S. J. La Placa, P. W. R. Corfield, R. Thomas, and B. A. Scott, *Solid State Comm.*, 1975, 17, 635.
- 18 C. K. Johnson and C. R. Watson, Jr., *J. Chem. Phys.*, 1976, 64, 2271.

- 19 H. Kobayashi and K. Kobayashi, *Bull. Chem. Soc. Jpn.*, 1977, 50, 3127.
- 20 L. Pauling, 'The Nature of the Chemical Bond,' 3rd edn., Cornell University Press, Ithaca, New York, 1960, p 246.
- 21 A. J. Berlinsky, J. F. Caorlan, and L. Weiler, *Solid State Comm.*, 1974, 15, 795; 1976, 19, 1165.
- 22 B. D. Silverman, *J. Chem. Phys.*, 1979, 70, 1614.
- 23 J. P. Lowe, *J. Am. Chem. Soc.*, 1980, 102, 1262.
- 24 T. J. Emge, F. M. Wiygul, J. P. Ferraris, and T. J. Kistenmacher, *Mol. Cryst. Liq. Cryst.*, 1981, 78, 295.
- 25 J. B. Torrance, B. A. Scott, B. Welber, F. B. Kaufman, and P. E. Seiden, *Phys. Rev. B*, 1979, 19, 730.
- 26 H. D. Hanson, K. Mertz, E. Veigel, and J. Weidlein, *Z. anorg. allgem. Chem.*, 1974, 410, 156.
- 27 A. G. Davis, H. J. Milledge, D. C. Puxley, and P. J. Smith, *J. Chem. Soc. (A)*, 1970, 2862.
- 28 T. Tanaka and T. Abe, *Inorg. Nucl. Chem. Lett.*, 1968, 4, 569.
- 29 T. Tanaka, K. Tanaka, and T. Yoshimitsu, *Bull. Chem. Soc. Jpn.*, 1971, 44, 112.

PREPARATION AND ELECTRICAL RESISTIVITIES OF TTF AND TSF SALTS WITH
THE $[\text{SnR}_2\text{Cl}_n]^{2-n}$ ANIONS ($n = 3$ or 4 : $R = \text{Et}$ or Ph) AND X-RAY
CRYSTAL STRUCTURE OF $[\text{TTF}]_3[\text{SnEt}_2\text{Cl}_4]$

1. Introduction

Tetrathiafulvalene (TTF) and tetraselenafulvalene (TSF) are known as good electron donors and can easily be oxidized to stable radical cations, forming electrically conductive salts with various anions.¹ Metal halide anions may be of much interest as the counterparts of TTF^+ or TSF^+ radical cation salt, since they assume various geometries and different formal charges which can affect the packings of donor molecules in crystals. Recently, the crystal structures and the electrical properties of $[\text{TTF}]_3[\text{SnCl}_6]$,² $[\text{TTF}]_3[\text{SnMe}_2\text{Cl}_4]$,³ and $[\text{TTF}][\text{SnMe}_2\text{Cl}_3]$ ³ were reported, in which $[\text{TTF}]_3[\text{SnMe}_2\text{Cl}_4]$ has a novel TTF-packing consisting of trimer units forming a two-dimensional layer and exhibits a low electrical resistivity ($16 \, \Omega \, \text{cm}$ at $25 \, ^\circ\text{C}$ as a compacted pellet).³ Thus, the author undertaken to investigate the TTF and TSF salts with more bulky diorganostannate (IV) anions.

This section describes the preparation and electrical resistivities, of TTF and TSF salts with some diorganochlorostannate anions, $[\text{SnEt}_2\text{Cl}_n]^{2-n}$ ($n = 3$ or 4) and $[\text{SnPh}_2\text{Cl}_4]^{2-}$. The arrangements of TTF and TSF molecules in the crystals also are discussed based on electronic reflectance spectra of the salts, together with an X-ray crystallographic analysis of $[\text{TTF}]_3[\text{SnEt}_2\text{Cl}_4]$.

2. Experimental

Materials. TTF,⁴ TSF,⁵ [TTF]₃[BF₄]₂,⁶ [TSF]₃[BF₄]₂,⁷ SnEt₂Cl₂,⁸ and SnPh₂Cl₂,⁹ were prepared according to the literature methods. [Ph₃PCH₂Ph]Cl was obtained by the equimolar reaction of triphenylphosphine with benzylchloride in benzene.

Preparation of the TTF Salts. To an acetonitrile (30 cm³) solution of [TTF]₃[BF₄]₂ (50 mg, 0.064 mmol) was added an acetonitrile (20 cm³) solution both containing SnEt₂Cl₂ (470 mg, 1.9 mmol) and [Ph₃PCH₂Ph]Cl (50 mg, 0.13 mmol) under nitrogen atmosphere. The mixture was allowed to stand in a refrigerator overnight to yield simple salt [TTF][SnEt₂Cl₃] (1), which were filtered and dried *in vacuo*, 44 % yield based on the TTF⁺ radical cation. A similar reaction taking SnPh₂Cl₂ for the place of SnEt₂Cl₂ afforded simple salt [TTF]₂[SnPh₂Cl₄] (2), 18 % yield.

On the other hand, a similar reaction of an acetonitrile (5 cm³) solution both containing SnEt₂Cl₂ (0.95 mg, 0.38 mmol) and [Ph₃PCH₂Ph]Cl (30 mg, 0.88 mmol) with an acetonitrile (30 cm³) solution of [TTF]₃[BF₄]₂ (30 mg, 0.038 mmol) in the presence of TTF (20 mg, 0.098 mmol) under nitrogen atmosphere afforded complex salt [TTF]₃[SnEt₂Cl₄] (3), 16 % yield. The same salt was obtained also by the electrolysis of an acetonitrile (10 cm³) solution containing TTF (51 mg, 0.25 mmol), SnEt₂Cl₂ (250 mg, 1.0 mmol), and [Ph₃PCH₂Ph]Cl (180 mg, 0.50 mmol) for 11 days under the conditions described elsewhere,¹⁰ 8 % yield based on TTF. By taking SnPh₂Cl₂ for the place of SnEt₂Cl₂, the electrolysis under the same condition gave complex salt [TTF]_{3.3}[SnPh₂Cl₄] (4), 16 % yield.

Preparation of the TSF Salts. In contrast to the TTF salts, electrocrystallization from an acetonitrile (10 cm^3) solution containing TSF (51 mg, 0.13 mmol), SnPh_2Cl_2 (340 mg, 1.0 mmol), and $[\text{Ph}_3\text{PCH}_2\text{Ph}]\text{Cl}$ (180 mg, 0.50 mmol) for 11 days afforded simple salt $[\text{TSF}]_2[\text{SnPh}_2\text{Cl}_4]$ (5), 33 % yield based on TSF. On the other hand, the reaction of an acetonitrile (5 cm^3) solution containing SnPh_2Cl_2 (190 mg, 0.56 mmol) and $[\text{Ph}_3\text{PCH}_2\text{Ph}]\text{Cl}$ (14 mg, 0.037 mmol) with an acetonitrile (30 cm^3) solution of $[\text{TSF}]_3[\text{BF}_4]_2$ (50 mg, 0.37 mmol) in the presence of TSF (20 mg, 0.51 mmol) under nitrogen atmosphere gave complex salt $[\text{TSF}]_{3.3}[\text{SnPh}_2\text{Cl}_4]$ (6), 36 % yield.

Ratios of the TTF^+ radical cation to neutral TTF^0 in the salts were determined from electronic absorption spectra in acetonitrile. The presence of diorganostannate groups in the salts obtained were confirmed from ^1H NMR spectra in conc. HNO_3 . The analyses and properties of the salts are listed in Table 1.

Physical Measurements. Electronic absorption spectra in acetonitrile and powder reflectance spectra were recorded as described elsewhere.² Electrical resistivities were measured as compacted samples by the conventional two-probe method.¹¹

X-Ray Crystal Structure Determination of Salt 3. The initial unit-cell parameters were determined from oscillation and Weissenberg photographs. Accurate parameters were obtained from the least-squares fit of angular coordinates of 25 reflections with 2θ values from 24° to 30° which were measured with a Rigaku automatic four-circle diffractometer with $\text{Mo-K}\alpha$ ($\lambda = 0.71069\text{ \AA}$) radiation.

Crystal data for 3. $\text{C}_{22}\text{H}_{22}\text{Cl}_4\text{S}_{12}\text{Sn}$, $M = 931.6$, tetragonal,

Table 1. Analyses and physical properties of the salts

No.	Salt	Color	m.p. (dec.)/°C	Found (calcd.)	
				C %	H %
1 ~	[TTF][SnEt ₂ Cl ₃]	Brown Plates	> 158	25.24 (24.64)	3.14 (2.89)
2 ~	[TTF] ₂ [SnPh ₂ Cl ₄]	Brown microcrystals	> 149	34.97 (35.01)	2.49 (2.20)
3 ~	[TTF] ₃ [SnEt ₂ Cl ₄]	Black Plates	> 197	28.71 (28.37)	2.60 (2.38)
4 ~	[TTF] _{3.3} [SnPh ₂ Cl ₄]	Brown microcrystals	> 137	34.98 (35.08)	2.40 (2.15)
5 ~	[TSF] ₂ [SnPh ₂ Cl ₄]	Dark green microcrystals	> 134	24.27 (24.05)	1.69 (1.51)
6 ~	[TSF] _{3.3} [SnPh ₂ Cl ₄]	Dark green microcrystals	> 155	21.91 (22.33)	1.54 (1.37)

space group $I4cm$, $a = 11.710(3)$, $c = 25.242(7)$ Å, $V = 3461(2)$ Å³, $Z = 4$, $D_C = 1.789(1)$ g cm⁻³, $\mu(\text{Mo-K}\alpha) = 17.6$ cm⁻¹.

The intensity data were collected for a specimen with the dimensions of 0.25 x 0.30 x 0.10 mm by the $2\theta - \omega$ scan rate of 8° min⁻¹ up to $2\theta = 50^\circ$. The scan width in ω was $(0.8 + 0.35\tan\theta)^\circ$ and three standard reflections were monitored before every 100 reflections. No intensity decay was observed during the data collection. Lorentz and polarization effects were corrected, but no absorption correction was made.

Positions of Sn atoms were determined by the heavy-atom method on the basis of 479 reflections of $|F_O| > 3\sigma(F)$ among the 926 independent reflections. Although three possible space groups, $I\bar{4}c2$, $I4cm$, and $I4/mcm$, were suggested from the intensity data on the basis of the absence rule, the $I4cm$ was proved to be suitable in a successful analysis, and the positions of all nonhydrogen atoms except for the methyl-carbon atoms of ethyl groups were given by the Fourier maps. A structure refinement was performed by the block-diagonal least-squares method assuming anisotropic thermal parameters for the nonhydrogen atoms to give residual indices $R = \Sigma ||F_O| - |F_C|| / \Sigma |F_O| = 0.082$ and $R' = [\Sigma w(|F_O| - |F_C|)^2 / \Sigma w|F_O|^2]^{1/2} = 0.11$. The weighting scheme was $1/w = \sigma^2(F_O) + 0.01$ $0.01(F_O)^2$. Atomic scattering factors were taken from the table.¹² The final atomic coordinates with standard deviations are given in Table 2.

Crystallographic calculations were performed on an ACOS 900S computer at the Crystallographic Research Center, Institute for Protein Research, Osaka University. Figures 1 - 3 are drawn by the local version of ORTEP-II program.¹³

Table 2. Final atomic coordinates ($\times 10^4$) for $[\text{TTF}]_3[\text{SnEt}_2\text{Cl}_4]$ with the estimated standard deviations in parentheses

Atom	X	Y	Z
Sn	0(0)	0(0)	0(3)
Cl(1)	0(0)	0(0)	1057(4)
Cl(2)	0(0)	0(0)	-1023(7)
Cl(3)	484(19)	2187(16)	40(10)
S(1)	1974(9)	1239(19)	3096(4)
S(2)	2062(9)	1178(9)	1806(4)
S(3)	885(9)	4115(9)	2781(8)
S(4)	873(10)	4127(10)	1494(7)
C(1)	2368(55)	1750(44)	3695(14)
C(2)	2917(30)	2083(30)	2721(17)
C(3)	2942(27)	2058(27)	2191(20)
C(4)	2422(30)	1766(28)	1155(12)
C(5)	414(65)	4586(65)	3345(29)
C(6)	0(0)	5000(0)	2365(23)
C(7)	0(0)	5000(0)	1867(23)
C(8)	375(42)	4625(42)	887(29)
C(9)	247(59)	1867(57)	-30(31)

3. Results and Discussion

The Crystal Structure of $[\text{TTF}]_3[\text{SnEt}_2\text{Cl}_4]$ (3). The crystal structure of **3** projected along a and c axes are shown in Figure 1 and 2, respectively, where atoms are drawn by using arbitrary isotropic thermal parameters for simplification. Bond lengths and angles as well as relevant intermolecular atom-atom contacts are summarized in Table 3.

The tin atoms of distorted octahedral $[\text{SnEt}_2\text{Cl}_4]^{2-}$ anions occupy the positions $(0, 0, 0)$, $(1/2, 1/2, 0)$, $(0, 0, 1/2)$, and $(1/2, 1/2, 1/2)$, where four-fold axes exist parallel to the c axis.

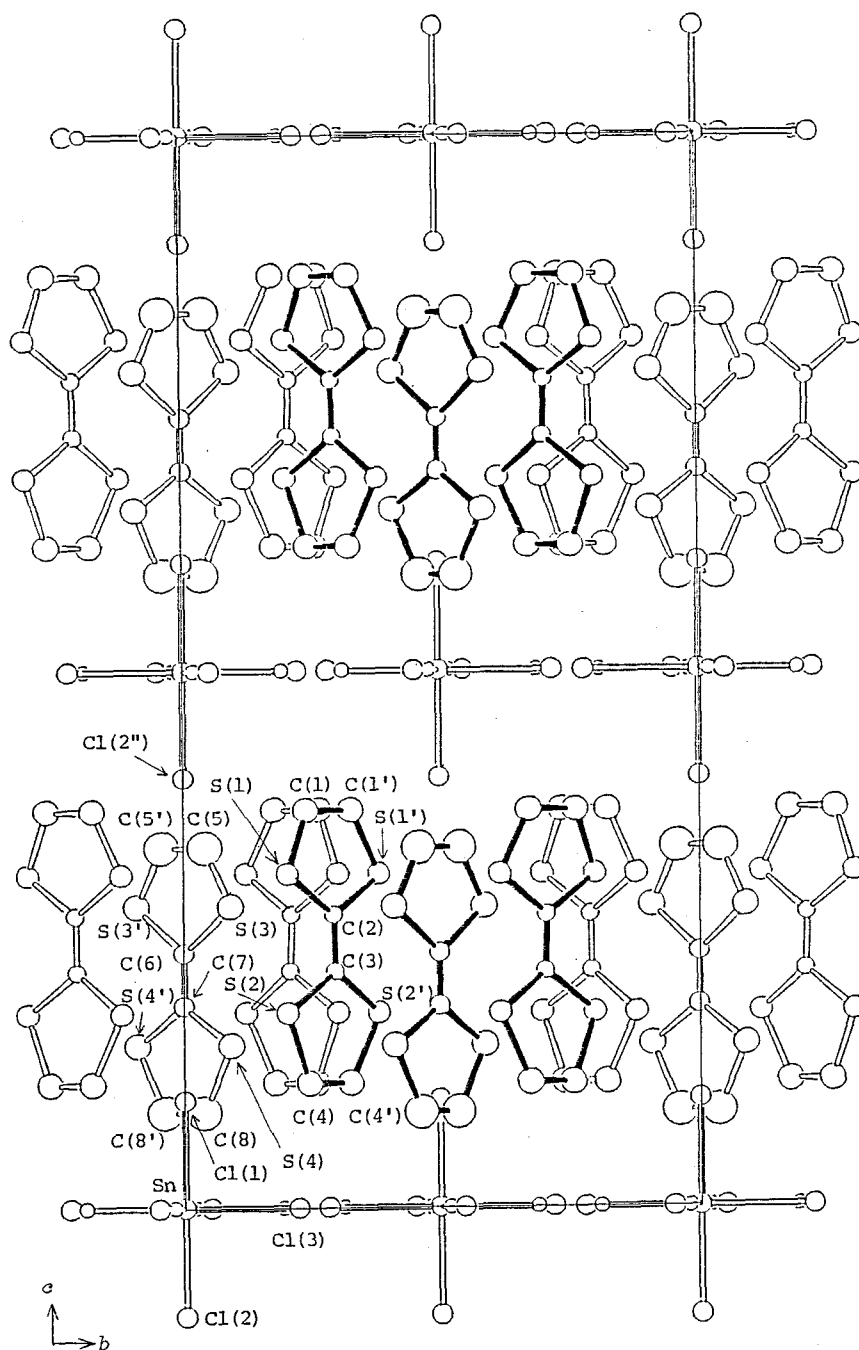


Figure 1. The crystal structure of 3 projected along the a axis. The atoms are drawn with arbitrary isotropic thermal factors for simplification.

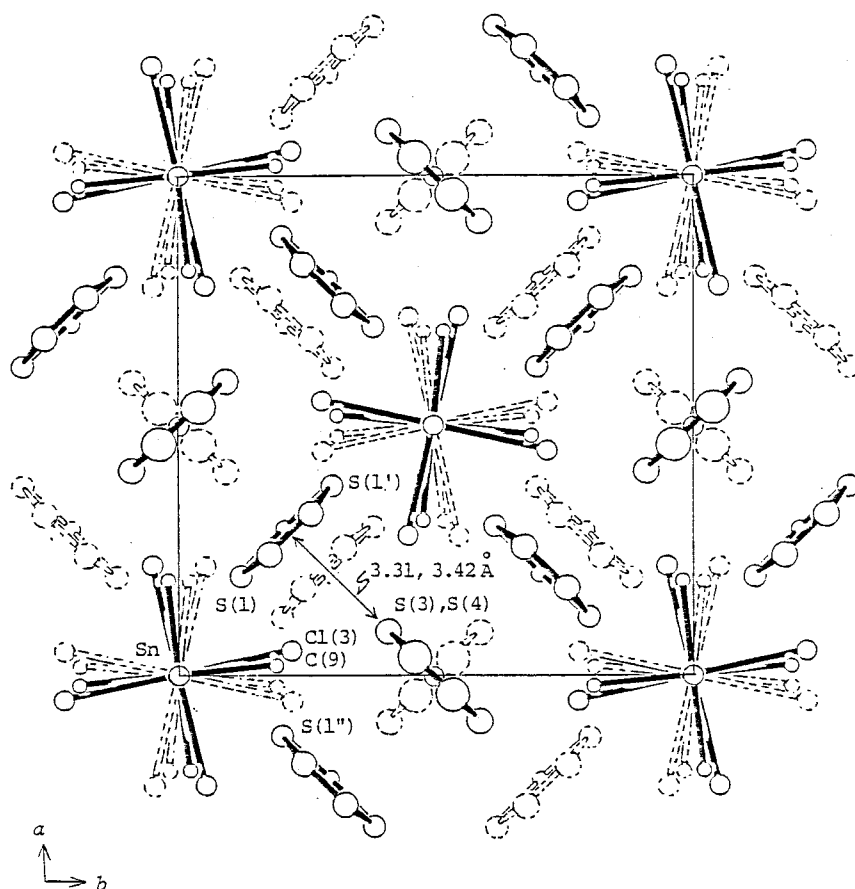


Figure 2. The crystal structure of **3** projected along the *c* axis. The atoms are drawn with arbitrary isotropic thermal factors for simplification.

Two chlorine atoms as well as two methylene-carbon atoms of the ethyl groups are almost on the (001) and (002) planes and they are disordered on these planes. A similar disorder with respect to chlorine atoms and methyl groups has been reported for $[\text{TTF}]_3^- [\text{SnMe}_2\text{Cl}_4]$.³ Positions of the methyl carbons have not been determined. The Sn-Cl distances (2.58(2), 2.62(2), and 2.67(1) Å) are close to those of $[\text{TTF}]_3 [\text{SnMe}_2\text{Cl}_4]$ (2.599(5) and 2.600(3) Å)³ and

Table 3. Selected bond distances (Å) and angles (°)^a of [TTF]₃[SnEt₂Cl₄] (3) with the estimated standard deviations in parentheses

Sn-Cl(1)	2.67(1)	S(3)-C(6)	1.80(4)
Sn-Cl(2)	2.58(2)	S(4)-C(7)	1.73(3)
Sn-Cl(3)	2.62(2)	S(4)-C(8)	1.74(7)
Sn-C(9) ^b	2.21(7)	C(1)-C(1')	1.46(13)
Cl(3)-C(9) ^b	0.50(7)	C(2)-C(3)	1.34(7)
S(1)-C(1)	1.69(4)	C(4)-C(4')	1.34(7)
S(1)-C(2)	1.76(3)	C(5)-C(5')	1.37(16)
S(2)-C(3)	1.75(4)	C(6)-C(7)	1.26(8)
S(2)-C(4)	1.83(3)	C(8)-C(8')	1.24(15)
S(3)-C(5)	1.62(7)		
Cl(1)-Sn-Cl(2)	0.0(0)	S(2)-C(3)-S(2')	113(2)
Cl(1)-Sn-Cl(3)	87.8(6)	C(3)-S(2)-C(4)	98(2)
Cl(2)-Sn-Cl(3)	92.2(6)	S(2)-C(4)-C(4')	115(3)
Cl(1)-Sn-C(9) ^b	92(2)	C(5')-C(5)-S(3)	119(6)
Cl(2)-Sn-C(9) ^b	88(2)	C(5)-S(3)-C(6)	97(3)
Cl(3)-Sn-C(9) ^b	7(2)	S(3)-C(6)-S(3')	109(2)
C(1')-C(1)-S(1)	115(5)	S(3)-C(6)-C(7)	126(2)
C(1)-S(1)-C(2)	96(2)	S(6)-C(7)-S(4)	123(2)
S(1)-C(2)-S(1')	115(2)	S(4)-C(7)-S(4')	114(2)
S(1)-C(2)-C(3)	113(2)	C(7)-S(4)-C(8)	95(2)
C(2)-C(3)-S(2)	124(2)	S(4)-C(8)-C(8')	118(6)
non-bonded distances ^c			
S(1) --- S(3)	3.69(3)	S(2) --- Cl(1)	3.36(2)
S(1'') --- S(3)	3.62(3)	S(1) --- Cl(2'')	3.52(3)

^a The atoms with the prime are in the mirror symmetry with respect to the atoms with the same number (see Figures 1 and 2).

^b The atom C(9) is the methylene carbon atom of the ethyl group.

^c See Figures 1 and 2.

[Pyridinium]₂[SnMe₂Cl₄] (2.603(2) and 2.625(2) Å).¹⁴ The Sn-C(9) bond (2.21(7) Å) is slightly longer than those respected for [Pyridinium]₂[SnMe₂Cl₄] (2.109(9) Å),¹⁴ [SnMe₂Cl(terpyridyl)]-[SnMe₂Cl₃] (2.11(5) and 2.12(4) Å for the anion moiety),¹⁵ and [Mo₃(h⁵-C₅H₅)₃S₄][SnMe₃Cl₂] (2.12(1) Å),¹⁶ whereas it is shorter than that for (EtSn(OH)Cl₂·H₂O)₂ (2.304(30) Å).¹⁷

TTF moieties exist as a trimer unit, where the cofacial molecular planes are located parallel to the *c* axis, spaced by the same distance. The molecular overlap of the TTF moieties within the trimer unit has a considerable lateral shift (0.79 Å) along the long molecular axis, as shown in Figure 3. This is different from the eclipsed overlap of the TTF moieties in [TTF]₃[SnCl₆]² and [TTF]₃[SnMe₂Cl₄].³ Moreover, the TTF-trimers are arranged perpendicularly to one another, the centers of two terminal TTF molecules of the trimer unit being on *z* = 0.245 and 0.745 (Figure 1). Thus, the two-dimensional TTF-layers are constructed parallel to the *c* plane, which is very similar to those of [TTF]₃[SnCl₆] and

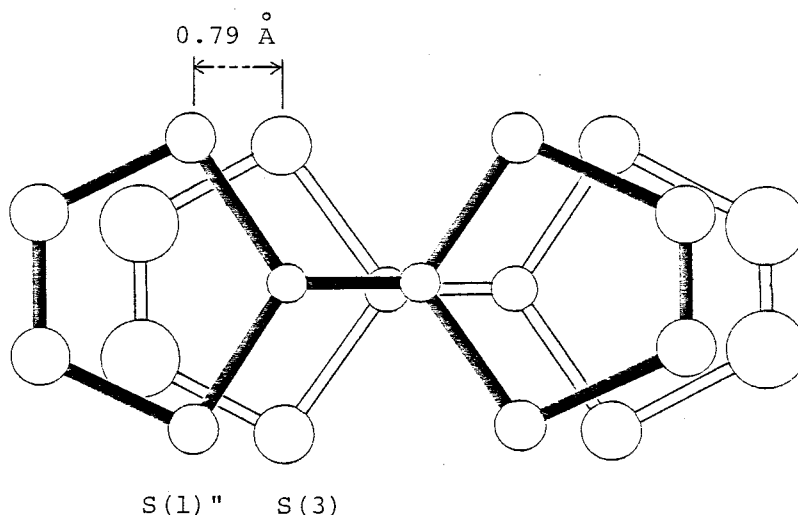


Figure 3. The overlap scheme of the TTF moieties in the trimer unit.

[TTF]₃[SnMe₂Cl₄], except for a significant shift from the TTF-eclipsed overlap within the trimer unit in the present salt.

The intermolecular spacing (3.46(2) Å) within the TTF-trimer unit is close to those of [TTF]₃[SnCl₆] (3.493(2) Å)² and [TTF]₃-[SnMe₂Cl₄] (3.499(2) Å).³ The sulfur-sulfur distance (3.62(3) Å) within the trimer unit is somewhat longer than those of the [SnCl₆]²⁻ and [SnMe₂Cl₄]²⁻ analogs (3.493(2) and 3.498(3) Å, respectively)^{2,3} owing to the considerable lateral shift in the TTF overlap in the present salt. The closest sulfur-sulfur contact between the TTF trimer units is 3.69(3) Å, which is almost equal to the sum of van der Waals radii of sulfur atoms,¹⁸ and is slightly longer than that of [TTF]₃[SnMe₂Cl₄] (3.649(3) Å)³ and rather close to that of [TTF]₃[SnCl₆] (3.705(2) Å).² On the other hand, the distances between the sulfur atoms (S(3) and S(4)) of the central TTF molecule and the neighbouring TTF molecular plane are 3.31(2) and 3.42(2) Å, respectively (see Figure 2), which are similar to the corresponding sulfur-TTF plane distances in [TTF]₃[SnCl₆] (3.40 Å)² and [TTF]₃[SnMe₂Cl₄] (3.34 Å). Thus, the present salt also forms the two-dimensional layer consisting of the TTF trimer units and a high electrical conductivity through the layer may be expected, as mentioned in the later section.

Although a weak interaction is observed between Cl(2) and S(1) atoms (3.52(3) Å), the Cl(1) - S(2) distance (3.362(2) Å)² is appreciably shorter than the sum of van der Waals radii of sulfur and chlorine atoms (3.65 Å),¹⁸ and is close to the shortest sulfur-chlorine distances reported for [TTF]₃[SnCl₆] (3.367(2) Å)² and [TTF]₃[SnMe₂Cl₄] (3.344(2) Å).³ This may be due to the electrostatic interaction between the rather positively polarized TTF-sulfur and the negatively polarized chlorine atoms. In accordance with the short Cl(1) - S(2) distance, the Sn - Cl(1) bond

(2.67(1) Å) is somewhat elongated in comparison with the Sn - Cl(2) bond (2.58(2) Å).

Electronic Spectra. Figure 4 illustrates the powder electronic reflectance spectra of salts 1, 3, 4, and 5. In the frequency region higher than 15000 cm⁻¹ are observed the local excitation (LE) bands of TTF⁺ or TSF⁺ radical cations and neutral TTF⁰ or TSF⁰ molecules.^{19,20} Salt 1 containing the TTF⁺ radical cation exhibits a band around 12500 cm⁻¹, which is assigned to the charge transfer (CT) transition within the TTF⁺ radical cation dimer.^{20,21} The same CT band was observed at 12800 cm⁻¹ in salt 2 (see Table 4). Analogously, salt 5 display the band due to the (TSF⁺)₂ dimer, the frequency being lower than that of the (TTF⁺)₂

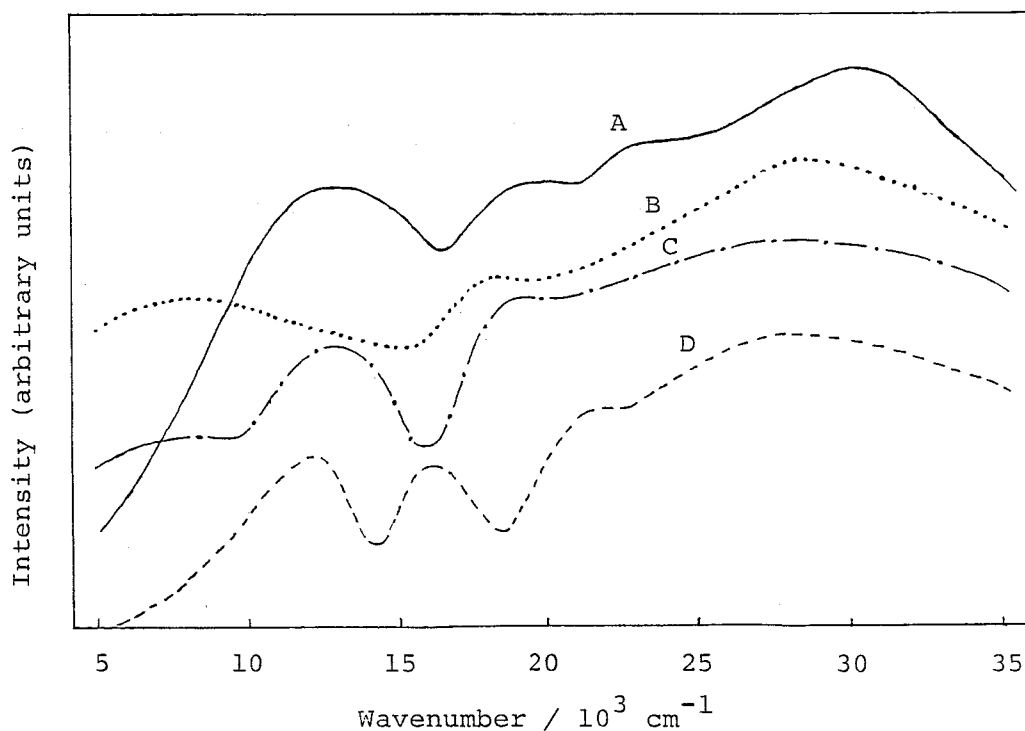


Figure 4. The powder electronic reflectance spectra of 1 (A), 3 (B), 4 (C), and 5 (D).

Table 4. The powder electronic reflectance spectra of the salts

No.	LE band/ 10^3 cm^{-1}			CT band/ 10^3 cm^{-1}	
				$D^{\dagger}/D^{\dagger^a}$	D^{\dagger}/D^{0^a}
1	30.1	22.9	19.4	12.5	
2	26.6	b	19.1	12.8	
3	28.1	b	18.2		8.7
4	28.1	b	19.1	12.8	8.8
5	27.2	22.3	16.1	12.2	
6	27.8	21.6	16.0	12.2	8.8

^a D = TTF or TSF. ^b Has not been determined owing to being obscured by the high frequency bands.

dimer. This is compatible with the fact that salt 5 has a considerably lower resistivity than salt 1, as described later.

Salt 3 in the solid state exhibits a broad band at 8700 cm^{-1} as well as LE bands with higher frequencies. The low frequency band is ascribed to the CT transition between the TTF^{\dagger} radical cation and neutral TTF^0 within the TTF trimer, suggesting the arrangement of the $\text{TTF}^{\dagger}/\text{TTF}^0/\text{TTF}^{\dagger}$ trimer. The same arrangement has been reported for $[\text{TTF}]_3[\text{SnCl}_6]^2$ and $[\text{TTF}]_3[\text{SnMe}_2\text{Cl}_4]^3$. On the other hand, salt 4 displays two broad bands around 12800 and 8800 cm^{-1} besides the LE bands in the higher frequency region. These can be ascribed to the CT transitions due to $\text{TTF}^{\dagger}/\text{TTF}^{\dagger}$ and $\text{TTF}^{\dagger}/\text{TTF}^0$, respectively. In view of this result together with a relatively low resistivity, as described in the later section, 4 may assume a columnar structure involving both $\text{TTF}^{\dagger}/\text{TTF}^{\dagger}$ and

Table 5. Electrical resistivities (ρ) and activation energies (E_a) of the salts

No.	$\rho_{25\text{ }^\circ\text{C}} / \Omega \text{ cm}$	E_a / eV
1	2.1×10^8	0.53
2	9.0×10^8	0.60
3	4.2×10^1	0.13
4	2.9×10^3	0.28
5	7.1×10^3	0.10
6	3.0×10^3	0.18

$\text{TTF}^{\dagger}/\text{TTF}^0$ interactions. A similar structure to 4 is suggested for salt 6, based on the similarity between the spectra of these salts (Table 4).

Electrical Resistivities. The temperature dependence of the electrical resistivities (ρ) of compacted samples has indicated that all the salts behave as typical semiconductors in the temperature range of $-20 - +30\text{ }^\circ\text{C}$. Table 5 summarizes the resistivities at $25\text{ }^\circ\text{C}$ ($\rho_{25\text{ }^\circ\text{C}}$) and activation energies (E_a) for electrical conduction. Salt 1 constructed from the TTF^{\dagger} radical cation dimers exhibits a large resistivity and a high activation energy, indicating that each $(\text{TTF}^{\dagger})_2$ dimer is located separately in the crystals, as was seen in $[\text{TTF}][\text{SnMe}_2\text{Cl}_3]$.³ A large resistivity is formed in salt 2 also containing the TTF^{\dagger} radical cation dimers, whereas the TSF^{\dagger} radical cation analog, 5, exhibits a considerably small resistivity. The same tendency has been observed also between the TTF and TSF salts with tris(oxalato)metallate anions ($M = \text{Si}, \text{Ge}, \text{and Sn}$).¹¹

Salt 3 displays fairly small resistivity and a low activation energy. The electrical conduction in this salt may occur through the two-dimensional layer consisting of the TTF trimer units, as clarified by the X-ray crystallographic analysis. On the other hand, salt 4 exhibits a resistivity and an activation energy larger than those of salt 3, although there exists neutral TTF^0 as well as the TTF^+ radical cations. This is indicative of the TTF stack being not suitable for the appearance of a high conductivity in spite of the observation of $\text{TTF}^+/\text{TTF}^+$ and $\text{TTF}^+/\text{TTF}^0$ charge transfer bands. The TSF analog, 6, also display the similar properties. Such TTF and TSF stacks and electrical resistivities have been observed in the TTF and TSF salts with bis(oxalato)cuprate and -platinate anions²¹ and with tetrahalogenometallate anions (MX_4^{2-} : M = Cd and Zn, X = Cl and Br).²²

4. Summary

Tetrathiafulvalene (TTF) and tetraselenafulvalene (TSF) salts with diorganochlorostannate anions, $[\text{TTF}][\text{SnEt}_2\text{Cl}_3]$ (1), $[\text{TTF}]_2[\text{SnPh}_2\text{Cl}_4]$ (2), $[\text{TTF}]_3[\text{SnEt}_2\text{Cl}_4]$ (3), $[\text{TTF}]_{3.3}[\text{SnPh}_2\text{Cl}_4]$ (4), $[\text{TSF}]_2[\text{SnPh}_2\text{Cl}_4]$ (5), and $[\text{TSF}]_{3.3}[\text{SnPh}_2\text{Cl}_4]$ (6), were prepared by the reactions of $[\text{TTF or TSF}]_3[\text{BF}_4]_2$ with SnR_2Cl_2 (R = Et or Ph) in the presence of $[\text{Ph}_3\text{PCH}_2\text{Ph}]\text{Cl}$ and by electrocrystallization of TTF or TSF in acetonitrile containing SnR_2Cl_2 and $[\text{Ph}_3\text{PCH}_2\text{Ph}]\text{Cl}$. All the salts behave as semiconductors with electrical resistivities in the order of $10^1 - 10^8 \Omega \text{ cm}$ as compacted samples at 25 °C. Electronic reflectance spectra of simple salts 1, 2, and 5 show a band due to the dimeric $(\text{TTF}^+)_2$ or $(\text{TSF}^+)_2$ unit in the 12200 - 12800 cm^{-1} region. Complex salt 3 exhibits a $\text{TTF}^+/\text{TTF}^0$ charge

transfer (CT) band at 8700 cm^{-1} , and the remaining complex salts 4 and 6 display both CT bands between the radical cations and between the radical cation and the neutral donor molecule. The crystal structure of 3 was determined by a single crystal X-ray diffraction. The tetragonal crystal, space group $I4cm$, has cell dimensions $a = 11.710(3)$, $c = 25.242(7)\text{ \AA}$, and $Z = 4$. The structure was solved by the heavy atom method and refined to the final R value 0.082 for 479 independent reflections with $|F_o| > 3\sigma(F)$. TTF molecules exist as trimers, in which a slight lateral shift from the eclipsed TTF overlap occurs, although TTF molecules are arranged with an equal spacing. The trimer units are located perpendicularly to each other, forming a two-dimensional layer. The $[\text{SnEt}_2\text{Cl}_4]^{2-}$ anion is disordered with respect to the two Sn-Et and two Sn-Cl bonds.

5. References

- 1 A. R. Siedle, G. A. Candela, T. F. Finnegan, R. P. van Duyne, T. Cape, G. F. Kokoszka, P. M. Woyciesjes, J. A. Hashmall, M. Glick, and W. Ilsley, *Ann. N. Y. Acad. Sci.*, 1978, 313.
- P. Kathirgamanathan, S. A. Mucklejohn, and D. Rosseinsky, *J. Chem. Soc., Chem. Commun.*, 1979, 86.
- A. R. Siedle, G. A. Candela, T. F. Finnegan, R. P. van Duyne, T. Cape, G. F. Kokoszka, P. M. Woyciejes, and J. A. Hashmall, *Inorg. Chem.*, 1981, 20, 2635.
- P. Kathirgamanathan and D. R. Rosseinsky, *J. Chem. Soc., Chem. Commun.*, 1980, 356.
- T. J. Kistenmacher, M. Rossi, C. C. Chiang, R. P. van Duyne, and A. R. Siedle, *Inorg. Chem.*, 1980, 19, 3604.
- K. Yakushi, S. Nishimura, T. Sugano, and H. Kuroda, *Acta Cryst.*, 1980, B36, 358.
- R. C. Teitelbaum,

- T. J. Marks, and C. K. Johnson, *J. Am. Chem. Soc.*, 1980, 102, 2986. G. C. Pavassiliou, *Mol. Cryst. Liq. Cryst.*, 1982, 86, 159. M. Bousseau, L. Valade, M. F. Bruniquel, P. Cassoux, M. Garbauskas, L. Interrante, and J. Kasper, *Nouv. J. Chim.*, 1984, 8, 3.
- 2 K. Kondo, G. Matsubayashi, T. Tanaka, H. Yoshioka, and K. Nakatsu, *J. Chem. Soc., Dalton Trans.*, 1984, 379.
- 3 G. Matsubayashi, K. Ueyama, and T. Tanaka, *J. Chem. Soc., Dalton Trans.*, in press.
- 4 L. R. Merby, H. D. Hartzler, and W. A. Sheppard, *J. Org. Chem.*, 1974, 39, 2456.
- 5 M. V. Lakshmikantham and M. P. Cava, *J. Org. Chem.*, 1976, 41, 882.
- 6 F. Wudl, *J. Am. Chem. Soc.*, 1975, 97, 1962.
- 7 W. M. Walsh, Jr., L. W. Rupp, Jr., F. Wudl, M. L. Kaplan, D. E. Schafer, G. A. Thomas, and R. Gemmer, *Solid State Commun.*, 1980, 33, 413.
- 8 K. A. Kozeshkow, *Ber.*, 1933, 66, 1661.
- 9 H. Gilman and L. A. Gist, Jr., *J. Org. Chem.*, 1957, 22.
- 10 K. Ueyama, G. Matsubayashi, and T. Tanaka, *Inorg. Chim. Acta*, 1984, 87, 143.
- 11 S. Araki, H. Ishida, and T. Tanaka, *Bull. Chem. Soc. Jpn.*, 1978, 51, 407.
- 12 'International Table for X-Ray Crystallography,' vol. IV, Kynoch press, Birmingham (1974).
- 13 C. K. Johnson. ORTEP-II: A FORTRAN Thermal-Ellipsoid Plot Program for Crystal Structure Illustrations, ORNL-5138, March 1976. Oak Ridge National Laboratory.
- 14 L. E. Smart and M. Webster, *J. Chem. Soc., Dalton Trans.*, 1976, 1923.

- 15 F. W. B. Einstein and B. R. Penfold, *J. Chem. Soc. (A)*, 1968, 3019.
- 16 P. J. Vergammi, H. Vahrenkamp, and L. F. Dahl, *J. Am. Chem. Soc.*, 1971, 93, 6327.
- 17 P. C. Lecomte, J. Protas, and M. Devaud, *Acta Cryst.*, 1976, B32, 923.
- 18 L. Pauling, 'The Nature of the Chemical Bond,' 3rd ed., Cornell University Press, Ithaca, New York, 1960, p. 246.
- 19 J. B. Torrance, B. A. Scott, B. B. Welba, F. B. Kaufman, and P. E. Sieden, *Phys. Rev. B*, 1979, 19, 730.
- 20 T. Sugano, K. Yakushi, and H. Kuroda, *Bull. Chem. Soc. Jpn.*, 1978, 51, 1041.
- 21 K. Ueyama, A. Tanaka, G. Matsubayashi, and T. Tanaka, *Inorg. Chim. Acta*, in press.
- 22 A. Tanaka, G. Matsubayashi, and T. Tanaka, to be published.

CHAPTER 4

X-RAY CRYSTAL STRUCTURE AND PROPERTIES OF TRIS(TETRATHIAFULVALENium) HEXACHLOROPLATINATE

1. Introduction

Several electrically conductive tetrathiafulvalene (TTF) salts with metal halide anions have been prepared,¹⁻⁶ some of which have been analysed by X-ray crystallography.³⁻⁵ Recently, a new type of TTF arrangement as the trimer unit was reported in the $[\text{TTF}]_3^- [\text{SnCl}_6]^{4-}$ and $[\text{TTF}]_3 [\text{SnMe}_2\text{Cl}_4]^{5-}$.

Previously Siedle and co-workers⁶ reported the reaction of TTF with K_2PtCl_4 to afford $[\text{TTF}]_2\text{PtCl}_2$ which may contain the TTF^+ radical cation and neutral TTF^0 , as confirmed from the Raman spectrum. The structure, however, has not been clarified. Although several attempts of the author for the reaction of TTF with K_2PtCl_4 have afforded no crystalline salts, the reaction of neutral TTF^0 with $[\text{Bu}^n_4\text{N}]_2[\text{PtCl}_6]$ in acetonitrile has yielded black plates formulated as $[\text{TTF}]_3[\text{PtCl}_6]$, which has the same composition as $[\text{TTF}]_3[\text{SnCl}_6]$, with a high conductivity. This chapter describes the crystal structure and properties of $[\text{TTF}]_3[\text{PtCl}_6]$.

2. Experimental

Diffusion of TTF and $[\text{Bu}^n_4\text{N}]_2[\text{PtCl}_6]$ in acetonitrile using a conventional U-tube⁷ gave black plates of $[\text{TTF}]_3[\text{PtCl}_6]$, m.p. (decomp.) > 300 °C. The chemical analysis (Found: C, 21.8; H, 1.4.

Calc. for $C_{18}H_{12}S_{12}Cl_6Pt$; C, 12.2; H, 1.2 %).

Powder electronic reflectance⁴ and X-ray photoelectron spectra⁸ were recorded as described elsewhere. Electrical resistivities were measured as compacted samples by the conventional two-probe method.⁹

X-Ray Crystal Structure of $[TTF]_3[PtCl_6]$. Oscillation and Weissenberg photographs indicated a tetragonal system and possible space group of $P\bar{4}b2$, $P4bm$, and $P4/mbm$. The latter was probed to be correct from the successful analysis. Accurate unit-cell parameters were obtained from the 25 reflections with 2θ values from $29 - 36^\circ$ measured with a computer-controlled Rigaku four-circle diffractometer with Mo-K α ($\lambda = 0.71069 \text{ \AA}$) radiation.

Crystal data. $C_{18}H_{12}S_{12}Cl_6Pt$, $M = 1020.8$, tetragonal, space group $P4/mbm$, $a = 11.757(2)$, $c = 11.707(2) \text{ \AA}$, $U = 1618.2(4) \text{ \AA}^3$, $Z = 2$, $D_c = 2.096(1) \text{ g cm}^{-3}$, $F(000) = 984$, and $\mu(\text{Mo-K}\alpha) = 58.1 \text{ cm}^{-1}$.

Intensity data were collected for a crystal of size $0.50 \times 0.35 \times 0.08 \text{ mm}$ by the ω - 2θ scan technique up to $2\theta = 55^\circ$ with the scan rate of $4^\circ/\text{min}$ in 2θ and the scan width in ω was $(1.5 + \tan\theta)^\circ$. 1143 Independent reflections were measured, of which 804 with $|F_o| > 3\sigma(F)$ were used in the subsequent calculations. The structure was solved by the Patterson method and the positions of non-hydrogen atoms clarified from the successive Fourier syntheses. Positions of hydrogen atoms were not determined. Block-diagonal least-squares refinement with anisotropic thermal parameters for all the non-hydrogen atoms gave the final indices $R = \Sigma ||F_o| - |F_c|| / \Sigma |F_o| = 0.11$ and $R' = [\Sigma w(|F_o| - |F_c|)^2 / \Sigma w|F_o|^2]^{1/2} = 0.15$ with the weighting scheme $1/w = \sigma^2(F_o) + 0.01(F_o)^2$. Atomic scattering factors were taken from the tabulation.¹⁰ The final atomic coordinates with the standard deviations are listed in Table 1.

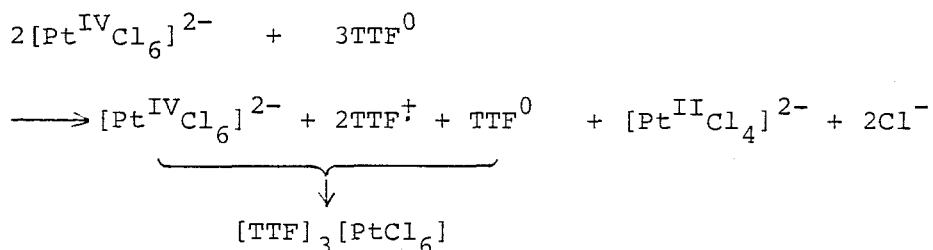
Table 1. Final atomic co-ordinates ($\times 10^4$) for $[\text{TTF}]_3[\text{PtCl}_6]$ with the estimated standard deviations in parentheses.

Atom	X	Y	Z
Pt	0(0)	0(0)	0(0)
Cl(1)	0(0)	0(0)	1986(6)
Cl(2)	1956(5)	324(5)	0(0)
S(1)	1220(3)	2024(4)	3520(4)
S(2)	4121(6)	879(6)	3602(23)
C(1)	1755(16)	2437(18)	2327(14)
C(2)	2085(12)	2915(12)	4439(18)
C(3)	4597(49)	4025(29)	2282(84)
C(4)	5000(0)	0(0)	4344(95)

Crystallographic calculations were performed on an ACOS 900S computer at the Crystallographic Research Center, Institute for Protein Research, Osaka University. Figures 1 and 2 were drawn by the local version of ORTEP-II program.¹¹

3. Results and Discussion

Since TTF has a low oxidation potential (0.33 V *vs.* SCE)¹² and the $[\text{Pt}^{\text{IV}}\text{Cl}_6]^{2-}$ anion also a considerably low reduction potential (0.68 V *vs.* NHE; corresponds to 0.44 V *vs.* SCE),¹³ $[\text{TTF}]_3^-$ $[\text{PtCl}_6]$ may be obtained by the redox reaction between TTF and the $[\text{Pt}^{\text{IV}}\text{Cl}_6]^{2-}$ anion forming the TTF^+ radical cation and the $[\text{Pt}^{\text{II}}\text{Cl}_4]^{2-}$ anion as formulated in the following equation.



The crystal structure of the salt is illustrated in Figures 1 and 2. Bond lengths and angles as well as relevant intermolecular atom-atom contacts are summarized in Table 2. The octahedral $[\text{PtCl}_6]^{2-}$ anion occupies the origin and $(1/2, 1/2, 0)$. The Pt-Cl distances $(2.325(7) \text{ \AA} \text{ and } 2.330(6) \text{ \AA})$ are very close to that of K_2PtCl_6 (2.33 \AA) .¹⁴ TTF molecules are arranged co-facially to form a trimer unit with the equal intermolecular spacing of $3.49(3) \text{ \AA}$, and overlapped in the eclipsed form within the trimer unit. These findings are the same as the case of $[\text{TTF}]_3[\text{SnCl}_6]^4$ and $[\text{TTF}]_3[\text{SnMe}_2\text{Cl}_4]$.⁵

The powder electronic reflectance spectrum has exhibited a broad band at 8900 cm^{-1} due to the $\text{TTF}^+/\text{TTF}^0$ charge transfer transition,^{15,16} which is compatible with the above-mentioned arrangement as the trimer. As is apparent from the Figures, the TTF trimers are located perpendicularly to each other with the sulfur-sulfur contact of $3.67(3) \text{ \AA}$ to form a two-dimensional layer parallel to the c plane. The S-S distances is somewhat smaller than the sum of van der Waals radii of the sulfur atoms (3.70 \AA) .¹⁷ The small electrical resistivity and the low activation energy of the present salt ($87 \text{ } \Omega \text{ cm}$ as a compacted pellet at $25 \text{ } ^\circ\text{C}$ and 0.05 eV , respectively) may result from the electrical conduction through the two-dimensional TTF layer.

The closest chlorine-sulfur contact ($\text{Cl}(1) \cdots \text{S}(1)$, $3.373(9) \text{ \AA}$), which is appreciably shorter than the sum of van der Waals radii

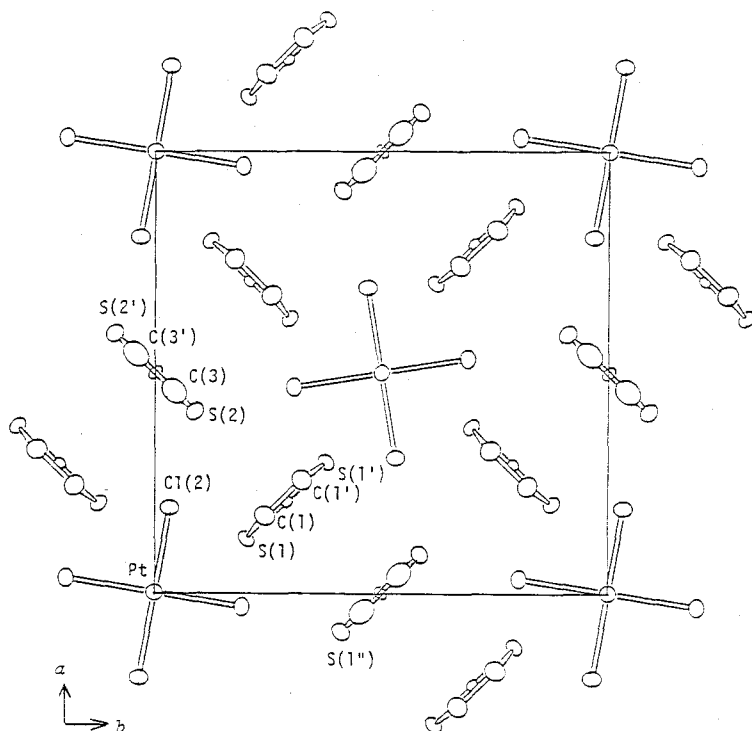


Figure 1. Crystal structure of $[\text{TTF}]_3[\text{PtCl}_6]$ projected along the c axis.

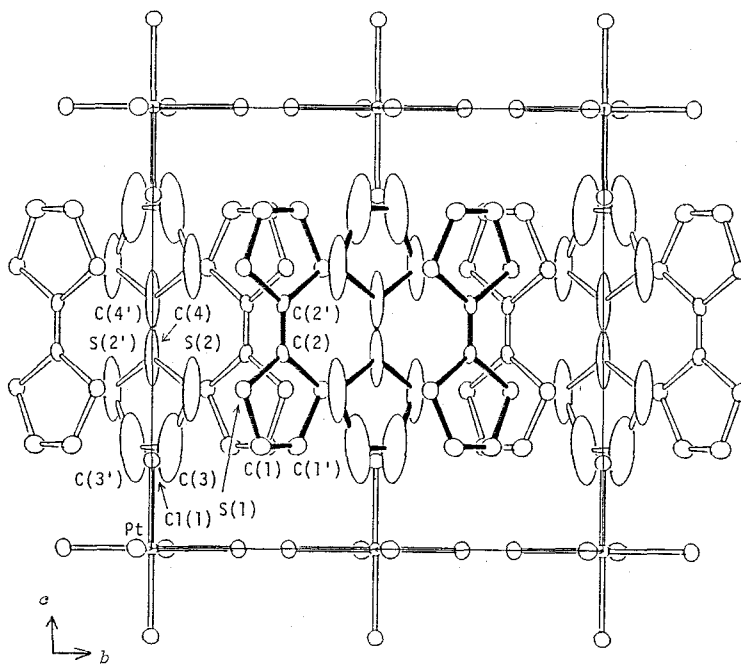


Figure 2. Crystal structure of $[\text{TTF}]_3[\text{PtCl}_6]$ projected along the a axis.

Table 2. Selected bond lengths (\AA) and angles ($^\circ$)^a together with the non-bonded contacts (\AA) for $[\text{TTF}]_3[\text{PtCl}_6]$ with the estimated standard deviations in parentheses

Pt-Cl(1)	2.325(7)	C(1)-C(1')	1.34(4)
Pt-Cl(2)	2.330(6)	C(2)-C(2')	1.31(4)
S(1)-C(1)	1.71(2)	C(3)-C(3')	1.34(20)
S(1)-C(2)	1.75(2)	C(4)-C(4')	1.54(20)
S(2)-C(3)	1.74(9)		
S(2)-C(4)	1.70(6)		
Cl(1)-Pt-Cl(2)	90(0)	S(1)-C(1)-C(1')	118(1)
C(1)-S(1)-C(2)	95.8(9)	S(2)-C(3)-C(3')	117(6)
C(3)-S(2)-C(4)	94(4)	S(1)-C(2)-C(2')	123(2)
S(1)-C(2)-S(1')	113.4(7)	S(2)-C(4)-C(4')	121(8)
S(2)-C(4)-S(2')	119(4)		
non-bonded contacts ^b			
S(1)---S(2)	3.67(3)	Cl(1)---S(1)	3.373(9)
S(1)---S(1'')	3.49(3)		

^a The atoms with the prime are in the mirror symmetry with respect to the atoms with the same number (see Figures 1 and 2). ^b See Figures 1 and 2.

of chlorine and sulfur atoms (3.65 \AA),¹⁸ indicating an electrostatic interaction between those two atoms. Binding energies of Pt $4f_{7/2}$ and Pt $4f_{5/2}$ electrons have been determined to be $70.9 \pm 0.2 \text{ eV}$ and $74.1 \pm 0.2 \text{ eV}$, respectively, from the X-ray photoelectron spectra, which are considerably smaller than those for $[\text{Bu}^n_4\text{N}]_2-[\text{PtCl}_6]$ (73.9 ± 0.2 and $77.1 \pm 0.2 \text{ eV}$), and rather close to those for $[\text{Bu}^n_4\text{N}]_2[\text{PtCl}_4]$ (71.2 ± 0.2 and $74.2 \pm 0.2 \text{ eV}$). This is suggestive of the occurrence of an appreciable reduction of the

Pt(IV) valence state of the $[\text{PtCl}_6]^{2-}$ anion of the present salt, as a result of the transfer of negative charge from the TTF molecules to the anion through the chlorine-sulfur interaction.

4. Summary

Tris(tetrathiafulvalenium) hexachloroplatinate, $[\text{TTF}]_3[\text{PtCl}_6]$, has been prepared by the diffusion of tetrathiafulvalene (TTF) and $[\text{Bu}_4\text{N}]_2[\text{PtCl}_6]$ in acetonitrile. Black plates are tetragonal, space group $P4/mbm$, with $a = 11.757(2)$, $c = 11.707(2)$ Å, and $Z = 2$. The block-diagonal least-squares refinement, based on 804 independent reflections with $|F_o| > 3\sigma(F)$, yields an R factor of 0.11. The structure comprises TTF-trimer units which are arranged perpendicularly to each other, forming a two-dimensional layer with somewhat close sulfur-sulfur contact among the trimers. The salt exhibits the electrical resistivity of 87 Ω cm as a compacted pellet at 25 °C. Binding energies of platinum 4f electrons of the $[\text{PtCl}_6]^{2-}$ anion suggest an extreme reduction from the platinum (IV) state.

5. References

- 1 A. R. Siedle, G. A. Candela, T. F. Finnegan, R. P. van Duyne, T. Cape, G. F. Kokoszka, P. M. Woyciesjes, J. A. Hashmall, M. Glick, and W. Ilsley, *Ann. N. Y. Acad. Sci.*, 1978, 313.
- 2 A. R. Siedle, G. A. Candela, T. F. Finnegan, R. P. van Duyne, T. Cape, G. F. Kokoszka, P. M. Woyciejes, and J. A. Hashmall, *Inorg. Chem.*, 1981, 20, 2635.

- 3 T. J. Kistenmacher, M. Rossi, C. C. Chiang, R. P. van Duyne, and A. R. Siedle, *Inorg. Chem.*, 1980, 19, 3604.
- 4 K. Kondo, G. Matsubayashi, T. Tanaka, H. Yoshioka, and K. Nakatsu, *J. Chem. Soc., Dalton Trans.*, 1984, 379.
- 5 G. Matsubayashi, K. Ueyama, and T. Tanaka, *J. Chem. Soc., Dalton Trans.*, in press.
- 6 Ref. 1, p. 377.
- 7 E. M. Engler, V. V. Patel, *J. Am. Chem. Soc.*, 1974, 96, 7376, and the references therein.
- 8 G. Matsubayashi, K. Kondo, and T. Tanaka, *Inorg. Chim. Acta*, 1983, 69, 167.
- 9 S. Araki, H. Ishida, and T. Tanaka, *Bull. Chem. Soc. Jpn.*, 1978, 51, 407.
- 10 'International Table for X-Ray Crystallography,' vol. IV, Kynoch press, Birmingham (1974).
- 11 C. K. Johnson. ORTEP-II: A FORTRAN Thermal-Ellipsoid Plot Program for Crystal Structure Illustrations, ORNL-5138, March 1976. Oak Ridge National Laboratory.
- 12 E. M. Engler, F. B. Kaufman, D. C. Green, C. E. Klotz, and R. N. Compton, *J. Am. Chem. Soc.*, 1975, 97, 2921, and references therein.
- 13 J. C. Bailar, Jr., H. J. Emeleus, Sir R. Nyholm, and A. F. Trotman-Dickenson, 'Comprehensive Inorganic Chemistry,' Vol 3. Pergamon Press (1973), p. 1330.
- 14 Ralph W. G. Wyckoff, 'Crystal Structures,' Vol II, Cap. IX, p. 10. p. 10. Interscience Publishers, INC., New York (1951).
- 15 J. B. Torrance, B. A. Scott, B. Welber, F. B. Kaufman, and P. E. Sieden, *Phys. Rev. B*, 1979, 19, 730.
- 16 T. Sugano, K. Yakushi, and H. Kuroda, *Bull. Chem. Soc. Jpn.*, 1978, 51, 1041.

17 L. Pauling, 'The Nature of the Chemical Bond,' 3rd ed., Conell University Press, Ithaca, New York (1960).

Conclusion

The results obtained from the present work are summarized as follows:

1. Several bulky tris(β -diketonato)siliconium(IV)-TCNQ salts have been prepared as the first silicon-containing TCNQ salts. Simple salts containing the $\text{TCNQ}^{\cdot -}$ radical anion exhibit resistivities of $1 \times (10^6 - 10^8) \, \Omega \text{ cm}$, and complex salts involving both the $\text{TCNQ}^{\cdot -}$ radical anion and neutral TCNQ display the resistivities of $1 \times (10^1 - 10^4) \, \Omega \text{ cm}$. The single crystal X-ray analysis of $[\text{Si}(\text{MeC}(\text{O})-\text{CHC}(\text{O})\text{Me})_3]^+(\text{TCNQ})_2^{\cdot -}$ has revealed that TCNQ molecules construct a one-dimensional columnar structure of tetrameric units consisting of two dimeric units. The resistivity measured in the crystalline state of this salt is the lowest along the TCNQ column. Thus, an effective TCNQ column may be constructed to exhibit high conductivities even with bulky counter cations.

2. TTF and TSF salts with some bulky octahedral metallate anions containing oxalato ligands ($[\text{M}(\text{C}_2\text{O}_4)_3]^{2-}$ where $\text{M} = \text{Si}(\text{IV}), \text{Ge}(\text{IV}),$ and $\text{Sn}(\text{IV})$, and $[\text{cis-}\text{R}_2\text{Sn}(\text{C}_2\text{O}_4)_2]^{2-}$ where $\text{R} = \text{Me}$ and Et) and some planar metallate anions ($[\text{M}(\text{C}_2\text{O}_4)_2]^{2-}$ where $\text{M} = \text{Cu}(\text{II})$ and $\text{Pt}(\text{II})$, and $[\text{Pt}(\text{C}_2\text{O}_4)\text{Cl}_2]^{2-}$) have been prepared. Electrical resistivities of these TTF and TSF salts as compacted samples at 25°C are $1 \times (10^3 - 10^5) \, \Omega \text{ cm}$ for $[\text{M}(\text{C}_2\text{O}_4)_3]^{2-}$, $1 \times (10^1 - 10^6) \, \Omega \text{ cm}$ for $[\text{cis-}\text{R}_2\text{Sn}(\text{C}_2\text{O}_4)_2]^{2-}$, and $1 \times (10^2 - 10^4) \, \Omega \text{ cm}$ for $[\text{M}(\text{C}_2\text{O}_4)_2]^{2-}$.

3. Several TTF and TSF salts with chlorodiorganostannate anions have been prepared; $[\text{TTF}][\text{SnR}_2\text{Cl}_3]$ ($\text{R} = \text{Me}$ and Et), $\text{D}_2[\text{SnPh}_2\text{Cl}_4]$, $[\text{TTF}]_3[\text{SnR}_2\text{Cl}_4]$ ($\text{R} = \text{Me}$ and Et), and $\text{D}_{3.3}[\text{SnPh}_2\text{Cl}_4]$ ($\text{D} = \text{TTF}$ and

TSF). They behave as semiconductors with the resistivities $1 \times (10^1 - 10^9) \Omega \text{ cm}$ as compacted pellets at 25°C . An X-ray crystallographic analysis has revealed that $[\text{TTF}][\text{SnMe}_2\text{Cl}_3]$ consists of both dimeric $(\text{TTF}^+)_2$ and $([\text{SnMe}_2\text{Cl}_3]^-)_2$, and $[\text{TTF}]_3[\text{SnR}_2\text{Cl}_4]$ (R= Me and Et) involve trimeric TTF units which are located perpendicularly to each other in the crystals, forming a two-dimensional layer with somewhat close sulfur-sulfur contacts among the trimers. Small resistivities of the latter two salts (16 and $42 \Omega \text{ cm}$ at 25°C , respectively) suggest the electrical conduction through the two-dimensional TTF layers.

4. The TTF complex salt with hexachloroplatinate(IV), $[\text{TTF}]_3[\text{PtCl}_6]$, has been prepared by the diffusion reaction of TTF with $[\text{Bu}^n_4\text{N}]_2^- [\text{PtCl}_6]$ in acetonitrile. The crystal structure consists of TTF trimeric units which are arranged perpendicularly to each other, forming a two-dimensional layer. The electrical conduction through the layer leads a small resistivity ($87 \Omega \text{ cm}$ at 25°C).

Acknowledgements

The author would like to express sincerest gratitude to Professor Toshio Tanaka at Department of Applied Chemistry, Faculty of Engineering, Osaka University for his continuous guidance and hearty encouragement throughout this work. The author is also deeply grateful to Associate Professor Gen-etsu Matsubayashi for his continuous advices and valuable discussions. Greatful acknowledgement is also given to Dr. Koji Tanaka and Dr. Shunichi Fukuzumi for their helpful suggestions.

The author acknowledges Professor Kazumi Nakatsu at Faculty of Science, Kwansei Gakuin University for his collaboration.

The crystallographic studies were generously supported by the Crystallographic Research Center, Institute for Protein Research, Osaka University, the author thanks for the guidance.

Furthermore, the author wishes to thank all the members of the Tanaka Laboratory for their occasional discussions, helpful assistances, and friendships.

Finally, great many thanks are given to the author's family for their understanding and perpetual support.